2009

The Influence of SPARC on Collagen Deposition in Asbestos-Induced Pulmonary Fibrosis

Aubrey Meghan Smartt
The University of Montana

THE INFLUENCE OF SPARC ON COLLAGEN DEPOSITION IN ASBESTOS-INDUCED PULMONARY FIBROSIS

By

AUBREY MEGHAN SMARTT

B.A. Biology and Chemistry, Carroll College, Helena, MT, 2004

Dissertation

Presented in partial fulfillment of the requirements
for the degree of

Doctor of Philosophy
in Biomedical Science

The University of Montana
Missoula, MT

January 2009

Approved by:

Perry Brown, Associate Provost for Graduate Education
Graduate School

Dr. Elizabeth Putnam, Chair
Department of Biomedical and Pharmaceutical Sciences

Dr. Andrij Holian
Department of Biomedical and Pharmaceutical Sciences

Dr. Stephen Lodmell
Department of Biological Sciences

Dr. Curtis Noonan
Department of Biomedical and Pharmaceutical Sciences

Dr. Mark Pershouse
Department of Biomedical and Pharmaceutical Sciences

Smartt, Aubrey, Ph.D., January 2009 Biomedical Science

The influence of SPARC on collagen deposition in asbestos-induced pulmonary fibrosis

Chairperson: Elizabeth Putnam, Ph.D.

Pulmonary fibrosis involves the invasion of lung tissue with fibrotic, scar tissue and affects roughly five million people total worldwide. Fibrotic development in the lung has several causes, including chronic inflammatory diseases, infections, medical compounds, and environmental agents. There is no known cure for the disease, but only therapies to improve quality of life. Scar tissue formation must be targeted in order to begin to provide any type of cure for fibrotic diseases. In this study, asbestos was used to induce pulmonary fibrosis in a mouse model and gene expression studies were then performed to identify potential candidate genes involved in asbestos response. One gene with the potential to regulate the fibrotic response is SPARC (secreted protein acidic and rich in cysteine), a matricellular protein involved in tissue repair, extracellular matrix (ECM) regulation, cellular proliferation, and cellular adhesion. The goal of this project was to determine the role of SPARC in fibrosis development after asbestos exposure, specifically targeting how lack of SPARC expression can influence collagen production. *I hypothesize that SPARC is a necessary component involved in the fibrotic response to asbestos through an influence on collagen deposition in the lung.* I have found that the expression of SPARC is increased in the lungs of C57Bl/6 wild-type mice exposed to asbestos. This increase in expression correlates to higher collagen deposition in the lung. The absence of SPARC in these treated mice resulted in a reduction of the level of collagen deposition back to baseline. To determine the therapeutic potential of these findings, SPARC expression was reduced by small interfering RNA (siRNA) in wild-type mice already suffering from fibrosis. Collagen deposition in the fibrotic mice that received the SPARC siRNA vector showed a significant decrease in collagen accumulation when compared to those that did not receive the vector. Overall, these results indicate that expression of SPARC is a significant step in the development of lung fibrosis through the modulation of collagen deposition and therefore, SPARC may be a potential therapeutic target.

ACKNOWLEDGEMENTS

First and foremost I would like to thank my parents, Scott and Kathleen Smartt, and grandparents, Roy and Phyllis Milne, for their unconditional love and for always believing in me and what I can accomplish. I have been fortunate enough in the pursuit of my dreams to constantly have both their support and encouragement to keep going. I would also like to thank my brother Ryan and all of my friends who helped me to maintain my sanity by making life much more enjoyable throughout this journey. This would include my lab mates Amy, Mary, Melanie, and Amber who not only became my friends, but also helped me a great deal in the laboratory. I would not be where I am today without the help and support of these individuals.

I would further like to thank my advisor, Dr. Elizabeth Putnam for her assistance and guidance in the development and completion of this project. Also, I would like to thank the members of my advisory committee Dr. Andrij Holian, Dr. Stephen Lodmell, Dr. Curtis Noonan, and Dr. Mark Pershouse for their time and expertise lent to make this a better project and me a better scientist.

Finally I would like to thank the Department of Biomedical and Pharmaceutical Sciences and the Center for Environmental Health Sciences at the University of Montana for both the funding and educational resources necessary for the completion of this degree. This includes Lou Herritt and the Histology Core, Corbin Schwanke and the Microarray Core, Laura Hoerner, Britten Postma, and Laboratory Animal Resources, as well as Dr. Donald Gardner at Rocky Mountain Laboratories.

TABLE OF CONTENTS

ABSTRACT ii

ACKNOWLEDGEMENTS iii

TABLE OF CONTENTS iv

LIST OF TABLES vii

LIST OF FIGURES viii

INTRODUCTION 1

i. Pulmonary Fibrosis 1

a. Asbestosis 6

ii. Asbestos 7

a. Libby Amphibole 11

b. Crocidolite 13

iii. SPARC 13

iv. Long-Term Asbestos Exposure Study 22

a. Abstract 22

b. Introduction 23

c. Materials and Methods 24

d. Results 26

e. Discussion 37

f. Conclusions 39

v. References 39

CHAPTER ONE: Collagen Accumulation After Short-Term Asbestos Exposure 50

I.i. Abstract 50

I.ii. Introduction 51

I.iii. Materials and Methods 53

I.iv. Results 56

I.v. Discussion 69

I.vi. Conclusion 73

I.vii. References 74

CHAPTER TWO: Collagen Accumulation in SPARC-null Mice After Asbestos Exposure 79

II.i. Abstract 79

II.ii. Introduction 80

II.iii. Materials and Methods 83

II.iv. Results 87

II.v. Discussion 117

II.vi. Conclusion 121

II.vii. References 122

CHAPTER THREE: SPARC Knockdown on Collagen Production in Pulmonary Fibrosis 128

III.i. Abstract 128

III.ii. Introduction 129

III.iii. Materials and Methods 131

III.iv. Results 136

III.v. Discussion 169

III.vi. Conclusion 171

III.vii. References 172

SUMMARY 175

APPENDIX A: Elutriated Libby Amphibole 181

APPENDIX B: Hevin 190

LIST OF TABLES

Table 1	Number of Gene Alterations After Long-term Exposure to Asbestos	36
Table 2	Inflammation Scoring of Wild-Type Lung Tissue	61
Table 3	Inflammation Scoring of Wild-Type/SPARC-null Lung Tissue	104
Table 4	SPARC shRNA Target Sequences	139
Table 5	Lentivirus Titers	141

LIST OF FIGURES

Figure 1	Scar Tissue Formation in Pulmonary Fibrosis	4
Figure 2	Worldwide Production of Asbestos	9
Figure 3	SPARC Structure	16
Figure 4	SPARC Pathway Leading to Collagen Synthesis	19
Figure 5	Trichrome Staining of Lung Tissue After a 1 Year or 6 Month Exposure	28
Figure 6	Quantitation of Lucifer Yellow In Lung Tissue 6 Months Post Exposure	31
Figure 7	GoMiner Analysis of RNA Expression Changes After Microarray Analysis	34
Figure 8	Wild-Type Lung Histology	58
Figure 9	Wild-Type Collagen qRT-PCR	64
Figure 10	Wild-Type Hydroxyproline Assay	67
Figure 11	1 Month SPARC Immunohistochemistry	88
Figure 12	Wild-Type SPARC qRT-PCR	91
Figure 13	Wild-Type SPARC Protein Expression	94
Figure 14	1 Week Wild-Type/SPARC-null Lung Histology	97
Figure 15	1 Month Wild-Type/SPARC-null Lung Histology	99
Figure 16	3 Month Wild-Type/SPARC-null Lung Histology	101
Figure 17	SPARC-null Collagen qRT-PCR	106
Figure 18	Wild-Type vs SPARC-null Collagen qRT-PCR	109
Figure 19	SPARC-null Hydroxyproline Assay	112
Figure 20	Wild-Type vs. SPARC-null Hydroxyproline Assay	115
Figure 21	MISSION RNAi pLKO.1-puro Vector Map	137
Figure 22	SPARC siRNA Virus Knockdown Ability	142

Figure 23 6 Hour SPARC Immunocytochemistry 145

Figure 24 12 Hour SPARC Immunocytochemistry 147

Figure 25 24 Hour SPARC Immunocytochemistry 149

Figure 26 In Vitro SPARC siRNA Virus PBS and CRO Western Blots 152

Figure 27 In Vitro SPARC siRNA Virus, -CNT Virus, and No Virus Western Blots 155

Figure 28 In Vitro SPARC siRNA Virus Sircol Assay 158

Figure 29 In Vivo SPARC siRNA Virus Western Blot 161

Figure 30 In Vivo SPARC siRNA Virus Histology 164

Figure 31 In Vivo SPARC siRNA Virus Hydroxyproline Assay 167

Figure 32 The Role of SPARC in Asbestos-Induced Pulmonary Fibrosis 176

Figure 33 Elutriated LA Hydroxyproline Assay 183

Figure 34 Normal vs. Elutriated LA Hydroxyproline Assay 186

Figure 35 Hevin qRT-PCR 192

Figure 36 Wild-Type/SPARC-null Hevin qRT-PCR 194

Figure 37 Hevin Western Blot 197

Figure 38 Wild-Type/SPARC-null Hevin Western Blot 199

INTRODUCTION

Pulmonary Fibrosis

Pulmonary fibrosis is the formation of fibrous connective tissue in the lung in excess of normal levels. Gradually, the alveoli at the base of the lung become filled with fibrotic tissue, a process known as scarring. This process represents the end stages of fibrotic lung diseases, a group of disorders that cause progressive lung scarring in response to repeated injury to the lining of the alveoli (MFMER, 2008). This scarring makes the exchange of oxygen and carbon dioxide during respiration very difficult. Due to the progressive nature of the disease, pulmonary fibrosis can eventually result in death. Of the roughly five million individuals that currently have pulmonary fibrosis, 40,000 will die each year from the disease (Pardo, 2005). There are currently no known cures for this disease, and the existing treatments often fail to slow its progression (MFMER, 2008).

The primary symptom of pulmonary fibrosis is dyspnea (shortness of breath), which can occur even when undertaking very simple and routine tasks. Individuals suffering from the disease may also experience a dry cough, fatigue, muscle aches, and an unexplained weight loss. The severity at which these symptoms occur often differs between individuals. Some people may become ill very quickly, while others may not experience the effects of fibrosis for several years. Because the scarring associated with pulmonary fibrosis cannot be reversed and there are currently no treatments that have the ability to halt the progression of the disease, current treatments focus mainly on improving quality of life and easing the effects of disease symptoms by reducing

inflammation (American Thoracic Society, 2000). Treatments include oxygen therapy to improve respiration and the use of corticosteroids like prednisone, often in combination with other anti-inflammatory agents, to suppress the activity of the immune system. About one in three patients respond to therapy, though this response is only temporary and is not effective over time (MFMER, 2008). Lung transplantations are also an option for young individuals with severe disease, however donor organs are rare.

The cause of pulmonary fibrosis is not always known. Disease development in individuals with no identifiable cause is known as idiopathic pulmonary fibrosis. There are, however, several known causes of pulmonary fibrosis, including exposure to asbestos (asbestosis), silica (silicosis), cigarette smoke, hard metal dust, or chemotherapy drugs, that can manifest in the scarring mentioned above (American Thoracic Society, 2000). Once the small air sacs at the bases of the bronchioles are irreversibly damaged through the build up of scar tissue, the lung no longer has the same elasticity thereby hindering respiration. Gradually the alveolar architecture is destroyed and the scarring results in air-filled cystic spaces giving the appearance of a honeycomb lung (West, 2007). Basically, instead of being soft and flexible, the alveoli become very stiff and thick like a dry sponge. This hinders the ability of the lung to transfer oxygen into the blood and remove carbon dioxide.

The pathology leading to the development of pulmonary fibrosis involves the complex interaction between several factors including epithelial cells, interstitial cells, inflammatory cells, cytokines, fibroblasts and the extracellular matrix (Bienkowski, 1995). After exposure to an insult like silica or asbestos, blood leukocytes and fibroblasts, which are widely distributed in lung structures, are recruited to the site of injury (Savani, 2000; Laurent, 2007). This mobilization is due to stimulation from

cytokines and growth factors like TGF-β, PDGF, and IL-1 (reviewed in Laurent, 2007). TGF-β, in particular, may be one of the central players involved in the development of remodeling diseases like pulmonary fibrosis (Coker, 1997). Once recruited to the area, fibroblasts begin to lay down collagen fibers and further stimulate the immune system through the recruitment and activation of macrophages. As the macrophages die over time, they release cytokines that recruit new macrophages and more fibroblasts. This constant activation of fibroblasts leads to continuous collagen accumulation in the lung and scar tissue formation. A simplified version of this cyclic pathology is depicted in Figure 1.

Figure 1: The Process of Scar Tissue Formation in Pulmonary Fibrosis

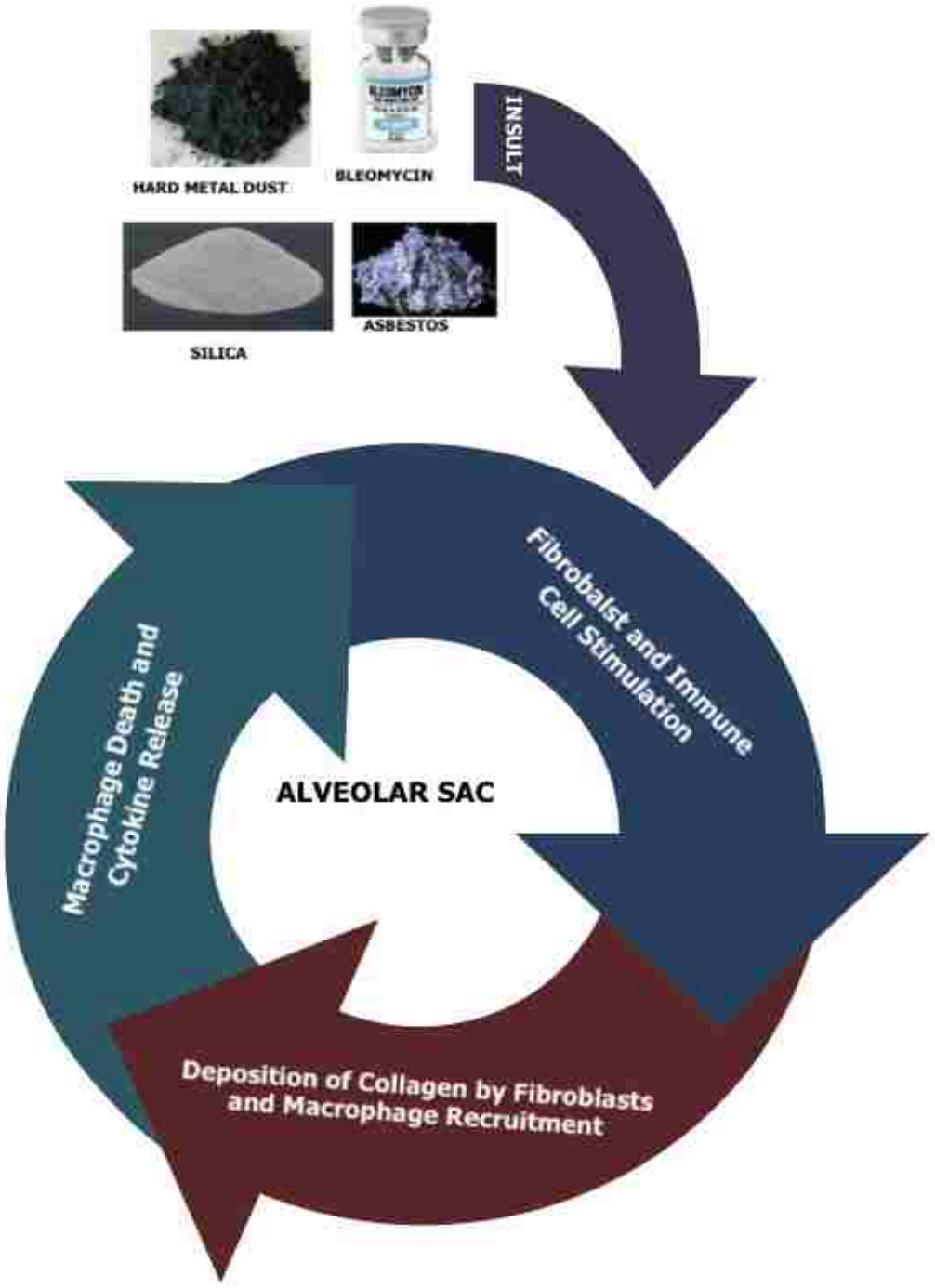

Figure 1 Legend: The cellular process leading to the development of pulmonary fibrosis is a cycle involving the continuous recruitment of macrophages and other immune cells, activation of fibroblasts, and constant collagen deposition leading to the formation of scar tissue at the lung bases. Insult images from:

http://farm4.static.flickr.com/3218/2849103016_ef7933bdcd.jpg (hard metal dust),

http://www.bedfordlabs.com/products/images/bleo.jpg (bleomycin),

http://msmc.gov.in/minerals/SilicaSand.jpg (silica)

http://www.umt.edu/libbyhealth/gifs/secondary/science/crocidolite.gif (asbestos)

Asbestosis

Asbestosis is defined as interstitial fibrosis, or pneumoconiosis, induced by the inhalation of asbestos fibers (American Thoracic Society, 2004). It is a progressive, long-term disease of the lung that will present with signs of decreased diffusion capacity, total lung capacity, and vital capacity (O'Reilly, 2007). The actual number of individuals suffering from asbestosis in the United States is unknown, however there were approximately 20,000 diagnoses in the year 2000 with 2,000 deaths where asbestosis was reported as the cause (U.S. Department of Health and Human Services, 2003; Centers for Disease Control and Prevention, 2004). The number of individuals that suffer from asbestosis is expected to rise within the next decade due to the long latency period associated with disease development. It is expected that a peak in disease will follow 30 to 40 years after the peak in mining/production, which occurred in the 1960s and 1970s. Therefore many more people will continue to develop asbestosis so we must strive to do what we can to find a cure in the near future.

The symptoms associated with asbestosis are typical of pulmonary fibrosis, with the primary symptoms including shortness of breath, chest pain, and a dry cough. Individuals suffering from asbestosis also have a higher risk of developing lung cancer (Van Loon, 1997) and this risk is magnified several-fold by smoking (Boffetta, 2004; Liddell, 2001; Berry, 2004). The disease appears to be most severe at the base of the lungs where the asbestos fibers deposit after inspiration. In the alveoli, fibroblasts are stimulated to lay down collagen to wall off the fibers and macrophages are recruited and activated to destroy them. Unfortunately, due to the natural resistance of asbestos to phagocytosis, this process becomes repetitive leading to the development of scar tissue as was previously described (Figure 1). Because the pathology of asbestosis is

congruent with typical lung fibrotic disease, it is a good model for further study into the development of pulmonary fibrosis in the hopes of developing an effective treatment or even a cure.

Asbestos

Asbestos is a naturally occurring mineral composed of long, thin fibrous crystals. The fibers have been used for over 2,000 years and were particularly popular in the building industry due to their high tensile strength, sound absorption, and resistance to heat, electricity, and chemical damage. These properties made asbestos ideal for use in products that required flame-retardation, flexibility, chemical resistance, and strength, which included insulation, house siding, electrical wiring, and brake pads among others.

There are two forms of asbestos, the needle-like amphibole fibers and the curly serpentine fibers. All forms of asbestos are fibrillar in nature in that they are made up of fibers with widths less than one micrometer. These fibers occur in bundles and can have long lengths. Chrysotile, which composes the serpentine group, is the most common form of asbestos used in industry and accounts for approximately 95% of the asbestos found in buildings in the United States (Wisconsin Department of Natural Resources, 2007). It is typically used in brake linings, pipe insulation, floor tiles, and cement roof sheets. The use of chrysotile asbestos has been banned in many countries, however it is allowed in the United States and Europe with limitations.

There are several members of the amphibole asbestos group including amosite, crocidolite, tremolite, actinolite, and anthophyllite (American Cancer Society, 2006). These fiber types are commonly used as fire retardant in thermal insulation products

and ceiling tiles. Like chrysotile, asbestiform amphibole can be found as soft friable fibers, but varieties such as amosite are much straighter. Amosite, or brown asbestos, is the second most common form of asbestos found in buildings (U.S. EPA, 2008).

The use of asbestos became very popular during the industrial revolution where it was utilized as insulation in the United States and Canada. Beginning in World War II, asbestos was also extensively used in the ship industries. By the middle of the 20th century, the use of asbestos had expanded to include materials composing lawn furniture, drywall, and concrete. This increase in the use and production of asbestos led to the discovery of its toxicity. During the early 1900's, researchers began to notice a higher incidence of lung disease and death in asbestos mining towns. By the 1930's England identified asbestos-induced lung fibrosis, or asbestosis, as a work-related disease, an insight that was not recognized by the United States for another ten years (American Cancer Society, 2006; Asbestos Resource Center, 2008). The United States government has been criticized for not acting quickly enough to prevent asbestos exposures after the toxicity of the fibers was recognized.

Since the mid 1980's, the use of asbestos in many countries has been banned due to its toxicity. However, exposures are still occurring. In 2006, 2.3 million tons of asbestos were still processed worldwide, mainly in Russia, China, Kazakhstan, and Canada (Hetherington, 2008) (Figure 2). The United States last mined asbestos in 2002 but exposures still arise because many homes still contain asbestos in their insulation/siding. In addition, the United States still uses asbestos in the production of new materials under limited conditions (EPA Asbestos Materials Bans, 1999).

Figure 2: Worldwide Production of Asbestos

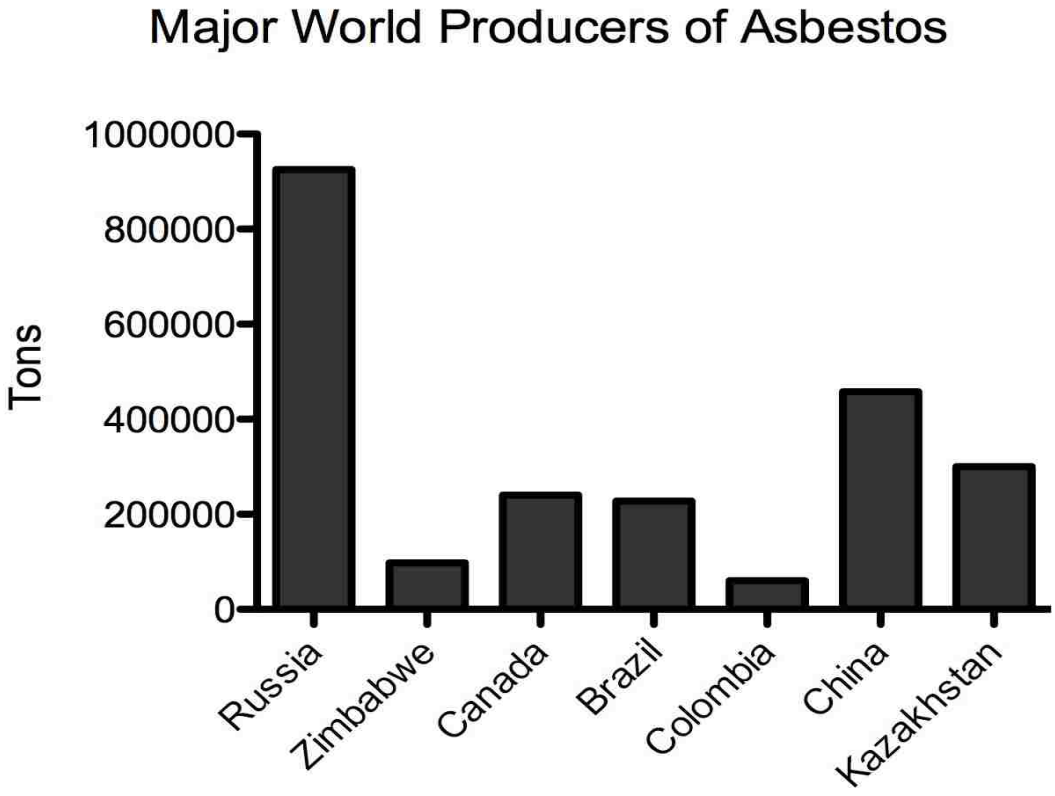

Figure 2 Legend: Many countries still produce asbestos today. In 2006 a total of 2.3 million tons of asbestos were produced worldwide with the major producers being Russia, China, and Kazakhstan. Data obtained from World Mineral Production 2002 – 2006, British Geological Survey (Hetherington, 2008).

The inhalation of airborne asbestos fibers can cause a variety of respiratory illnesses including asbestosis, lung cancer, and malignant mesothelioma. It is estimated that approximately 10,000 people die from an asbestos-related disease each year, and this number is expected to rise (Environmental Working Group, 2004). This rise is based on the knowledge that asbestos related diseases have approximately a 40 year latency period, which means that individuals who previously worked in the asbestos mines and factories may just now be showing signs of disease. Because there appears to be no end in sight for mining/use of asbestos or the destruction of all of its existing products, people will continue to be exposed to asbestos. Therefore, a thorough understanding of asbestos-related diseases is necessary to help those individuals.

For the purpose of this project, I focused on the development of asbestos-induced fibrosis (asbestosis) after exposure to one of two forms of asbestos: the amphibole found as a contaminant in the vermiculite mines in Libby, Montana (Libby amphibole) and the well-studied crocidolite amphibole fibers.

Libby Amphibole

The small town of Libby is located in the northwestern corner of Montana, approximately 30 miles south of the Canadian border. The economy of Libby has primarily been supported by the utilization of natural resources through mining and logging. Prior to 1990 the main sources of employment were the logging industry and vermiculite mining. Vermiculite ore was found in the area in 1881 and was mined from 1919 to 1990 (U.S. EPA Region 8, 2008). Vermiculite is typically defined as a hydrated laminar magnesium-aluminum-iron silicate resembling mica in appearance (U.S. EPA,

2008). The vermiculite was used in the production of Zonolite, the trademarked product made from vermiculite. In 1953 the vermiculite was found to be contaminated with asbestiform fibers, though, the fibers were not extensively studied until the late 1970's (McDonald, 2004). This contamination could explain the high number of asbestos-related diseases affecting Libby residents (Zalac, 2003).

W. R. Grace and Company bought the vermiculite mine in 1963 and continued to operate it until 1990 even though it had been known since 1956 that the vermiculite was contaminated with asbestos. Unfortunately, exposure to the vermiculite was not isolated to the Libby community as the vermiculite was shipped for use as insulation in homes all over the United States. In fact, it is estimated that 35 million homes in the United States still contain the Zonolite insulation (U.S. EPA, 2008). Today, the town of Libby is an EPA superfund site and has been the subject of 120 million dollars in cleanup efforts (Office of Inspector General Report, 2007).

The asbestos found in Libby vermiculite is a combination of amphibole fibers and cleavage fragments that include tremolite, actinolite, soda tremolite, richterite, and winchite (Meeker, 2001). These fibers can form blocky crystals, non-flexible cleavage fragments, or long flexible fiber bundles (Meeker, 2003). They also differ in their length and in the cations expressed on their surface, where the various fibers that compose Libby asbestos all have different proportions of cations like Mg^{2+}, Ca^{2+}, Fe^{2+}, Na^{2+}, and K^{+} (Webber, 2008). Based on the varied composition of Libby amphibole, the fibers are very different from other amphiboles and may therefore induce different effects in exposed tissues.

Crocidolite

Crocidolite, or blue asbestos, is mainly found in Africa but deposits also occur in Australia. It is the asbestiform of the mineral riebeckite. Crocidolite asbestos accounts for roughly 4% of the total asbestos used in the United States and is considered by some to be the most hazardous of the amphibole group (Mesothelioma & Asbestos Wellness Center, 2008). Because it is much less resistant to heat than other forms of asbestos, crocidolite was most often utilized in asbestos-cement products. Due to its hazardous nature, crocidolite asbestos provides a good fiber type for the further study of asbestos-induced pulmonary fibrosis.

SPARC

A protein that may be involved the lung's fibrotic response to an insult like asbestos through the mediation of cell-matrix interactions is Secreted Protein Acidic and Rich in Cysteine (SPARC), also known as osteonectin or BM-40 (Lane, 1994; Reed, 1996). SPARC is a 43kD protein that belongs to a group of structurally distinct proteins with similar functions that include thrombospondin, tenascin, and Hevin. These matricellular proteins can interact with cell-surface receptors, the extracellular matrix, growth factors and proteases while not contributing directly to the structural properties of the extracellular matrix (Bornstein, 2002). They are activated during tissue renewal, tissue remodeling, tissue repair, and embryonic development (Bornstein, 1995; Sage, 1989), and since its discovery, SPARC has been shown to function as a modulator of growth factor activity (Raines, 1992; Kupprion, 1998; Murphy-Ullrich, 1991; Schiemann,

2003), a counteradhesive protein (Murphy-Ullrich, 1991; Rosenblatt, 1997), a modulator of cell proliferation (Funk, 1991; Kupprion, 1998) and migration (Hasselaar, 1992; Wu, 2006), a regulator of the extracellular matrix (Tremble, 1993; Barker, 2005), and a cell cycle inhibitor (Funk, 1991).

SPARC expression is widespread during early development, but in the adult expression is mainly localized to tissues undergoing repair or remodeling, such as the bone and lining of the gut (Sage, 1989). These processes can be the result of wound healing, disease, or natural processes. Expression of SPARC is localized to several cell types including steroidogenic cells, chrondrocytes, placental trophoblasts, vascular smooth muscle cells, and endothelial cells (Porter, 1995). In injured tissues it is highly expressed in fibroblasts, epithelial cells, and macrophages (Porter, 1995; Puolakkainen, 1999; Reed, 1993; Latvala, 1996). As these are some of the primary cell types involved in pulmonary fibrosis, SPARC may play a significant role in the development of the disease, and has already been shown to accumulate in the fibrotic lung (Kuhn, 1995; Strandjord, 1999).

Protein crystallization has allowed for the identification of three structural modules in SPARC that include an acidic domain, a follistatin-like domain, and an extracellular calcium binding domain (Figure 3). The acidic domain or NH_2-terminal domain (amino acids 1-52) is involved in the inhibition of cell spreading (Hasselaar,1992), causes cell rounding and de-adhesion (Lane, 1990) and can influence the expression of extracellular matrix protein (Lane, 1992). The follistatin-like domain (amino acids 52-137) has been shown to inhibit cell proliferation (Funk, 1993), delay the cell cycle (Funk, 1991; Funk, 1993), and be involved in SPARC's recruitment to its cell surface receptors (Hohenester, 1997). The extracellular calcium-binding domain (amino

acids 138-286) has also been shown to inhibit cell spreading and proliferation (Kupprion, 1998; Motamed, 1998). Furthermore, this third domain is known to stabilize the binding of Ca^{2+} to the protein (Hohenester, 1997), which then allows the binding of collagen types I, III, and V to this extracellular module in a calcium dependent manner (Sasaki, 1997). As most of the functions of SPARC are calcium dependent, this third domain is primarily responsible for SPARC's involvement as a tumor suppressor and in cell-matrix interactions.

Figure 3: SPARC Structure

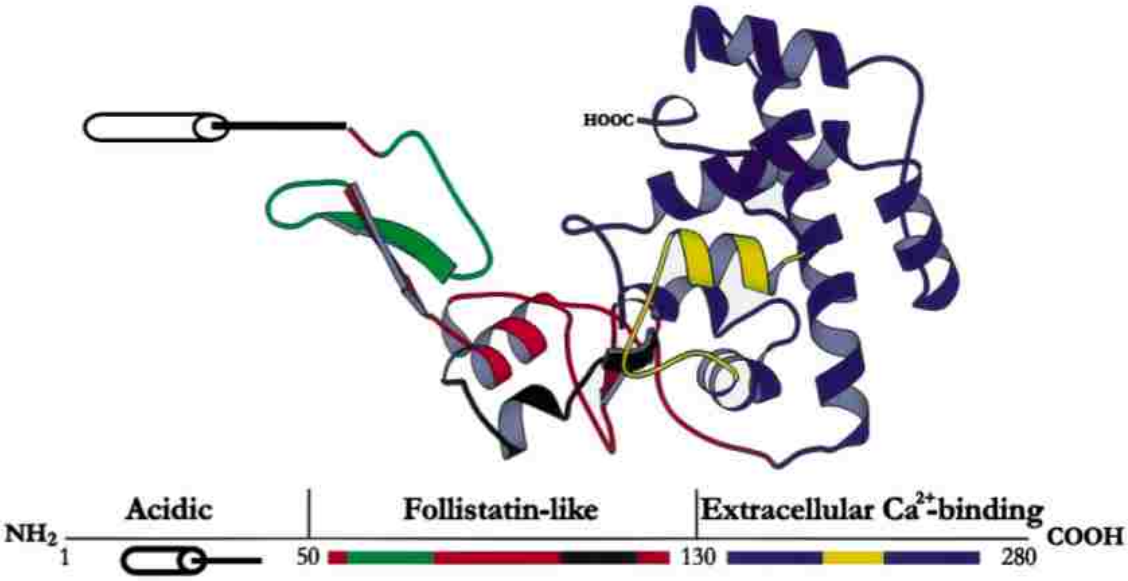

Figure 3 Legend: SPARC has three structural domains: an acidic domain (black), follistatin-like domain (red, green, black), and an extracellular calcium-binding domain (blue, yellow). Adapted from Hohenester et al. (1997), Brekken et al. (2001), and the RCSB Protein Data Bank, formerly the Brookhaven Protein database, accession number 1BMO.

A mediator of SPARC expression is the cytokine transforming growth factor β (TGF-β). TGF-β is a multifunctional growth factor involved in growth, differentiation, proliferation, tissue remodeling, and wound healing (Pepper, 1997). It is also responsible for the stimulation of fibroblasts to both proliferate and increase the synthesis of extracellular matrix components (Border, 1994). In addition, it has recently been found that exogenous TGF-β1 induces an increase in both SPARC and collagen type I expression (Reed, 1994).

SPARC is capable of stimulating the TGF-β pathway through interactions with the TGF-β receptor complex only if TGF-β is already bound to the receptor (Franki, 2004). If TGF-β1 is bound to the TGF-β type II receptors it can recruit and phosphorylate TGF-β type I receptors and initiate a signal cascade (Heldin, 1997). It had been suggested that if SPARC is also bound to this receptor complex, it could dictate which of the TGF-β signaling pathways is activated, and it was later discovered that it does. Though more research is needed on the precise mechanism by which SPARC triggers TGF-β signaling events, there are several possibilities for which specific cascades are activated in SPARC's presence. These include the activation of either JNK or SMAD2/3 pathways, both of which result in an increased synthesis of collagen (Franki, 2004). Figure 4 depicts these pathways. Aside from interacting directly with extracellular membrane components like collagen, it is now known that SPARC can increase the transcription of collagen as well.

Figure 4: SPARC's Involvement in the Pathway Leading to the Synthesis of Collagen

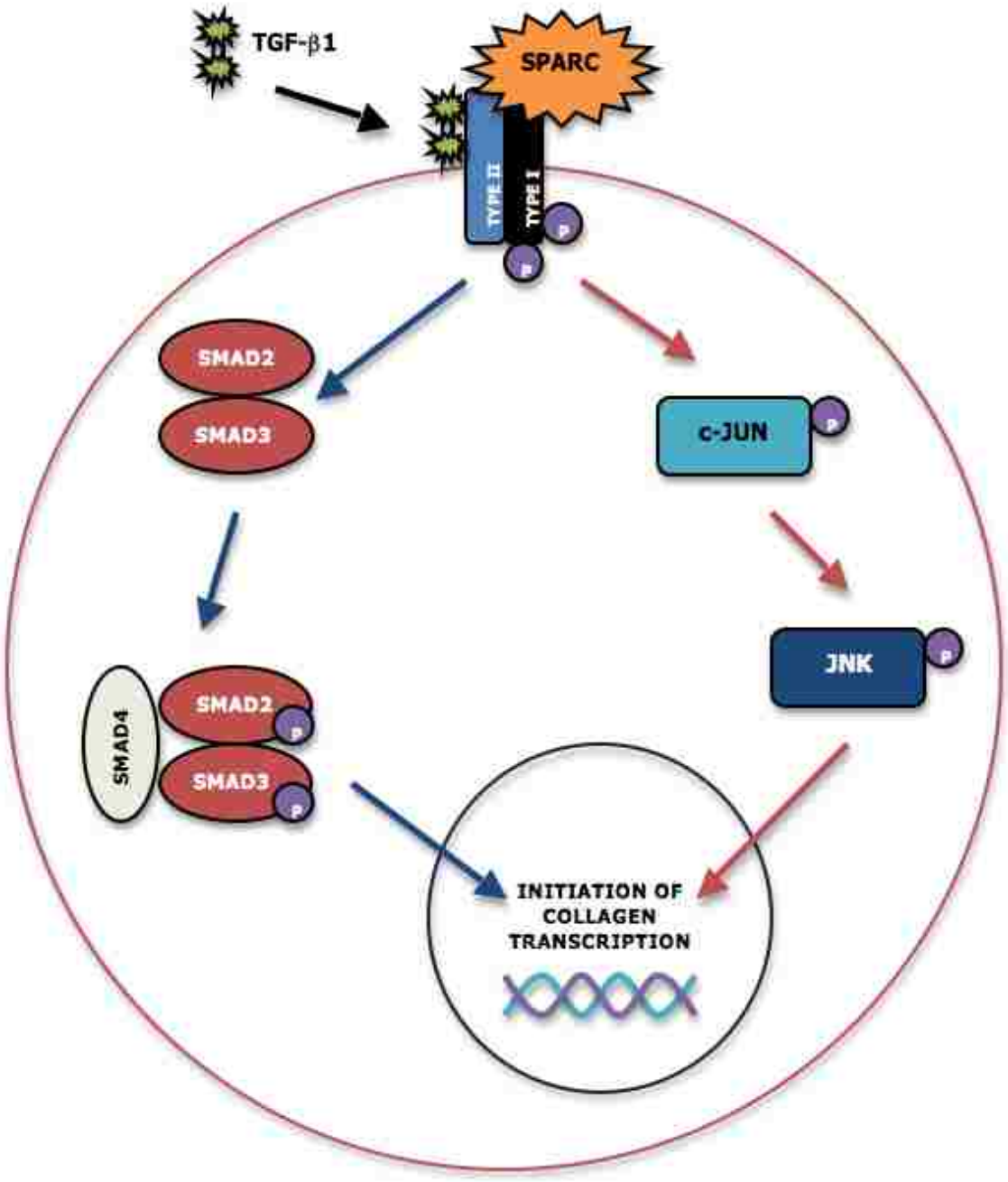

Figure 4 Legend: In a ligand-dependent manner, SPARC can bind the TGF-β receptor complex and initiate the activation of either the JNK (red arrows) or SMAD2/3 (blue arrows) signaling cascades to stimulate the transcription of collagen mRNA. This model is based on one published by Francki et al. in 2004.

To better understand the relationship between SPARC and collagen, SPARC-null (SP-null) mice were created. Previous investigations have used the SP-null mice in conjunction with bleomycin treatment to elucidate the influence of SPARC on collagen accumulation in a fibrotic lung. Bleomycin is a chemotherapeutic agent whose administration is known to cause lung fibrosis in several species of animals (Schrier, 1983; Snider, 1978; Starcher, 1978; Swiderski, 1998) that undergo a sequence of inflammatory cell migration, edema, cell proliferation, and collagen accumulation characteristic of fibrotic disease in humans (Brown, 1988; Lazenby, 1990). Results of these investigations have been conflicting, though the conditions under which they were performed were somewhat different. The first study was performed in a C57Bl/6-129 cross mouse using a low dose of bleomycin to induce fibrosis through a transtracheal puncture. It was discovered in this study that lack of SPARC significantly decreased total collagen accumulation in the lung (Strandjord, 1999). The second study used 129 mice and a high dose of bleomycin injected intratracheally to show that lack of SPARC leads to an increase in collagen accumulation in the fibrotic lung (Savani, 2000). Regardless of the opposing outcomes, it is apparent from these studies that SPARC does play a role in the amount of collagen deposited in the fibrotic lung and therefore may be interesting to study in terms of asbestosis.

In order to determine if SPARC is a potential candidate for further study in a model of fibrosis induced by asbestos, a long-term exposure (1 year & 6 months) study was performed.

Long-Term Asbestos Exposure Study

A version of this study has been published: Putnam EA, Smartt A, Groves A, Schwanke C, Brezinski M, Pershouse MA. Gene expression changes after exposure to six-mix in a mouse model. *J. Immunotoxicol.* 5: 139-144. 2008.

Abstract

The exposure of Libby MT residents to amphibole-contaminated vermiculite has been well documented in the literature (Amandus, 1987; McDonald 1986, 2004; Sullivan, 2007). To explore the gene-environment interactions in the development of asbestos-related diseases (ARD), a mouse model of asbestos exposure using Libby amphibole (a combination of amphibole fibers gathered from six sites at the Libby vermiculite mine), crocidolite asbestos, or phosphate buffered saline as a negative control was used to both determine gene expression responses by using mouse 10,000 oligonucleotide array and to visualize histological changes. One year and six months following exposure via intratracheal instillation, mice were sacrificed and whole lungs harvested for histology and microarray analysis. Using an arbitrary cutoff of 1.25 fold change, genes whose RNA expression levels were specifically altered in response to the different amphibole exposures were grouped into categories by a gene ontology analysis program, GoMiner. Our hypothesis was that assessment of asbestos-responsive genes would provide a better understanding of response mechanisms. These experiments have provided new candidate genes that may be involved in the asbestos response pathways.

Introduction

A serious public health situation has been identified in Libby, Montana where miners and town residents were exposed to hazardous levels of asbestos from the local mining operation. Vermiculite was mined, transported, and processed in the area from 1923 to 1990. Most vermiculite ore is not a health hazard and is used in many consumer products including insulation, fireproofing material, and lawn/garden products. However, the Libby ore is different in that it is contaminated 21-26% with asbestos by weight (Atkinson, 1982). As a result of the asbestos contamination, Libby has been designated as an Environmental Protection Agency (EPA) Superfund site.

Prolonged exposures to asbestos can manifest in a variety of health problems including asbestosis, lung cancer, and mesothelioma. In December 2000 the Agency for Toxic Substances and Disease Registry (ATSDR) conducted a mortality study on the Libby population for a twenty-year period encompassing 1979 – 1998. It was reported that there was a 20% to 40% increase in malignant and nonmalignant respiratory deaths. In particular mesothelioma mortality was elevated, asbestosis mortality was 40 to 80 times higher than expected, and lung cancer mortality was 1.2 to 1.3 times higher than expected when compared to the rest of the United States (ATSDR, 2000).

Previous studies in mice have shown that after asbestos exposure, a complex network of cytokines, growth factors, and receptors are involved in initial inflammation and ensuing asbestosis and carcinogenesis (Geist, 2000; Shukla, 2003). We have used gene expression studies in a mouse model to identify potential candidate genes involved in asbestos response. In addition, exposed lungs were visualized for histological changes consistent with fibrosis. Thus, the goal of this study was to identify the fibrotic effects of

crocidolite asbestos and the amphibole fibers from the Libby, Montana vermiculite mine and to indicate specific pathways of response to these fibers for future studies.

Materials and Methods

Amphiboles: Libby amphibole comprised of samples 20, 23, 25, 27, 28 and 30 from the vermiculite mine in Libby, MT as described (Meeker et al., 2003) were generously provided by the U.S. Geological Survey. This amphibole has been characterized in detail (Wylie, 2000; Gunter, 2003; Meeker, 2003) and the Libby amphibole samples used also have a particle size distribution matching air sample size distribution data (Meeker, 2003). Crocidolite asbestos was obtained from the Research Triangle Institute (Research Triangle Park, NC). The fiber size distribution of both Libby amphibole and crocidolite asbestos has been previously reported (Blake, 2007). For reference, size parameters of the Libby amphibole sample were 0.61 μm in diameter, 7.21 μm in length, with 22.52 for the aspect ratio. Size parameters of the crocidolite were 0.16 μm in diameter and 4.59 μm in length, with a 34.05 aspect ratio. Samples were freshly prepared in sterile phosphate-buffered saline (PBS, pH 7.4) and sonicated before instillation.

Mouse Treatment: C57Bl/6 mice six to eight weeks of age were divided into three groups of at least seven mice each and treated via intratracheal instillation with 100μg of Libby amphibole or crocidolite asbestos in 30 μL of sterile phosphate buffered saline (PBS). PBS alone was instilled in vehicle control mice. The mice were sacrificed and the lungs harvested for study one year or six months after instillation.

RNA Isolation: Treated mouse lungs were homogenized in the presence of TRIzol reagent and RNA was isolated following the manufacturer's protocol (Invitrogen, Carlsbad, CA). Additional purification of the total RNA was performed using an RNeasy kit (Qiagen, Valencia, CA).

Microarray Analysis: RNA was analyzed by microarray hybridization to a 10K element mouse oligonucleotide array based on set A from MWG-Biotech (High Point, NC). Gene expression was analyzed relative to mouse reference standard RNA (Stratagene, La Jolla, CA), enabling experiment-to-experiment comparison. Alterations of transcript levels were characterized by fold-change, k-means cluster analysis, and principle components analysis. Genes with expression changes were organized into biologically relevant categories and assessed for significance using the GoMiner program (http://discover.nci.nih.gov/gominer/). Assays and analyses were performed in the Microarray core at The University of Montana Center for Environmental Health Sciences.

Histology: Mouse lung samples were perfused and immersed in Histochoice fixative (Amresco, Solon, OH), embedded in paraffin, and sliced into 7μm sections for analysis. Routine Gomori's trichrome staining was performed in the Molecular Histology & Fluorescence Imaging Core and the sections examined under light microscopy.

Lucifer yellow (LY) staining: LY has been shown to bind to collagen, enabling quantification of the extent of fibrosis based on the amount of collagen present (Antonini, 2000; Taylor, 2002. Briefly, histologic tissue sections were incubated in Lucifer Yellow-CH (1 mg/mL) (Molecular Probes, Eugene, OR) for one hour at room

temperature, washed in dI water and cover-slipped with water soluble, anti-fade mounting medium (Immuno Concepts, Sacramento, CA). LY-stained tissue was quantitated using a Laser Scanning Confocal Microscope (LSC), (CompuCyte, Cambridge, MA) in the Fluorescence Cytometry Core fitted with an argon-ion laser. Wincyte software (CompuCyte Corporation) was used in the analysis.

Statistics: Mean values obtained from quantitation of the LY-stained sections of amphibole and PBS-exposed mouse lungs were compared using One-Way ANOVA with a Newman-Keuls Multiple Comparison Test.

Results

Six months after instillation, lungs from animals exposed to Libby amphibole (LA) and crocidolite asbestos (CRO) demonstrated fibrosis development with increased cellularity (inflammation) and elaboration of extracellular matrix (collagen appears blue-green in Gomori Trichrome-stained sections, Figure 5B and 5C). Arrows indicate areas of increased collagen deposition. Although fibrotic areas were identified in the LA treated mouse lung sections, the level of collagen deposition around the airways appeared to be less than that seen in crocidolite asbestos treated lung sections included as positive control. No fibrotic areas were identified in sections from mouse lungs instilled with PBS as the vehicle control (Figure 5A).

At one year post instillation, collagen is no longer deposited in increased amounts in the amphibole treatment groups as is seen at six months post-exposure (Figure 5E and 5F). There still appears to be a significant increase in inflammation made

apparent by the increased cellularity and appearance of macrophages (large red cells). Again, the PBS control animals show no signs of inflammation or increased collagen deposition (Figure 5D). Due to the lack of collagen deposition around the airways, it appears as though the fibrotic disease process is resolving from six months to one year.

Figure 5: Mouse Lung Sections Exposed for 1 Year or 6 Months to Crocidolite Asbestos (CRO), Libby Amphibole (LA), or a PBS Control.

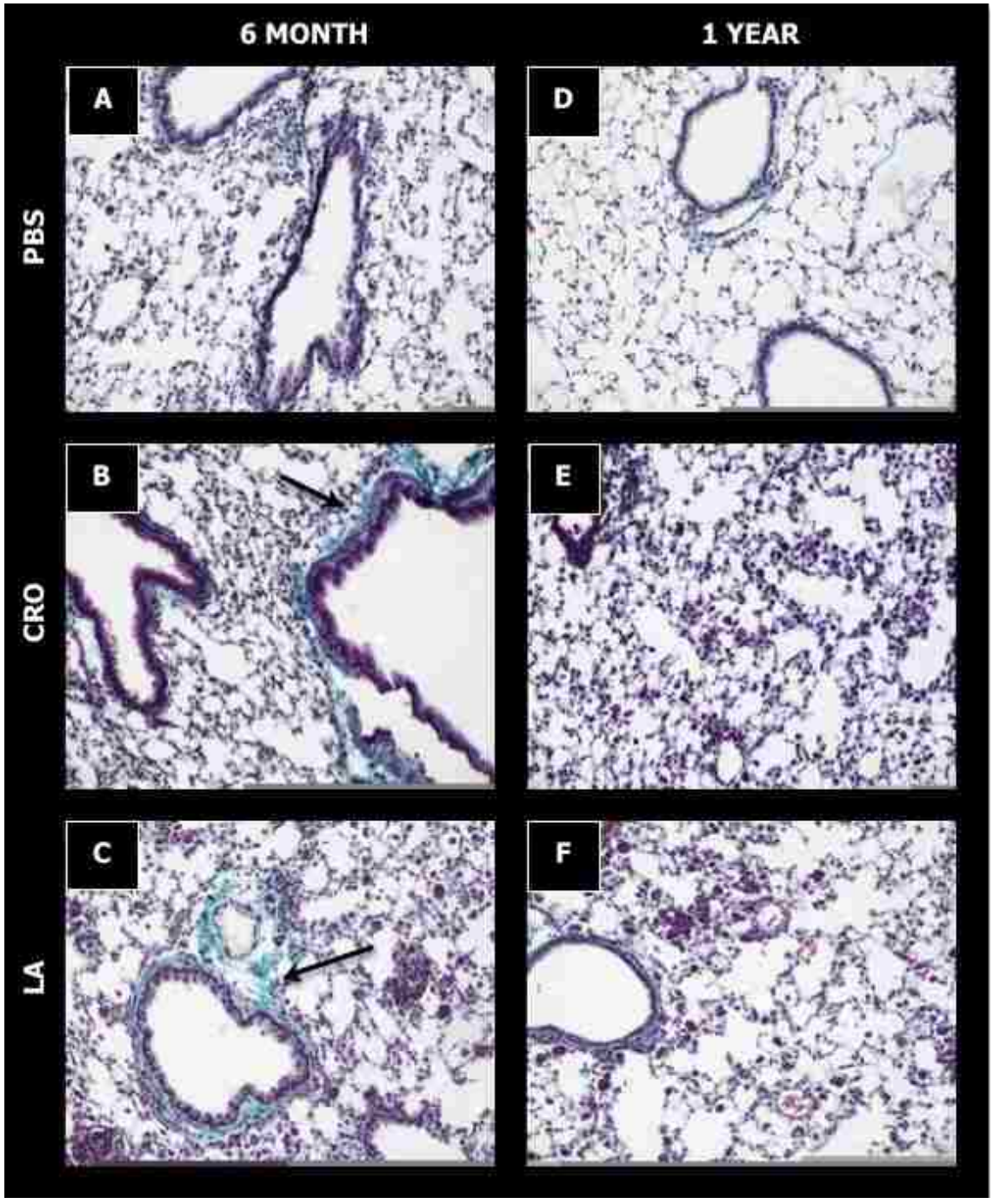

Figure 5 Legend: Gomori Trichrome-stained 7μM sections of mouse lungs from animals instilled with crocidolite asbestos (CRO), Libby amphibole (LA), or sterile saline (PBS) as a vehicle control for comparison (200X original magnification). Blue-green staining indicates collagen deposition and arrows point to areas of increased accumulation.

To quantify mouse lung collagen deposition, an assay using lucifer yellow to stain for collagen was performed. This assay allows for collagen quantitation without the tissue destruction required by a hydroxyproline assay. Figure 6 demonstrates the mean fluorescence intensities seen in histology sections of mouse lungs. While mean fluorescence intensity was increased in lungs from both treatment groups, lungs from the crocidolite-treated mice demonstrated a statistically significant increase over PBS-treated control mice (n = four in each group). Collagen levels in LA instilled mice, while elevated, did not rise to statistical significance when compared to control animals. This lack of significance could be due to the limited number of mice used in the assay or the exposure time. As there appeared to be no difference in collagen accumulation one year after treatment, the lucifer yellow assay was not performed.

Figure 6: Quantitation of Lucifer Yellow Stained Lung Tissue 6 Months Post Exposure.

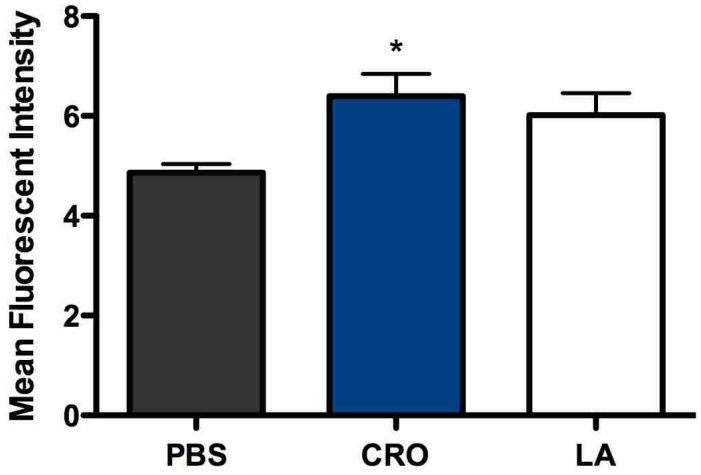

Figure 6 Legend: Quantitation of Lucifer Yellow stained tissue. Stained tissue was scanned using a Laser Scanning Confocal Microscope fitted with an argon-ion laser. A circular area having a radius of 700 microns was scanned at approximately the same location on each section using a series of smaller scan areas called phantoms, each having a radius of 8mm. The mean fluorescent intensity for the phantoms in each scan area was recorded and analyzed using Wincyte software. The phantoms that were saturated or below a set threshold were gated out and were not included in the analysis. This eliminated background areas and artifacts from the analysis. Intensity values were obtained from every tenth section (for a total of 15 sections) for each lung and added together for each animal. Angie Groves performed this assay while working as an undergraduate in our lab. I completed the statistical analysis using one-way ANOVA with a Newman-Keuls Multiple Comparison test. (* = $p < 0.05$)

Gene expression analysis was performed on pooled aliquots of RNA from seven to eight animals per exposure and the results analyzed with the GoMiner program from NCBI. Results from LA and CRO exposed animals demonstrated gene expression changes in multiple pathways at both time points (Figure 7, Table 1). Similar responses were seen at both one year and six months with the highest number of expression changes occurring in the regulation of cell proliferation functional group. Numerous changes were also seen in the extracellular matrix and the regulation of signal transduction functional groups. Expression changes were also seen in groups with genes involved in apoptosis, fibrosis, tumor formation, and oxidative stress. Overall, it is also apparent that expression changes are not as frequent at one year as six months, again indicating that the disease process in mice may be resolving from six months to one year.

Figure 7: GoMiner analysis of RNA expression changes determined by microarray analysis both 1 Year and 6 Months post exposure.

A.

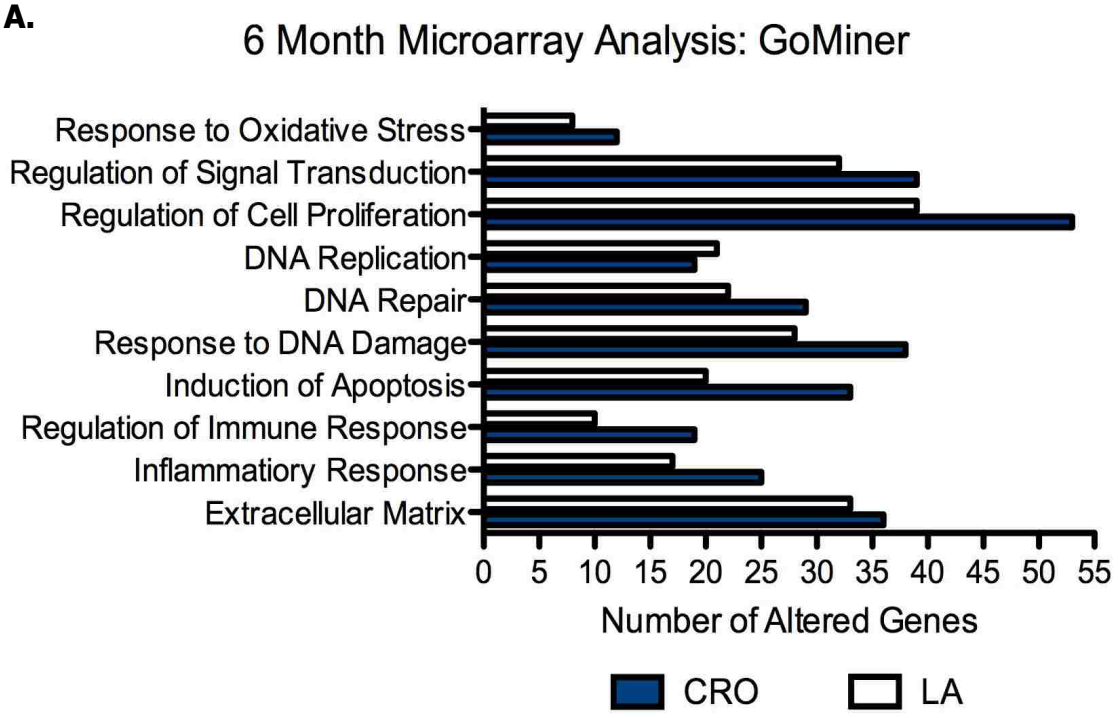

B.

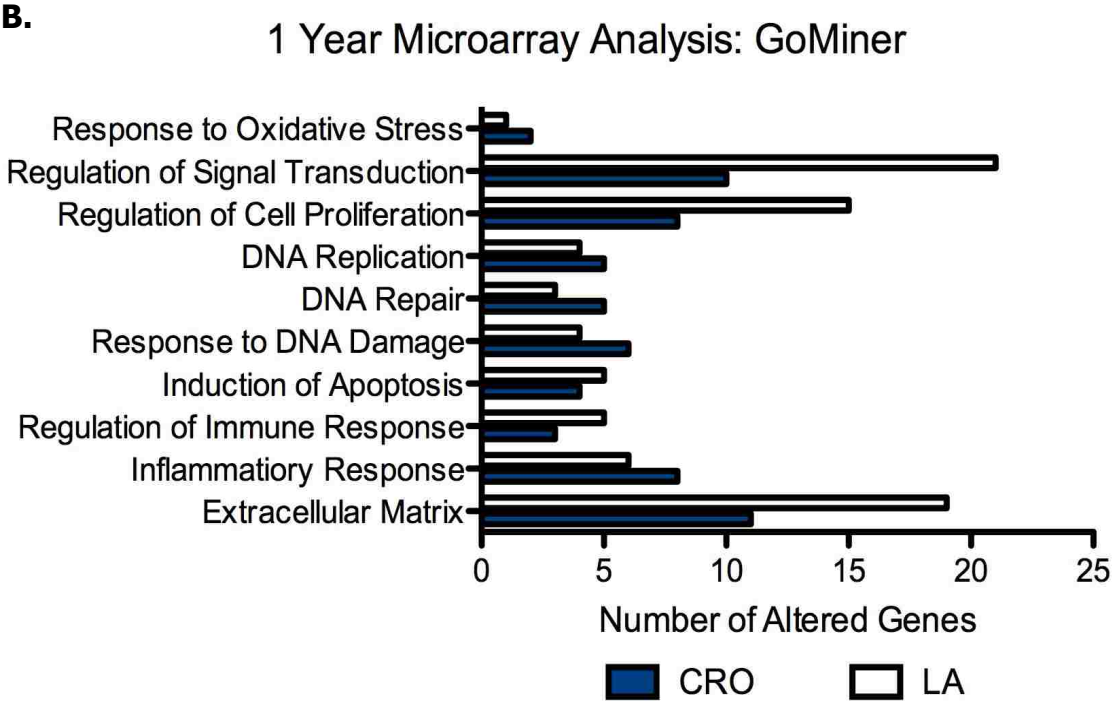

Figure 7 Legend: GoMiner analysis of RNA expression changes determined by microarray analysis. Genes exhibiting at least 1.25 fold up- or down-regulation in treated lungs compared to controls were grouped with GoMiner (NCBI) into functional categories. The functional groups are graphed to include the total number of genes with changed expression.

Table 1: Number of Gene Alterations After Long-term Exposure to Asbestos

Pathway	6 Month Genes		1 Year Genes	
	# Down	# Up	# Down	# Up
Induction of Apoptosis	13 [11]	7 [22]	1 [3]	4 [1]
Extracellular Matrix	19 [15]	14 [21]	13 [7]	6 [4]
Regulation of Cell Proliferation	30 [18]	9 [35]	9 [6]	6 [2]
Response to Oxidative Stress	4 [3]	4 [9]	1 [2]	0 [0]
Regulation of Signal Transduction	21 [11]	11 [28]	14 [6]	7 [4]
Inflammatory Response	12 [10]	5 [15]	5 [6]	1 [2]
DNA Replication	11 [7]	10 [12]	4 [4]	0 [1]
DNA Repair	13 [11]	9 [18]	2 [3]	1 [2]
Regulation of Immune Response	8 [9]	2 [10]	3 [3]	2 [0]
Response to DNA Damage	16 [13]	12 [25]	2 [3]	2 [3]

* LA altered genes / [CRO altered genes]

Discussion

Despite intensive investigation, the mechanisms of asbestos toxicity have yet to be delineated. The development of lung disease has been related to both the cumulative dose and the time since first exposure, with asbestos-related diseases (ARD) typically arising after a 15-40 year latent period. Recent reviews have detailed evidence of various pathogenic pathways of asbestos-induced lung diseases, which include: 1) the chemical and structural properties of the fibers, 2) the lung fiber burden, 3) fiber uptake by lung epithelial cells, 4) iron-catalyzed free radicals, 5) DNA damage, 6) cytokines/growth factors, and 7) exposure to cigarette smoke and other pulmonary toxicants (reviewed in Kamp 1999, Manning 2002). No single mechanism has been found to explain the abnormalities caused by asbestos, and the exact pathogenic pathways and their regulation have not been determined. Through the analysis of gene expression changes found in mouse lungs after asbestos exposure, our studies will aid in determining the contribution of these various mechanisms on the initiation and progression of asbestos-related diseases.

The physiological effects of crocidolite asbestos have been well studied for many years, but the effects of the Libby amphibole (LA) are still under investigation. The asbestos-related diseases seen in the exposed Libby population make it essential to determine the mechanism of action of this material, and to compare the effects of the LA to the effects of other, well-characterized amphiboles. Using crocidolite asbestos as a well-characterized fiber for comparison (Hamilton, 2004; Wang, 2006; Baldys, 2007), we studied the effects of the LA in a mouse model of exposure. LA and crocidolite both produced increased collagen deposition in a mouse model of asbestosis, as

demonstrated by both Trichrome staining and lucifer yellow quantitation. In both exposures, the extent of fibrosis in terms of collagen deposition was consistently reduced in LA exposed mouse lungs compared to lungs exposed to crocidolite asbestos. This could have been due to some of the differences between LA and CRO including fiber length, diameter, and surface charge. For example, crocidolite is smaller in both length and diameter than LA.

Gene expression changes after asbestos exposure have been studied *in vitro* (Nymark, 2007). The analysis of changes in gene expression in whole lung tissue after exposure to asbestos may provide new directions for research into the mechanisms of fibrosis development. Our results demonstrate that after a long-term exposure (1 year, 6 months) to either LA or crocidolite, there are both similarities and differences in the gene expression changes seen as analyzed with the gene ontology analysis program from NCBI, GoMiner. This program assigns genes to functional categories and assesses the significance of the expression level differences from control (PBS) before the expression of a particular gene is included as "altered" in the category. As expected after exposure to fibers that cause fibrosis, the greatest number of expression changes were seen in the regulation of cell proliferation functional category after both LA and crocidolite exposure. Similarly, the functional categories of extracellular matrix genes and regulation of signal transduction genes also had numerous changes in expression levels. At six months, the number of altered genes was greater after crocidolite exposure compared to LA exposure in every category found to be significant except for the expression of genes involved in DNA repair. This effect is the opposite for the major categories of alteration at one year, with mice exposed to LA having more genetic alterations than CRO exposed mice. This may indicate that fibrotic disease in mice

exposed to CRO may resolve faster than in mice exposed to LA. As the disease process does not resolve in humans, it will be important to assess fibrotic and gene expression changes at earlier times after exposure in order to better understand the mechanisms underlying fibrotic disease development as it relates to humans.

Conclusions

Both Libby amphibole and crocidolite asbestos induce gene expression changes in mice exposed long term. However, these changes are not as numerous at one year as they are at six months indicating that in order to use mice as a model of the fibrosis seen in humans, earlier exposure time points must be used. Also it is apparent that though LA induces fibrosis like crocidolite, it may do so in a different way as the gene alterations between the two groups differ. Further study is needed to determine the influence these differences have on fibrosis development, and to potentially identify candidate genes that may play a significant role in the disease process.

This project was supported by CCR822092 (CDC) and RR017670 (NCRR).

References

Amandus HE, Wheeler R. The morbidity and mortality of vermiculite miners and millers exposed to tremolite-actinolite. Part II: mortality. *Am. J. Ind. Med.* 11: 15-26. 1987.

American Cancer Society. Asbestos. Revised January 31, 2006. Accessed December 9, 2008.
http://www.cancer.org/docroot/PED/content/PED_1_3X_Asbestos.asp?sitearea=PED

American Thoracic Society. Diagnosis and initial management of nonmalignant diseases related to asbestos. Am. J. Respir. Crit. Care Med. 170: 691-715. 2004.

American Thoracic Society. Idiopathic Pulmonary Fibrosis: Diagnosis and Treatment. American Journal of Respiratory and Critical Care Medicine. 161: 646-664, 2000.

Antonini JM, Hemenway DR and Davis GS. Quantitative image analysis of lung connective tissue in murine silicosis. *Exp. Lung. Res.* 26: 71-88. 2000.

Asbestos Resource Center. 2003-2008 http://www.asbestosresource.com/. Accessed December 7, 2008.

Atkinson GR, Rose D, Thomas K, Jones D, Chatfield EJ, Going JE. Collection, analysis and characterization of vermiculite samples for fiber content and asbestos contamination. MRI report for EPA, project No. 4901-A32 under EPA contract 68-01-5915. 1982.

ATSDR. Health Consultation on Mortality from Asbestosis in Libby, Montana. Atlanta, GA: US Dept. of Health and Human Services. 2000.

Baldys A, Pande P, Moseih T, Park SH, Aust AE. Apoptosis induced by crocidolite asbestos in human lung epithelial cells involves inactivation of Akt and MAPK pathways. *Apoptosis* 12: 433-47. 2007.

Barker TH, Barneyx G, Cardo-Vila M, et al. SPARC regulates extracellular matrix organization through its modulation of integrin-linked kinase activity. *J. Biol. Chem.* 280: 36483-36493. 2005.

Berry G, Liddell FK. The interaction of asbestos and smoking in lung cancer: a modified measure of effect. *Ann. Occup. Hyg.* 48: 459-462. 2004.

Bienkowski RS and Gotkin MG. Control of collagen deposition in mammalian lung. *Proc. Soc. Exp. Biol. Med.* 209: 118-140. 1995

Blake DJ, Bolin CM, Cox DP, Cardozo-Pelaez F, Pfau JC. Internalization of Libby amphibole asbestos and induction of oxidative stress in muring macrophages. Toxicol. Sci. 99(1): 277-288, 2007.

Boffetta P. Epidemiology of environmental and occupational cancer. *Oncogene.* 23: 6392-6403. 2004.

Border WA, Noble NA. Transforming growth factor β in tissue fibrosis. *N. Engl. J. Med.* 331: 1286-1292. 1994.

Bornstein P. Diversity of function is inherent in matricellular proteins: an appraisal of thrombospondin 1. *J. Cell. Biol.* 130: 503-506. 1995.

Bornstein P, Sage EH. Matricellular proteins: extracellular modulators of cell function. *Curr. Opin. Cell. Biol.* 14: 608-616. 2002.

Brekken RA, Sage EH. SPARC, a matricellular protein: at the crossroads of cell-matrix communication. Matrix Biology. 19: 816-827. 2001.

Brown RFR, Drawbaugh RB, Marrs TC. An investigation of possible models for the production of progressive pulmonary fibrosis in the rat. The effects of repeated intratracheal instillation of bleomycin. Toxicology. 51: 101-110. 1988.

Centers for Disease Control and Prevention. Changing patterns of pneumoconiosis mortality – United States 1968-2000. *Morb. Mortal. Wkly. Rep.* 53: 627-632. 2004.

Coker RK, Laurent GJ. Anticytokine approaches in pulmonary fibrosis: brining factors into focus. *Thorax*. 52: 294-296. 1997.

Environmental Working Group. Asbestos: Think Again. 2004. Data compiled from the Centers for Disease Control and Prevention.

Francki A, McClure TD, Brekken RA, Motamed K, Murri C, Wang T, Sage EH. SPARC regulates TGF-beta1-dependent signaling in primary glomerular mesangial cells. *J. Cell. Biochem.* 91: 915-925. 2004.

Funk SE, Sage EH. Differential effects of SPARC and cationic SPARC peptides on DNA synthesis by endothelial cells and fibroblasts. *J. Cell. Physiol.* 154: 53-63. 1993.

Funk SE, Sage EH. SPARC modulates cell cycle progression in bovine aortic endothelial cells. *Proc. Natl. Acad. Sci.* 88: 2648-2652. 1991.

Geist, LJ, Powers LS, Monick MM, Hunninghake GW. Asbestos stimulation triggers differential cytokine release from human monocytes and alveolar macrophages. *Exp. Lung Res*. 26: 41-56. 2000.

Gunter ME, Dyar DM, Twamley B, Foit FF, and Cornelius S. Composition, Fe+3/Fe and crystal structure of non-abestiform and asestiform amphiboles from Libby, Montana, USA. *Am. Mineral.* 89:1579. 2003.

Hamilton RF, Holian A, Morandi M. A comparison of asbestos and urban particulate matter in the in vitro modification of human alveolar macrophage antigen-presenting cell function. *Exp. Lung Re.s* 30: 147-62. 2004.

Hasselaar P, Sage EH. SPARC antagonizes the effect of basic fibroblast growth factor on the migration of bovine aortic endothelial cells. *J. Cell. Biochem.* 49: 272-283. 1992.

Heldin CH, Miyazono K, Ten Dijke P. TGF-beta signaling from cell membrane to nucleus through SMAD proteins. *Nature.* 390: 465-471. 1997.

Hetherington LE, Brown TJ, Benham AJ, Bide T, Lusty PAJ, Hards VL, Hannis SD, Idoine NE. World Mineral Production 2002-2006. British Geological Survey. 2008

Hohenester E, Maurer P, Timpl R. Crystal structure of a pair of follistatin-like and EF-hand calcium-binding domains in BM-40. *EMBO J.* 16: 3778-3786. 1997.

Kamp DW, SA Weitzman SA. The molecular basis of asbestos induced lung injury. *Thorax*. 54: 638-52. 1999.

Kuhn C, Mason RJ. Immunolocalization of SPARC, tenascin, and thrombospondin in pulmonary fibrosis. *Am. J. Pathol.* 147: 1759-1769. 1995.

Kupprion C, Motamed K, Sage EH. SPARC (BM-40, osteonectin) inhibits the mitogenic effect of vascular endothelial growth factor on microvascular endothelial cells. *J. Biol. Chem.* 273: 29635-29640. 1998.

Lane TF, Sage EH. The biology of SPARC, a protein that modulates cell-matrix interactions. FASEB J. 8: 163-173. 1994.

Lane TF, Iruela-Arispeg ML, Sage EH. Regulation of gene expression by SPARC during angiogenesis in vitro. Changes in fibronectin, thrombospondin-1, and plasminogen activator inhibitor-1. *J. Biol. Chem.* 267: 16736-16745. 1992

Lane TF, Sage EH. Functional mapping of SPARC: peptides from two distinct Ca^{++}-binding sites modulate cell shape. *J. Cell. Biol.* 111: 3065-3076. 1990.

Latvala T, Puolakkainen P, Vesaluoma M, Tervo T. Distribution of SPARC protein (osteonectin) in normal and wounded feline cornea. *Exp. Eye Res.* 63: 579-584. 1996.

Laurent GJ, Chambers RC, Hill MR, McAnulty RJ. Regulation of matrix turnover: fibroblasts, forces, factors, and fibrosis. *Biochemical Society Transactions*. 35: 647-651. 2007.

Lazenby AJ, Crouch EC, McDonald JA, Kuhn C. Remodeling of the lung in bleomycin-induced pulmonary fibrosis in the rat. An immunohistochemical study of laminin, type IV collagen, and fibronectin. *Am. Rev. Respir. Dis.* 142: 206-214. 1990.

Liddell FD. The interaction of asbestos and smoking in lung cancer. *Ann. Occup. Hyg.* 45: 341-356. 2001.

Manning CB, Vallyathan V, Mossman BT. Diseases caused by asbestos: mechanisms of injury and disease development. *Int. Immunopharm.* 2: 191-200. 2002.

Mayo Foundation for Medical Education and Research (MFMER). www.mayoclinic.com/health/pulmonary-fibrosis/DS00927. March 14, 2007. Accessed December 8, 2008.

McDonald JC, Harris J, and Armstrong B. Mortality in a cohort of vermiculite miners exposed to fibrous amphibole in Libby, Montana. *Occupational and Environmental Medicine.* 61: 363-366. 2004.

McDonald JC, Harris J, and Armstrong B. Cohort study of mortality of vermiculite miners exposed to tremolite. *British J. Ind. Med.* 43: 436-444. 1986.

Meeker GP, Bern AM, Brownfield IK, Lowers HA, Sutley SJ, Hoefen TM, and Vance JS. The composition and morphology of amphiboles from the Rainy Creek complex, near Libby, Montana. *Am Mineral* 88:1955-1969. 2003

Meeker GP, Brownfield IK, Clark RN, Vance JS, Hoefen TM, Sutley SJ, and Gent CA. The Chemical Composition and Physical Properties of Amphibole from Libby, Montana: A Progress Report, Abstract, 2001 health Effects of Asbestos, Oakland, CA. 2001.

Mesothelioma & Asbestos Wellness Center. Crocidolite Asbestos. 2008. Accessed December 9, 2008. http://www.maacenter.org/asbestos/crocidolite.php.

Motamed K, Sage EH. SPARC inhibits endothelial cell adhesion but not proliferation through a tyrosine phosphorylation-dependent pathway. *J. Cell. Biochem.* 70: 543-552. 1998.

Murphy-Ullrich JE, Lightner VA, Aukhil I, et al. Focal adhesion integrity is downregulated by the alternatively spliced domain of human tenascin. *J. Cell. Biol.* 115: 1127-1136. 1991.

Nymark P, Lindholm PM, Korpela MV, Lahti L, Ruosaari S, Kaski S, Hollmen J, Anttila S, VL Kinnula and S Knuutila. Gene expression profiles in asbestos-exposed epithelial and mesothelial lung cell lines. *BMC Genomics.* 8: 62. 2007

Office of Inspector General Report. EPA's Actions Concerning Asbestos-Contaminated Vermiculite in Libby, Montana. 2001-S-7. March 31, 2007

O'Reilly KM, Mclaughlin AM, Beckett WS, Sime PJ. Asbestos-related lung disease. *Am. Fam. Physician.* 75: 683-688. 2007.

Pardo A, Gibson K, Cisneros J, Richards TJ, Yang Y, Becerril C, Yousem S, Herrera I, Ruiz V, Selman M, Kaminski N. Up-regulation and profibrotic role of osteopontin in human idiopathic pulmonary fibrosis. *PLoS Med.* 2: 251. 2005.

Pepper MS. Transforming growth factor-beta: Vasculogenesis, angiogenesis, and vessel wall integrity. *Cytokine Growth Factor Rev.* 8: 21-43. 1997.

Porter PL, Sage EH, Lane TF, et al. Distribution of SPARC in normal and neoplastic human tissue. *J. Histochem. Cytochem.* 43:791-800. 1995

Pulmonary Fibrosis Foundation. www.pulmonaryfibrosis.org/home.htm. Updated June 27, 2008. Accessed December 8, 2008.

Puolakkainen P, Reed M, Vento P. et al. Expression of SPARC (Secreted Protein, Acidic and Rich in Cysteine) in healing intestinal anastomoses and short bowel syndrome in rats. *Dig. Dis. Sci.* 44: 1554-1564. 1999.

Raines EW, Lane TF, Iruela-Arispe ML, et al. The extracellular glycoprotein SPARC interacts with platelet-derived growth factor (PGDF)-AB and –BB and inhibits the binding of PDGF to its receptors. *Proc. Natl. Acad. Sci. USA.* 89: 1281-1285. 1992.

Reed MJ, Sage EH. SPARC and the extracellular matrix: implications for cancer and wound repair. *Curr. Top. Microbiol. Immunol.* 213: 81-94. 1996.

Reed MJ, Vernon RB, Abrass IB, Sage EH. TGF-beta 1 induces the expression of type I collagen and SPARC, and enhances contraction of collagen gels, by fibroblasts from young and aged donors. *J. Cell. Physiol.* 158: 169-179. 1994.

Reed MJ, Puolakkainen P, Lane TF, et al. Differential expression of SPARC and Thrombospondin 1 in wound repair: immunolocalization and in situ hybridization. *J. Histochem. Cytochem.* 41: 1467-1477. 1993.

Rosenblatt S, Bassuk JA, Alpers CE, et al. Differential modulation of cell adhesion by interaction between adhesive and counter-adhesive proteins: characterization of the binding of vitronectin to osteonectin (BM40, SPARC). *Biochem. J.* 324: 311-319. 1997.

Sage EH, Vernon RB, Decker J, Funk S, Iruela-Arispe ML. Distribution of the calcium-binding protein SPARC in tissues of embryonic and adult mice. *J. Histochem. Cytochem.* 37: 819-829. 1989.

Sasaki T, Gohring W, Mann K. Limited cleavage of extracellular matrix protein BM-40 by matrix metalloproteinases increases its affinity for collagens. *J. Biol. Chem.* 272: 9237-9243. 1997.

Savani RC, Zhou Z, Arguiri E, Wang S, Vu D, Howe CC, DeLisser HM. Bleomycin-induced pulmonary injury in mice deficient in SPARC. *Am. J. Physiol. Lung Cell. Mol. Physiol.* 279: 743-750. 2000.

Schiemann BJ, Neil JR, Schiemann WP. SPARC inhibits epithelial cell proliferation in part through stimulation of the transforming growth factor-beta-signaling system. *Mol. Biol. Cell.* 14: 3977-3988. 2003.

Schrier DJ, Kunkel RG, Phan SH. The role of strain variation in murine bleomycin-induced pulmonary fibrosis. *Am. Rev. Respir. Dis.* 127: 63-66. 1983.

Shukla A, Ramos-Nino M, and Mossman BT. Cell signaling and transcription factor activation by asbestos in lung injury and disease. *Intl. J. Biochem. Cell. Biol.* 35: 1198-1209. 2003.

Snider GL, Celli BR, Goldstein RH, O'Brien JJ, Lucey EC. Chronic interstitial pulmonary fibrosis produced in hamsters by endotracheal bleomycin. Lung volumes, volume pressure relations, carbon monoxide uptake, and arterial blood gas studied. *Am. Rev. Respir. Dis.* 117: 289-297. 1978.

Starcher BC, Kuhn C, Overton JE. Increased elastin and collagen content in the lungs of hamsters receiving an intratracheal injection of bleomycin. *Am. Rev. Respir. Dis.* 117: 299-305. 1978.

Strandjord TP, Madtes DK, Weiss DJ, Sage EH. Collagen accumulation is decreased in SPARC-null mice with bleomycin-induced pulmonary fibrosis. *Am. J. Physiol. Lung Cell. Mol. Physiol.* 277: 628-635. 1999.

Sullivan PA. Vermiculite, respiratory disease, and asbestos exposure in Libby, Montana: update of a cohort mortality study. *Environ. Health. Perspect.* 115: 579-85. 2007.

Swiderski RE, Dencoff JE, Floerchinger CS, Shapiro SD, Hunninghake GW. Differential expression of extracellular matrix remodeling genes in a murine model of bleomycin-induced pulmonary fibrosis. *Am. J. Pathol.* 152: 821-828. 1998.

Tremble PM, Lane TF, Sage EH, Werb Z. SPARC, a secreted protein associated with morphogenesis and tissue remodeling, induces expression of metalloproteinases in fibroblasts through a novel extracellular matrix-dependent pathway. *J. Cell. Biol.* 121: 1433-1444. 1993.

Taylor MD, Roberts JR, Hubbs AF, Reasor MJ, Antonini JM. Quantitative image analysis of drug-induced lung fibrosis using laser scanning confocal microscopy. *Tox. Sci.* 67: 295-302. 2002.

U.S. Department of Health and Human Services, Division of Respiratory Disease Studies, Public Health Service, Centers for Disease Control and Prevention. Work-Related Lung Disease Surveillance Report 2002. NIOSH number 2003-111. May 2003.

U.S. Environmental Protection Agency. Asbestos. Updated 2008. Accessed December 7, 2008. http://www.epa.gov/oppt/asbestos/index.html.

U.S. Environmental Protection Agency. Region 8: Libby Asbestos. Updated 2008. Accessed December 7, 2008. http://www.epa.gov/region8/superfund/libby/.

U.S. Environmental Protection Agency Asbestos Materials Bans: Clarification, May 18, 1999

Van Loon AJ, Kant IJ, Swaen GM, Goldbohm RA, Kremer AM, Van Den Brandt PA. Occupational exposure to carcinogens and risk of lung cancer: results from the Netherlands cohort study. *Occup. Environ. Med.* 54: 817-824. 1997.

Wang X, Samet JM, Ghio AJ. Asbestos-induced activation of cell signaling pathways in human bronchial epithelial cells. *Exp. Lung Res.* 32: 229-43. 2006.

Webber JS, Blake DJ, Ward TJ, Pfau JC. Separation and characterization of respirable amphibole fibers from Libby, Montana. *Inhalation Toxicology.* 20: 733-740. 2008.

West JB. Chapter 5 Restrictive Diseases: Pathology. Pulmonary Pathophysiology: The Essentials. Seventh Edition. Published by Lippincott Williams & Wilkins, 2007.

Wisconsin Department of Natural Resources. Asbestos: History and Uses. http://dnr.wi.gov/air/compenf/asbestos/asbes3.htm. Revised August 31, 2007. Accessed December 9, 2008.

Wu RX, Laser M, Han H, et al. Fibroblast migration after myocardial infarction is regulated by transient SPARC expression. *J. Mol. Med.* 84: 241-252. 2006.

Wylie AG, Verkouteren JR. Amphibole asbestos from Libby, Montana, aspects of nomenclature. *Am. Mineral.* 85: 1540-1542. 2000.

Zalac F. Deadly Dust. CBC News. February 7, 2003. Updated March 2005

CHAPTER ONE

Collagen Accumulation After Short-Term Exposure to Crocidolite Asbestos or Libby Amphibole

This study is in press: Smartt AM, Brezinski M, Trapkus M, Gardner D, Putnam EA. Collagen accumulation over time in the murine lung after exposure to crocidolite asbestos or Libby amphibole. *Environmental Toxicology.* 2009.

Abstract

Libby, MT is the site of a closed vermiculite mine that produced ore contaminated with asbestos-like amphiboles. Worldwide distribution of the material and the long latency period for manifestation of asbestos-related diseases (ARDs) has created a significant health threat for many years to come. The composition of the Libby material (termed the Libby amphibole, LA) differs from other well-studied types of asbestos in that it is a mixture of several amphibole fibers. The purpose of this study was to determine the fibrotic effects of LA exposure in a mouse model and to compare these effects to those of a well-characterized amphibole fiber, crocidolite asbestos. We exposed C57Bl/6 mice to LA or crocidolite and analyzed lung RNA, protein, and morphology at one week, one month, and three months post instillation. Our results indicate that both forms of amphibole studied induced increased collagen types I and III mRNA expression and collagen protein deposition in exposed murine lungs compared to the PBS-instilled control lungs. These collagen increases were the most significant at one month after exposure. Overall, crocidolite exposed mice demonstrated greater increases

in collagen deposition than those exposed to LA, indicating that the fibrotic effects of LA exposure, although not as severe as those of crocidolite in this model system, were still able to induce collagen deposition.

Introduction

Vermiculite ore, a hydrated laminar magnesium-aluminum-iron silicate, expands to between 10 and 20 times its original size when heated and has several useful commercial applications including those in construction, industrial, and agricultural products (U.S. EPA, 2008; Moatamed, 1986). Libby, Montana was the site of a vermiculite mining operation from 1920 to 1990, and may have produced as much as 80% of the world's supply. This vermiculite was later found to contain 21-26% asbestos, explaining both occupational and environmental asbestos exposures in the Libby community (Wake, 1962; Wright, 2002). The Libby mine was closed in 1990 and the last ore was shipped to processing plants in 1993, but asbestos-related health problems continue to develop for exposed workers and their families. This is primarily due to the fact that asbestos related diseases (ARD) have a long latency period of 15-40 years, which indicates that many more people will continue to develop ARD in the future.

Asbestos fibers are divided into two distinct groups consisting of either straight amphibole fibers consisting of double-chain silicates or curved serpentine fibers consisting of thin-walled sheet silicates. Libby amphibole (LA) is a combination of amphibole fibers and cleavage fragments that include tremolite, actinolite, soda tremolite, richterite, and winchite amphiboles (Meeker, 2001). Exposure to LA is associated with several ARD including asbestosis, lung cancer, mesothelioma, and

pleural plaques (McDonald, 1986; Amandus, 1987a; Amandus, 1987b). In 1999 the Agency for Toxic Substance Disease Registry (ATSDR) and the Environmental Protection Agency (EPA) conducted studies on respiratory disease in Libby residents and found a 20% to 40% increase in malignant and nonmalignant respiratory deaths. In particular, the asbestosis mortality rate was 40 to 60 times greater than the national average (ATSDR, 2000).

Asbestosis can be defined as bilateral diffuse interstitial fibrosis of the lungs caused by the inhalation of asbestos fibers (American Thoracic Society, 1986; Craighead, 1982). The pathogenesis of asbestosis begins with the characteristic of amphibole fibers like those contained in LA to penetrate deep into the lungs where they become lodged in the alveoli (Brody, 1981; Brody, 1983). Here the fibers cause the initiation of a chronic inflammatory reaction as the local immune system attempts to eradicate the foreign matter (Chang, 1988). Specifically, macrophages are stimulated to ingest the fibers and fibroblasts lay down connective tissue to wall off the fibers respectively. Eventually the macrophages begin to die as they become subject to the natural resistance asbestos has to phagocytosis. As this occurs, cytokines are released by the immune system to attract additional macrophages and fibroblasts to further deposit fibrous tissue eventually resulting in the creation of a fibrous mass surrounding the asbestos fibers (Cutroneo, 2003; Chapman, 2004).

The deposition of fibrous tissue is a typical response to lung injury. Animals suffering from bleomycin-induced pulmonary fibrosis endure a characteristic sequence of inflammatory cell migration, edema, cellular proliferation, and accumulation of collagen, as occurs in human lungs after similar exposure (Brown, 1988; Lazenby, 1990). Following the exposure, the lung will undergo remodeling of the extracellular matrix.

Studies show that several changes then occur, in particular there are increases in the steady-state levels of type I and III procollagen mRNA (Hoyt, 1988; Swiderski, 1998). Whether a similar process occurs in a model of pulmonary fibrosis induced by Libby amphibole has yet to be examined.

Due to its unique composition, the amphibole contained in the Libby vermiculite may have characteristics that make its overall health effects different than that of other asbestos fibers. Using a mouse model, the purpose of this investigation was to examine the fibrotic effects of LA in the lung compared to the effects of crocidolite, a well-characterized asbestos fiber, and to examine these effects over time. Many individuals in the Libby area currently suffer from asbestosis, and the exact mechanism leading to progression of the disease has yet to be determined. This study may help to answer some of the questions regarding this unknown mechanism by bringing to light some of the similarities and differences between LA and crocidolite asbestos. For instance, the similarities between the lungs response to either LA or crocidolite can be compared to the similarities between the two fiber types. This would identify some of the mechanisms involved in the response to LA by referring to some of the known mechanisms involved in the response to crocidolite based on fiber properties.

Materials and Methods

Asbestos. A sample of the Libby amphibole was generously provided by the U.S. Geological Survey. The amphibole used is a chemical representation from six locations at the mine and has been characterized in detail (Wylie, 2000; Gunter, 2003; Meeker, 2003). This amphibole sample also has a particle size distribution matching air sample

size distribution data (Meeker, 2003). Crocidolite asbestos was obtained from the Research Triangle Institute (Research Triangle Park, NC). The fiber size distribution of both Libby amphibole and crocidolite asbestos has been previously reported (Blake, 2007). For reference, size parameters of the Libby amphibole sample were 0.61 μm in diameter, 7.21 μm in length, with 22.52 for the aspect ratio. Size parameters of the crocidolite were 0.16 μm in diameter and 4.59 μm in length, with a 34.05 aspect ratio. Samples were freshly prepared in sterile phosphate-buffered saline (PBS, pH 7.4) and sonicated before instillation (Putnam, 2008).

Mouse Treatment. All animal protocols were approved by the Institutional Animal Care and Use Committee. Mice were exposed to amphiboles according to methods previously described (Adamson, 1987). Briefly, pathogen-free 6-8 week old female and male C57Bl/6 mice were instilled intratracheally with 100 μg of crocidolite asbestos or Libby amphibole in 30μl sterile PBS while under anesthesia. Control mice received only sterile PBS. Mice were euthanized 1 week, 1 month, or 3 months after instillation. Treated mice were then divided into two groups. The left lung of the mice in the first group was removed for RNA isolation, while the right lung was perfused and immersed in Histochoice (Amresco, Solon, OH) before being embedded in paraffin. The caudal aspect of the left lung of the mice in the second group was removed, rinsed in PBS and collagen content quantified by hydroxyproline analysis. The remaining lung tissue was snap frozen in liquid nitrogen until protein could be isolated. Eight to ten mice were included in each treatment group.

Histology. Fixed lungs were embedded in paraffin and processed into 7μm sections. Routine Gomori's trichrome staining was performed in order to visualize fibrillar collagen localization in the lung, and the sections examined under light microscopy.

Inflammation Scoring. Scoring was performed by a board certified veterinary pathologist, Donald Gardner at Rocky Mountain Laboratories, MT. 3 to 6 mice from each treatment group/time point were scored through the analysis of at least 9 sections per mouse. Scores were determined by general appearance and the amount of infiltrating lymphocytes as seen by hematoxylin and eosin staining. Scores of mouse sections were averaged with numerical values representing the following stages of inflammation: 0 = absent, 1 = minimal, 2 = mild, 3 = moderate, and 4 = severe.

RNA Isolation and Quantitative RT-PCR. Lung tissue was homogenized in 1 ml of TRIZOL and RNA isolated following the manufacturer's protocol (Invitrogen, Carlsbad CA). The resulting RNA was purified using the RNeasy kit (Qiagen, Valencia, CA) and subsequently treated with DNAse (Qiagen). For qRT-PCR, initially first strand synthesis of cDNA was accomplished using a First-Strand Synthesis kit (Invitrogen, Carlsbad, CA). Target cDNA was subsequently amplified using predesigned TaqMan probes (ABI, Foster City, CA) for Collagen 1A1, Collagen 1A2 and Collagen 3A1, as well as probes to detect both GAPDH and β-Actin transcripts as controls. qPCR was performed on an iQ5 Optical System (Bio-Rad, Hercules, CA).

Hydroxyproline Assay. Quantitation of lung collagen content from exposed and control mice was determined by an assay for hydroxyproline content according to methods

previously described (Woessner, 1961) with some modifications. Lung tissue was rinsed in PBS, minced and hydrolyzed in 1.5 ml of 6N HCl overnight at 110°C. To 5 µl of the hydrolysate were added 10 µl of 0.02% methyl red and 2 µl of 0.04% bromothymol blue. The sample volume was adjusted to 200 µl with assay buffer (0.024 M Citric Acid, 0.02 M Glacial Acetic Acid, 0.088 M Sodium Acetate, and 0.085 M NaOH). The colorimetric assay was performed by the addition of 100 µl of chloramine T solution and incubation at room temperature for 20 minutes. Following incubation, 100 µl of dimethyl benzaldehyde solution was added and the solution incubated in a 60°C water bath for 15 minutes. Absorbance was measured at 550 nM for each lung sample in a 96-well plate and quantitation of hydroxyproline was determined by comparison to a standard curve.

Statistical Analysis. Mean values for the hydroxyproline assay were compared by one-way ANOVA with Newman-Keuls test for multiple comparisons. Results are presented as mean values ± SEM. Results from Real-time PCR on triplicate pools of RNA for each treatment group were normalized to both Gapdh and β-actin and statistically analyzed with a two-tailed *t*-test on the treatment means. Results are presented as mean fold difference ± SEM versus PBS. Inflammation scores were first averaged for each mouse, then treatment groups analyzed by one-way ANOVA with a Bonferroni test for multiple comparisons. In all cases, significant results were determined by $p < 0.05$.

Results

C57Bl/6 mice, a strain sensitive to induced fibrosis, were exposed to crocidolite asbestos (CRO), Libby amphibole (LA), or sterile phosphate buffered saline (PBS) as a

vehicle control by intratracheal instillation. One week, one month, and three months after instillation, the mice were sacrificed and lungs removed for analysis.

Histological examination revealed that collagen deposition around the airways was increased in the crocidolite treated animals (collagen appears blue-green in Gomori Trichrome-stained sections, indicated by the arrows, Figure 8B, 8E, and 8H), which represented the typical pattern of fibrosis seen in animals exposed to this amphibole. By three months post instillation, the presence of multi-nucleated giant cells and macrophages became apparent in crocidolite-exposed animals (Figure 8H), a further indication of the chronic inflammation and fibrosis. The histologic effects seen in LA treated mice were similar to those seen in crocidolite treated mice, though these effects appeared less severe at all time points examined (Figure 8C, 8F, and 8I). No major differences among the three time points were seen in the PBS treatment group (Figure 8A, 8D, and 8G). Morphology of the airways appeared normal and the alveolar architecture was not disordered. In addition, no changes at the pleura of the lungs indicative of potential mesothelioma were detected, although that would be unexpected at such short time frames.

Figure 8: Wild-Type Lung Histology

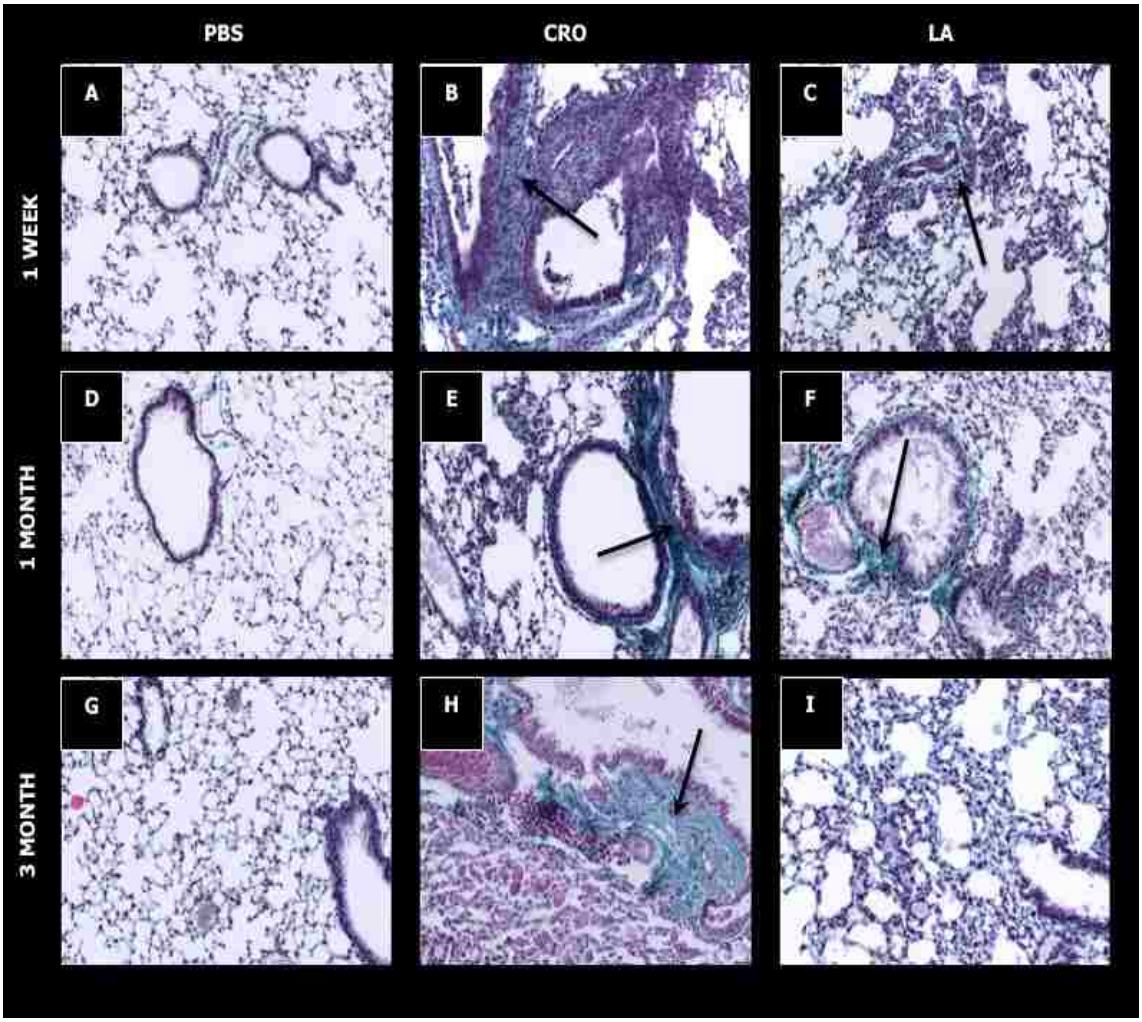

Figure 8 Legend: Histopathology of lungs from C57Bl/6 mice exposed to PBS, CRO, or LA (Magnification 200X). Mice were intratracheally instilled for 1 week (A-C), 1 month (D-F), or 3 months (G-I) and lung sections were stained with Gomori's trichrome stain to identify the distribution of collagen. Collagen containing areas appear blue-green. The lungs of control mice exposed to PBS (A, D, and G) have a much lower level of collagen deposition than the lungs of either the CRO exposed mice (B, E, and H) or LA exposed mice (C, F, and I). Arrows are used to identify examples of fiber accumulation.

Lung sections were also scored for inflammation to determine the severity of disease (Table 2). On average, crocidolite exposed mice presented minimal inflammation at one week (score of 1.2) and a progressive worsening of the response to mild inflammation by three months (score of 1.8). Mice treated with LA, while scored as demonstrating minimal inflammation at the one week time point (score of 0.9), were evaluated as slightly less involved than the crocidolite exposed animals. The disease process in the LA exposed group was maintained at one month after instillation with a score of 0.7 and did not appear to worsen over time, as inflammation in the lungs appeared to be resolving over time with a final 3 month score of 0.4. These data indicated that, as expected, the lungs of mice exposed to either crocidolite or LA demonstrated inflammatory response after only one week. Statistical analysis demonstrated a significant increase in inflammation for the crocidolite treated mice compared to the PBS treated controls at the one month time point only. Control mice instilled with PBS demonstrated minimal to no inflammation at all time points (scores of 0.0 to 0.1). It is apparent from the histological sections that asbestos exposure increases inflammation in both crocidolite and LA treated animals.

Table 2: Inflammation Scoring of Wild-Type Lung Tissue

TIME POINT	TREATMENT	INFLAMMATION SCORE[1]	NUMBER OF MICE	NUMBER OF SECTIONS
1 Week	PBS	0.0	4	48
1 Week	CRO	1.2	6	60
1 Week	LA	0.9	5	81
1 Month	PBS	0.1	4	36
1 Month	CRO	1.8*	5	39
1 Month	LA	0.7	4	36
3 Month	PBS	0.0	3	27
3 Month	CRO	1.8	3	27
3 Month	LA	0.4	3	27

[1]Inflammation scoring values are as follows: 0.0 = absent, 1.0 = minimal, 2.0 = mild, 3.0 = moderate, and 4.0 = severe; * = $p < 0.05$

Collagen accumulation and scar tissue production have been shown to play a significant role in the development of fibrosis, therefore, quantitative RT-PCR was utilized to determine gene expression changes of the type I collagen genes, Col1A1 and Col1A2, in response to asbestos exposure (Figure 9). One week after instillation the expression of Col1A1 mRNA in the lungs of both crocidolite asbestos and LA exposed mice was increased compared to PBS-exposed control mice (Figure 9A). Only LA treated mice demonstrated increased expression of Col1A2 at this time point (Figure 9B). One month after instillation both Col1A1 and Col1A2 expression in lungs from crocidolite asbestos and LA treated mice were increased over that seen in PBS treated mice, but in both exposures only Col1A1 expression was significantly increased (Figure 9A and 9B). At the three month post-instillation time point, the expression levels of the type I collagen genes in mRNA from the crocidolite asbestos and LA treated mice were not different from expression levels of the PBS treated group (Figure 9A and 9B). These analyses demonstrated that after exposure to crocidolite asbestos and LA, type I collagen mRNA synthesis initially increased but returned to baseline levels over time.

To further demonstrate the idea of a return to baseline collagen levels, analyses were performed on the differential expressions of each gene over time (Figure 9, upper significance bars). In terms of type I collagen, I found that there is significantly less type IA1 collagen mRNA at one month and three months post exposure compared to one week for both amphibole treatment groups. I also found there to be a significant decrease in type IA2 collagen mRNA over time in the Libby amphibole treatment group. This demonstrates that the synthesis of type I collagen mRNA in response to asbestos in mice is immediate and begins to fade over time.

I also examined changes in gene expression of type III collagen (Figure 9C). The qRT-PCR results indicated that there was a significant increase in the expression of Col3A1 mRNA at one month post instillation in the LA treated mice and also an increase, though not significant, at this time point in Col3A1 mRNA from the crocidolite treated mice. By three months post instillation, Col3A1 mRNA levels were still elevated in the treatment groups but the increase was no longer significant for the LA treated mice. Similar to the type 1 collagen gene mRNA expression profile, the expression of type III collagen gene mRNA peaked at the one month time point after amphibole instillation, followed by a return to baseline levels.

Figure 9: Wild-Type Collagen qRT-PCR

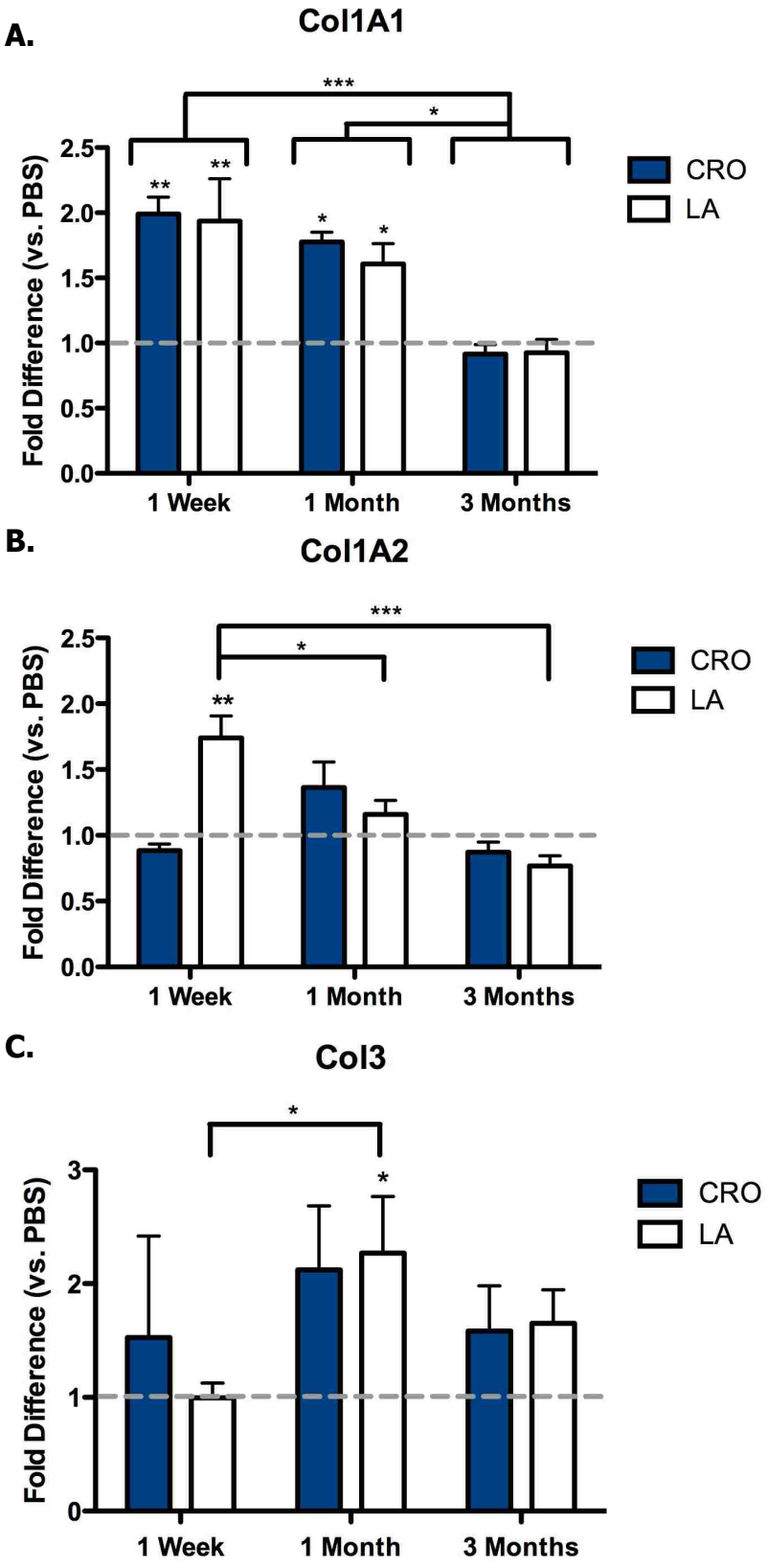

Figure 9 Legend: Real-Time PCR of pro-collagen types 1A1, 1A2 and 3 mRNA from the lungs of C57Bl/6 mice exposed to PBS, CRO, or LA. RNA was isolated from the lungs of replicate animals intratracheally 1 week, 1 month, or 3 months after instillation and the fold difference of lung pro-collagen 1A1 mRNA (A), pro-collagen 1A2 (B), and pro-collagen type 3 (C) between the asbestos treated mice and the PBS controls was determined. Each experiment was repeated three times. Results on triplicate pools of RNA for each treatment group (n = 10 – 12 per group) were normalized to both Gapdh and β-actin and are presented as mean fold difference ± SEM. Both the CRO and LA treatment groups have an increased amount of pro- collagen 1A1 mRNA over PBS at 1 week and 1 month. The LA treatment group also has significantly more pro-collagen 1A2 mRNA than the PBS group at 1 week. Both the CRO and LA treatment groups had higher levels of pro-collagen type 3 at 1 month and 3 month than the PBS group though the increase was only significant at 1 month. When looking at changes over time, both LA and CRO have significantly more Col1A1 mRNA at one week than at one or three months post exposure. LA also has significantly more Col1A2 mRNA at one week than at one and three months and more Col3 mRNA at one month than at one week. (* = $p < 0.05$, ** = $p < 0.01$, *** = $p < 0.001$)

Because of the pattern of changes in collagen mRNA expression compared to the histologic changes over the time course studied, it was important to examine the relationship between type I and III collagen gene expression changes and resultant collagen protein levels. Therefore, total collagen content was determined by measuring the hydroxyproline content in the caudal aspect of the left lung (Figure 10). One week after instillation, hydroxyproline levels in lungs of both the crocidolite and LA treated mice were significantly increased over levels seen in the lungs of PBS treated mice (Figure 10A). This increase in hydroxyproline content was also detected at one month post-instillation for lungs from the amphibole treated mice compared to the PBS treated control mice (Figure 10B). However, by three months post-instillation, the level of hydroxyproline in the crocidolite treated mice remained significantly higher than that of the PBS treated mice (Figure 10C), while the hydroxyproline level in the LA treated mice, though elevated, was not significantly different from the PBS treated mice. There were no significant differences in hydroxyproline content in each treatment group over time. The increase in collagen protein levels in the treatment groups correlated with the initial increase seen in type I collagen mRNA production. However, the persistence and accumulation of collagen protein production was independent of mRNA expression levels in crocidolite treated mice, while collagen deposition in LA treated mouse lungs did not persist. These results indicated that the fibrotic response of the murine lung to LA was different from the response to crocidolite.

Figure 10: Wild-Type Hydroxyproline Assay

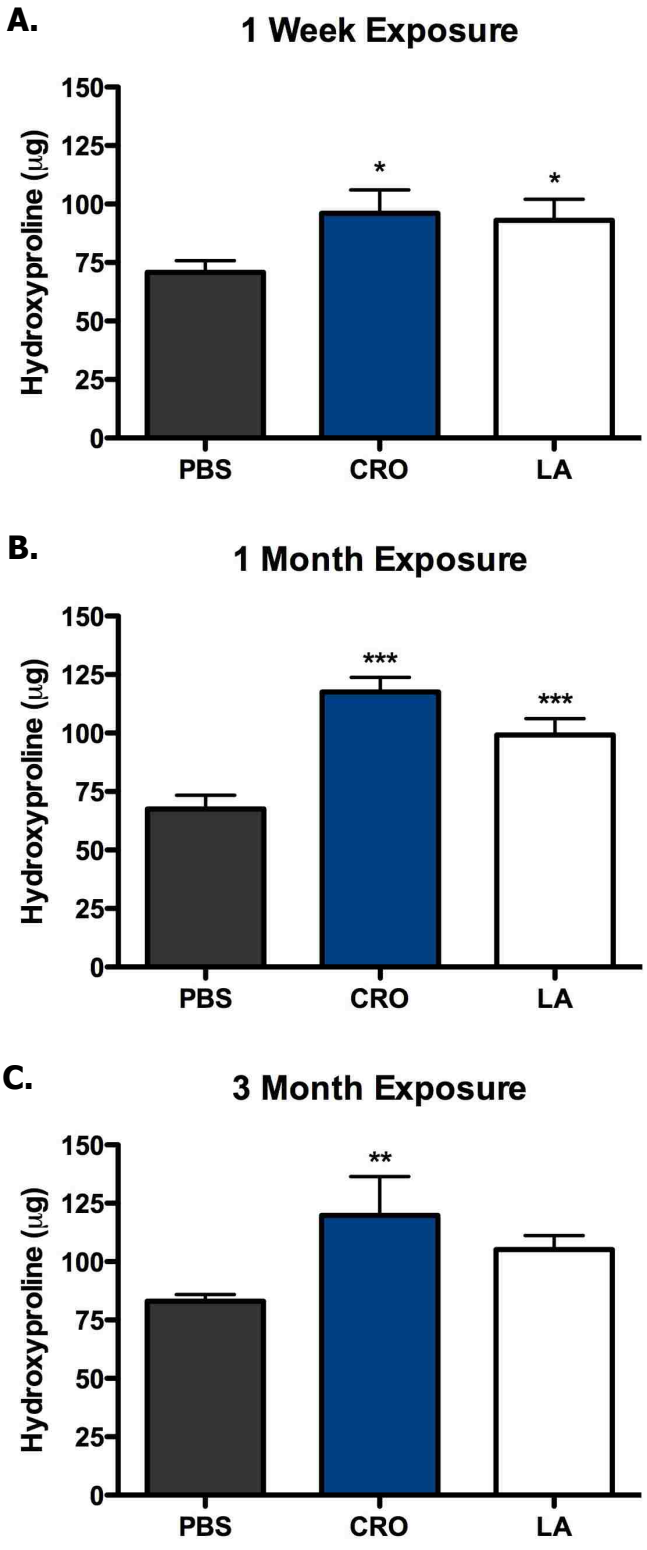

Figure 10 Legend: Total hydroxyproline content from the lungs of C57Bl/6 mice exposed to PBS, CRO, or LA. Mice were intratracheally instilled for 1 week (A), 1 month (B), or 3 months (C) and collagen content of the left lung was determined by measuring hydroxyproline levels in replicate animals. All experiments were done in triplicate. Mean values for the hydroxyproline assay were compared by one-way ANOVA with Newman-Keuls test for multiple comparisons. Results are presented as mean values ± SEM for each treatment/time (all groups have n = 10 except the 3 month CRO exposed mice with n = 8). The CRO and LA exposed mice had significantly more lung collagen than the PBS control (* = $p<0.05$, ** = $p<0.01$, *** = $p<0.001$). There were no significant differences in any individual exposure type over time.

Discussion

Investigations into asbestos toxicity have been carried out previously on well-characterized amphiboles such as crocidolite, yet in spite of the increase in knowledge, gaps still exist. Recent studies have suggested a variety of mechanisms by which asbestos may induce ill health effects including the chemical and structural properties of the fibers, lung fiber burden, fiber uptake by epithelial cells, iron-catalyzed free radicals, DNA damage, cytokine release, growth factor release, generation of reactive oxygen species, and synergy with tobacco smoke exposure (Kamp, 1999; Manning, 2002). The purpose of this investigation was to compare the effects of LA to those of crocidolite in order to both determine the differences between the lungs response to either amphibole and begin to delineate the mechanism of LA toxicity in terms of fibrotic disease.

The effects of crocidolite asbestos have been studied for many years, however investigations into the physiological effects of LA are still relatively new (Hamilton, 2004; Baldys, 2007; Blake, 2007; Putnam, 2008). The description of the asbestosis found in Libby miners and residents has been consistently different than that of patients exposed to other amphiboles (Peipens, 2003; Sullivan, 2007). It has been previously suggested that these differences could be due to the mixed fiber composition of LA, which is different from other types of more extensively studied amphiboles. I used exposure to crocidolite asbestos as a well-characterized positive control fiber for comparison in these studies, and have demonstrated response differences in both inflammation and collagen accumulation after exposure to crocidolite or LA. The studies presented here showed that disease progression differed between the two treatment groups with the crocidolite exposed group developing more inflammation over time while inflammation in the LA

exposed animals progressively lessened from one week to three months. Additional differences between the groups included an increase in collagen accumulation in mice exposed to crocidolite compared to those exposed to LA as demonstrated histologically by Trichrome staining and quantitatively by hydroxyproline analysis. Mice exposed to LA exhibited slightly less collagen deposition than crocidolite, though this difference was not significant. These results are not unexpected, and are probably related to the chemical characteristics of LA compared to crocidolite. As described by both Meeker et al. (2003) and Blake et al. (2007), the LA used here was comprised of mixed samples from multiple sources at the Libby mine. The majority of the amphiboles were in the winchite-richterite series, with minor components represented by tremolite as approximately 6% of the respirable fraction. Winchite and richterite have not previously been assessed for the fibrotic endpoints used in the present study, however, examination of richterite in immunologic studies using human macrophage cultures have found this amphibole to have a lesser effect compared to crocidolite as a control fiber (Collan, 1986). Tremolite asbestos studies in rats have demonstrated pulmonary fibrosis development in the time frame studied here (Bernstein, 2005). The small proportion of tremolite asbestos in LA may explain the reduced fibrosis seen with LA exposure in our mice, thus, our results are consistent with previously published investigations. As mentioned above, these differences may also be responsible for the differences in the disease process that develops between individuals exposed to LA and those exposed to crocidolite asbestos.

Initial visualization of mouse lungs after crocidolite exposure via histology indicated that noticeable quantities of collagen were associated with increased cellularity around the alveoli; more so than what was usually seen deposited for structural support.

Morphologically, the increase in cellularity consisted of both fibroblasts and macrophages, key members of the initial immune response to the foreign fibers (Chang, 1988). These cell types are known to express pro-inflammatory cytokines responsible for increasing TGF-β expression and thus type I collagen expression (Cutroneo, 2003). Areas of lung exposed to LA also showed an increase in both collagen deposition and cellularity, however to a lesser degree than the collagen levels seen in the lungs of mice exposed to crocidolite. The time points examined were also used to establish a course of disease progression. We found that the initial response evaluated at one week consisted mainly of mixed cellular inflammation. By one month, fibrosis had become apparent with an even greater amount of collagen deposition. At three months, chronic inflammation was visualized by the increased presence of multi-nucleated giant cells and activated macrophages as well as continued collagen deposition, similar to what is seen in human fibrotic diseases (Chapman, 2004). To verify these visual findings the levels of both collagen mRNAs and protein were further evaluated.

Quantification of collagen mRNA confirmed the increased collagen levels seen in the trichrome stained lung sections at the early time points. In particular, the levels of collagen1A1 mRNA were increased to a similar extent for both the crocidolite and LA exposed mice. However, levels of collagen1A2 mRNA were higher in the LA treated mice than mRNA levels in the crocidolite treated animals at the one week time point. This may be an indication that the initial response to LA versus crocidolite differed in the stimulation of collagen1A2. Transcription of both type I collagen genes is coordinately regulated, and there is a 2:1 ratio of pro-mRNA for Col1A1 to Col1A2 transcripts, reflecting the 2:1 ratio of the peptides in the mature collagen fibril (Ghosh, 2002; Cutroneo, 2003). However, this coordination is achieved through different TGF-β

signaling pathways for the collagen 1A1 and collagen1A2 genes. Thus, the differential effects seen on transcript levels of the collagen 1A2 gene after exposure to LA may be due to specific pathway activation. It is important to note that by the three month time point expression of neither collagen mRNA was increased over PBS treatment, even though collagen was still visualized histochemically and quantitated by hydroxyproline assay. This may have been due to regulation by cytokines (Cutroneo, 2003) or it could be due to a decreased activity of collagen proteases as the level of hydroxyproline appears to be constant from one month to three months. Therefore existing levels of collagen remain constant with minimal degradation or synthesis.

The hydroxyproline assay was used as a measure of collagen protein expression. This assay further confirmed the increased levels of collagen by demonstrating an increase in hydroxyproline in lungs of amphibole-exposed mice. Mice exposed to crocidolite had elevated levels of collagen compared to mice exposed LA, again being an indication that LA sample used was less effective in inducing fibrosis as crocidolite as previously discussed. The amount of collagen accumulated continued to increase at the one month time point and remained at a steady level at the three month time point. The lack of continued collagen deposition could be due to achievement of steady state collagen levels through remodeling, as has been demonstrated in a bleomycin model of fibrosis (Swiderski, 1998).

Previous investigations have demonstrated gene expression changes after a six month exposure to crocidolite and LA, as well as an increase in collagen deposition (Putnam, 2008; Introduction). For this study, I have used earlier time points to delineate the progression of fibrotic indicators after intratracheal instillation of LA as compared to crocidolite, a fiber extensively studied in mouse models. I have

demonstrated that both fibers are capable of inducing fibrosis as measured histologically and by increased hydroxyproline content of the exposed lungs. The fibrotic reaction induced by LA does not reach the level induced by crocidolite within the same time course, an expected outcome considering the mixed mineral composition of LA. A difference between human asbestosis in individuals from Libby, MT and the endpoints observed in our study is that pleural disease is predominant in individuals exposed to LA, whereas the mice in this study did not demonstrate observable pleural changes (Peipins, 2003). This could have been due to differences in the route or duration of exposure as well as the latent period since exposure. Thus, although the murine model may be an imperfect representation of the human disease, it is possible that this model can be used to determine some of the differences between LA and other forms of asbestos as well as to allow study of the time course of disease progression. This investigation has begun to point out some of the differences between LA and crocidolite asbestos, but further study needs to be conducted to determine the actual mechanistic differences between the two.

Conclusion

In order to study the fibrotic process using mice, short-term exposures must be used, as mice appear to heal over time whereas humans do not. It is important to mimic the human disease as much as possible to ensure that any results found may be applicable to human pulmonary fibrosis. Results of this short-term study indicated that both the inflammatory process and collagen accumulation play the largest roles in fibrosis development. Therefore it may be important to look into those genes that

influence these processes. Looking back at the long-term microarray study, we focused on those extracellular matrix genes whose expression was altered, as they are potential candidate genes for further study. We found that *Sparc*, a gene previously found to play a role in bleomycin-induced fibrosis, was upregulated 2.686 fold in crocidolite-exposed mice and 3.672 fold in Libby amphibole exposed animals. Based on its upregulation after asbestos exposure as well as its implicated involvement in fibrosis development, we chose to look further into the role of SPARC in the development of fibrosis.

References

Adamson IY, Bowden DH. Response of mouse lung to crocidolite asbestos. 2. Pulmonary fibrosis after long fibres. *J. Pathol.* 152, 109-117. 1987.

Agency for Toxic Substances and Disease Registry (ATSDR). Health consultation: mortality from asbestosis in Libby, Montana, 1979-1998. ATSDR December 12, 2000.

Amandus HE, Wheeler R, Jankovic J, Tucker J. The morbidity and mortality of vermiculite miners and millers exposed to tremolite-actinolite. Part I: exposure estimates. *Am. J. Ind. Med.* 11: 1-14. 1987a.

Amandus HE, Wheeler R. The morbidity and mortality of vermiculite miners and millers exposed to tremolite-actinolite. Part II: mortality. *Am. J. Ind. Med.* 11: 15-26. 1987b.

American Thoracic Society. Diagnosis of nonmalignant diseases related to asbestos. *Am. Rev. Respir. Dis.* 134: 363-8. 1986.

Baldys A, Pande P, Mosleh T, Park SH, Aust AE. Apoptosis induced by crocidolite asbestos in human lung epithelial cells involves inactivation of Akt and MAPK pathways. *Apoptosis.* 12: 433-47. 2007.

Bernstein DM, Chevalier J, Smith P. Comparison of Calidria chrysotile asbestos to pure tremolite: final results of the inhalation biopersistence and histopathology examination following short-term exposure. *Inhal. Toxicol.* 17: 427-449. 2005.

Blake DJ, Bolin CM, Cox DP, Cardozo-Pelaez F, Pfau JC. Internalization of Libby amphibole asbestos and induction of oxidative stress in murine macrophages. *Toxicol. Sci.* 99: 277-288. 2007.

Brody AR, Hill LH, Adkins B Jr., O'Connor RW. Chrysotile asbestos inhalation in rats: deposition pattern and reaction of alveolar epithelium and pulmonary macrophages. *Am. Rev. Respir. Dis.* 1283: 670-679. 1981.

Brody AR, Roe MW. Deposition pattern of inorganic particles at the alveolar level in the lungs of rats and mice. *Am. Rev. Respir. Dis.* 128: 724-729. 1983.

Brown RFR, Drawbaugh RB, Marrs TC. An investigation of possible models for the production of progressive pulmonary fibrosis in the rat. The effects of repeated intratracheal instillation of bleomycin. *Toxicology* 51: 101-110. 1988.

Chang LY, Overby LH, Brody AR, Crapo JD. Progressive lung cell reactions and extracellular matrix production after a brief exposure to asbestos. *Am. J. Pathol.* 131: 156-170. 1988.

Chapman HA. Disorders of lung matrix remodeling. *J. Clin. Invest.* 113: 148-157. 2004.

Collan Y, Kosma VM, Anttonen H, Kulju T. Toxicity of richterite in hemolysis test and macrophage cultures. *Arch. Toxicol. Suppl.* 9: 292-295. 1986.

Craighead JE, Abraham JL, Churg A, Green FHY, Kleinerman J, Pratt PC, et al. Asbestos-associated diseases. *Arch. Pathol. Lab. Med.* 106:541-96. 1982.

Cutroneo KR. How is type I procollagen synthesis regulated at the gene level during tissue fibrosis. *J. Cell. Biochem.* 90: 1-5. 2003.

Ghosh AK. Factors involved in the regulation of type I collagen gene expression: Implication in fibrosis. *Exp. Biol. Med.* 227: 301-314. 2002.

Gunter ME, Dyar DM, Twamley B, Foit FF, Cornelius S. Composition, Fe+3/Fe and crystal structure of non-abestiform and asestiform amphiboles from Libby, Montana, USA. *Am. Mineral.* 89:1579. 2003.

Hamilton RF, Holian A, Morandi MT. A comparison of asbestos and urban particulate matter in the in vitro modification of human alveolar macrophage antigen-presenting cell function. *Exp Lung Res.* 30: 147-62. 2004.

Hoyt DG, Lazo JS. Alterations in pulmonary mRNA encoding procollagens, fibronectin and transforming growth factor-beta precede bleomycin-induced pulmonary fibrosis in mice. *J. Pharmacol. Exp. Ther.* 246: 765-771. 1988.

Kamp DW, Weitzman SA. The molecular basis of asbestos induced lung injury. *Thorax.* 54: 638-652. 1999.

Lazenby AJ, Crouch EC, McDonald JA, Kuhn C. Remodeling of the lung in bleomycin-induced pulmonary fibrosis in the rat. An immunohistochemical study of laminin, type IV collagen, and fibronectin. *Am. Rev. Respir. Dis.* 142: 206-214. 1990.

Manning CB, Vallyathan V, Mossman BT. Diseases caused by asbestos: mechanisms of injury and disease development. *Int Immunopharmacol.* 2: 191-200. 2002.

McDonald JC, Harris J, and Armstrong B. Cohort study of mortality of vermiculite miners exposed to tremolite. *British J. Ind. Med.* 43: 436-444. 1986.

Meeker GP, Brownfield IK, Clark RN, Vance JS, Hoefen TM, Sutley SJ, Gent CA. The Chemical Composition and Physical Properties of Amphibole from Libby, Montana: A Progress Report, Abstract, 2001 health Effects of Asbestos, Oakland, CA. 2001.

Meeker GP, Bern AM, Brownfield IK, Lowers HA, Sutley SJ, Hoefen TM, Vance JS. The composition and morphology of ampiboles from the rainy creek complex, near Libby, Montana. *Am. Mineral.* 88:1955-1969. 2003.

Moatamed F, Lockey JE, Parry WT. Fiber contamination of vermiculites: A potential occupational and environmental health hazard. *Env. Res.* 41: 207-218. 1986.

Peipins LA, Lewin M, Campolucci S, Lybarger JA, Miller A, Middleton D, Weis C, Spence M, Black B, Kapil V. Radiographic abnormalities and exposure to asbestos-contaminated vermiculite in the community of Libby, Montana, USA. *Environ. Health Perspect*. 111: 1753-1759. 2003.

Putnam EA, Smartt A, Groves A, Schwanke C, Brezinski M, and Pershouse MA. Gene expression changes after exposure to six-mix in a mouse model. *J. Immunotoxicol.* 5: 139-144. 2008.

Solomon A. Computerized tomographic identification of visceral pleural changes other than in interlobar lung fissures. *Am. J. Ind. Med.* 15: 557-563. 1989.

Sullivan PA. Vermiculite, respiratory disease, and asbestos exposure in Libby, Montana: update of a cohort mortality study. *Environ. Health. Perspect.* 115: 579-85. 2007.

Swiderski RE, Dencoff JE, Floerchinger CS, Shapiro SD, Hunninghake GW. Differential expression of extracellular matrix remodeling genes in a murine model of bleomycin-induced pulmonary fibrosis. *Am. J. Pathol.* 152: 821-828. 1998.

United States Environmental Protection Agency. Asbestos contamination in Vermiculite. Vermiculite and Its Uses. Available: http://www.epa.gov/asbestos/pubs/verm.html Accessed 22 April 2008.

Wake B. A Report on an Industrial Hygiene Study of the Zonolite Company, Libby, Montana. April 19, 1962. Helena, MT: Montana State Board of Health. Division of Disease Control. 1962.

Woessner JF. The determination of hydroxyproline in tissue and protein samples containing small proportions of this imino acid. *Arch. Biochem. Biophys.* 93: 440-447. 1961.

Wright RS, Abraham JL, Harber P, Burnett BR, Morris P, West P. Fatal asbestosis 50 years after brief high intensity exposure in a vermiculite expansion plant. *Am. J. Respir. Crit. Care Med.* 165: 1145-1149. 2002.

Wylie AG, Verkouteren JR. Amphibole asbestos from Libby, Montana, aspects of nomenclature. *Am. Mineral.* 85: 1540-1542. 2000.

CHAPTER TWO

Mice Deficient in SPARC Show Decreased Collagen Accumulation After Asbestos Exposure

Abstract

Asbestos fibers are toxic substances that can cause serious health problems including cancer, asbestosis, and mesothelioma when they become airborne and are inhaled. Studies in mice have shown that after asbestos exposure, a complex network of cytokines, growth factors, and receptors are involved in initial inflammation and ensuing asbestosis. However, it has yet to be determined how genetic differences in these factors influence asbestos related disease development in humans. We have used gene expression studies in a mouse model to identify potential candidate genes involved in asbestos response, one such gene being *Sparc*. SPARC (secreted protein acidic and rich in cysteine) is a matricellular protein involved in tissue repair, extracellular matrix (ECM) regulation, cellular proliferation, and cellular adhesion. The ability of SPARC to regulate the ECM makes it a novel gene candidate for involvement in the fibrosis that occurs after asbestos exposure. The goal of this investigation was to determine the role of SPARC in fibrosis development after exposure to crocidolite asbestos or Libby amphibole, specifically targeting how lack of SPARC expression can influence ECM production. We speculated that SPARC is required for the accumulation of collagen seen in asbestos-induced pulmonary fibrosis. C57Bl/6 wild-type and SPARC-null mice were instilled intratracheally with crocidolite, Libby amphibole, or PBS for various durations. Through real-time PCR, fluorescent staining, and Western Blotting I found that

expression of SPARC is increased in both crocidolite and Libby amphibole treated mice compared to control. This increase in expression results in higher collagen deposits verified both visually through trichrome staining and via hydroxyproline levels. Lack of SPARC in these treated mice mitigated the level of collagen deposition. Overall, these results indicate that expression of SPARC is a significant step in the development of lung fibrosis through the modulation of ECM production.

Introduction

Libby, Montana was the site of a vermiculite mining operation from 1920 to 1990, and may have produced as much as 80% of the world's supply. This Libby vermiculite was contaminated with asbestos, which subsequently led to both occupational and environmental exposures in the Libby community. Libby asbestos (LA) is a combination of amphibole fibers that include tremolite, actinolite, soda tremolite, richterite, and winchite (Meeker, 2001). Exposure to LA is associated with several asbestos related diseases (ARDs) including asbestosis, lung cancer, mesothelioma.

Asbestos-induced pulmonary fibrosis, or asbestosis, can be defined as bilateral diffuse interstitial fibrosis of the lungs caused by the inhalation of asbestos fibers (American Thoracic Society, 1986; Craighead, 1982). It primarily occurs after prolonged exposure to the fibers through mining, manufacturing, handling, or the removal of asbestos fibers (Becklake, 1976). The disease is characterized by a scarring of lung tissue around the terminal bronchioles and alveolar ducts (A Medical Dictionary, 2004). This scar tissue can cause the thickening of alveolar walls, which will hinder the ability of the alveoli to transfer oxygen to the blood and remove carbon dioxide. Individuals who

contract this disease suffer from severe dyspnea, which can lead to respiratory failure, lung cancer or mesothelioma. In 1999 the Agency for Toxic Substance Disease Registry (ATSDR) and the EPA conducted studies on respiratory disease in Libby residents and found that the asbestosis mortality rate was 40 to 60 times greater than the national average (ATSDR, 2000).

The development of pulmonary fibrosis involves complex interactions between a number of cell types, including epithelial, interstitial, and inflammatory, and cellular components like cytokines and the extracellular matrix (Bienkowski, 1995). One class of proteins with a potential to modulate fibrosis is the matricellular proteins that bind to matrix components as well as to cell surface receptors. A member of the matricellular class of secreted proteins with the potential to modulated collagen deposition in response to fiber inhalation is SPARC (secreted protein acidic and rich in cysteine), also known as osteonectin or BM-40. SPARC has been shown to accumulate in the lung in idiopathic pulmonary fibrosis (Kuhn, 1995) and also play a role in collagen deposition in bleomycin-induced pulmonary fibrosis (Strandjord, 1999; Savani, 2000). Other members of this family of structurally distinct secreted proteins with counteradhesive properties include tenascin and the thrombospondins (Sage, 1991).

SPARC is a 43kD glycoprotein that plays a significant role in tissue repair and remodeling through the regulation of cell-matrix interactions (Bornstein, 1995; Reed, 1996). Expression of SPARC is widespread in developing fetal tissues but in the adult, expression occurs in tissues exhibiting a high turnover rate like the gut, skin, and glandular tissue (Lane, 1994) and also occurs in tumors (Schulz, 1988). SPARC is synthesized in and secreted from platelets, macrophages, fibroblasts, and endothelial cells under the regulation of transforming growth factor-β (TGF-β) and platelet-derived

growth factor (PDGF) (Jendraschak, 1996; Wrana, 1991). However, in terms of pulmonary fibrosis, SPARC has been localized primarily to fibroblasts, epithelial cells, and macrophages (Porter, 1995; Puolakkainen, 1999; Reed, 1993; Latvala, 1996). SPARC is a calcium-binding glycoprotein that interacts with many ECM components including the fibrillar collagens (types I, II, III, and V) as well as type IV, thrombospondin1, vitronectin, and fibrinogen fragments D and E (Bradshaw, 2001; Wang, 2006). SPARC has also been shown to be a modulator of growth factors involved in fibrosis and has also been implicated in the development of cancers (Schiemann, 2003; Framson, 2004; Siddiq, 2004).

Previous investigations into the role of SPARC in bleomycin-induced pulmonary fibrosis have shown conflicting results in terms of collagen deposition. It was shown that SPARC-null mice demonstrate a decrease in collagen accumulation with low-dose bleomycin injury (Strandjord, 1999). However, with a high-dose bleomycin lung injury, it was reported that lack of SPARC results in a significant increase in collagen deposition (Savani, 2000). Regardless of the dose it appears as though SPARC definitely plays a role in fibrotic disease development, therefore we felt it would be important to study the effects of a SPARC deficiency in a model of asbestos-induced pulmonary fibrosis.

The purpose of this study was to determine the effect of a SPARC deficiency on collagen deposition in the murine lung after exposure to LA or crocidolite asbestos. Crocidolite was used as a well-documented amphibole fiber for comparison. SPARC-null (SP-null) mice on a C57Bl/6 background and wild-type C57Bl/6 (WT) controls were intratracheally instilled with either asbestos suspended in phosphate buffered saline (PBS) or PBS alone as a vehicle control. The goal of this study is to determine if SPARC

plays a role in the regulation of pulmonary fibrosis through the modulation of collagen deposition.

Materials and Methods

Asbestos: A sample of the Libby amphibole was generously provided by the U.S. Geological Survey. The amphibole used is a chemical representation from six locations at the mine and has been characterized in detail (Wylie, 2000; Gunter, 2003; Meeker, 2003). This amphibole sample also has a particle size distribution matching air sample size distribution data (Meeker, 2003). Crocidolite asbestos was obtained from the Research Triangle Institute (Research Triangle Park, NC). The fiber size distribution of both Libby amphibole and crocidolite asbestos has been previously reported (Blake, 2007). For reference, size parameters of the Libby amphibole sample were 0.61 μm in diameter, 7.21 μm in length, with 22.52 for the aspect ratio. Size parameters of the crocidolite were 0.16 μm in diameter and 4.59 μm in length, with a 34.05 aspect ratio. Samples were freshly prepared in sterile phosphate-buffered saline (PBS, pH 7.4) and sonicated before instillation (Putnam, 2008).

Mouse Treatment: All animal protocols were approved by the Institutional Animal Care and Use Committee. Mice were exposed to amphiboles according to methods previously described (Adamson, 1987). Briefly, pathogen-free 6-8 week old female and male C57Bl/6 WT mice and SPARC-null mice (SP-null) were instilled intratracheally with 100 μg of crocidolite asbestos or LA in 30μl sterile PBS while under anesthesia. Control mice received only sterile PBS as a vehicle control. Mice were euthanized 1 week, 1 month, or

3 months after instillation. Treated mice were then divided into two groups. The left lung of the mice in the first group was removed for RNA isolation, while the right lung was perfused and immersed in Histochoice (Amresco, Solon, OH) before being embedded in paraffin. The caudal lobe of the left lung of the mice in the second group was removed, rinsed in PBS and collagen content quantified by hydroxyproline analysis. The remaining lung tissue was snap frozen in liquid nitrogen until protein could be isolated.

Histology: Fixed lungs were embedded in paraffin and sliced into seven μm sections. Routine Gomori's trichrome staining was performed in order to visualize fibrillar collagen localization in the lung, and the sections examined under light microscopy.

Fibrosis Scoring: Scoring was performed by a licensed veterinary pathologist (Donald Gardner, Rocky Mountain Laboratories, MT). 3 to 6 mice from each treatment group/time point were scored through the analysis of at least 9 sections per mouse. Scores of mouse sections were averaged with numerical values representing the following stages of fibrosis: 0.0 = absent, 1.0 = minimal, 2.0 = mild, 3.0 = moderate, and 4.0 = severe.

RNA Isolation: Lung tissue samples were homogenized in 1ml of TRIZOL and RNA isolated following the manufacturer's protocol (Invitrogen, Carlsbad CA). The resulting RNA was purified using the RNeasy kit (Qiagen, Valencia, CA) and subsequently treated with DNAse (Qiagen, Valencia, CA).

Quantitative RT-PCR: RNA isolated from lung tissue was analyzed by quantitative RT-PCR. Initially, first strand synthesis of cDNA was carried out using a First-Strand Synthesis kit (Invitrogen, Carlsbad, CA). Target cDNA was subsequently amplified using predesigned TaqMan probes (ABI, Foster City, CA) for Collagen 1A1, Collagen 1A2, Collagen 3, and Sparc as well as probes to detect both Gapdh and β-Actin transcripts as controls. PCR was performed on an iQ5 Optical System (Bio-Rad, Hercules, CA).

Protein Isolation: Lung tissue was homogenized in lysis buffer (PBS, Triton X-100, sodium desoxycholate, sodium dodecyl sulfate, EDTA, phenylmethylsulphonylfluride, and protease inhibitor) and centrifuged to isolate protein. Total protein concentration was measured with the Lowry-like DC Protein Assay (Bio-Rad, Hercules, CA).

Western Blotting: Lung protein samples were separated by electrophoresis through 4-12% Bis-Tris NuPAGE gels (Invitrogen, Carlsbad, CA) then transferred to PVDF membrane (Millipore, Billerica, MA). Membranes were blocked in 5% milk in PBS-Tween20. Specific antibodies for both SPARC (R & D Systems, Minneapolis, MN) and β-Actin (Santa Cruz Biotechnology, Santa Cruz, CA) were used to detect protein levels, which were quantified using chemiluminescence on a Fuji gel documentation system (Fujifilm Life Sciences, Stamford, CT).

Immunofluroescence: SPARC expression was detected by incubation with anti-SPARC (R & D Systems, Minneapolis, MN) antibodies followed by labeling with Alexa Fluor 568. Original magnification was 200X.

Hydroxyproline Assay: Quantitation of lung collagen content from exposed and control mice was determined by an assay for hydroxyproline content according to methods previously described (Woessner, 1961) with some modifications. The lower left lobe was rinsed in PBS, minced and hydrolyzed in 1.5ml of 6N HCl overnight at 110°C. To 5µl of the hydrolysate were added 10µl of 0.02% methyl red and 2µl of 0.04% bromothymol blue. Sample volume was adjusted to 200µl with assay buffer (0.024M Citric Acid, 0.02M Glacial Acetic Acid, 0.088M Sodium Acetate, and 0.085M NaOH). The colorimetric assay was performed by the addition of 100µl of chloramine T solution and incubation at room temperature for 20 minutes. Following incubation, 100µl of dimethyl benzaldehyde solution was added and the solution incubated in a 60°C water bath for 15 minutes. Absorbance was measured at 550nM for each lung sample in a 96-well plate and quantitation of hydroxyproline was determined by comparison to a standard curve.

Statistical Analysis: Mean values for the hydroxyproline assay were compared by one-way ANOVA with a Newman-Keuls test for multiple comparisons. Results are presented as mean values ± SEM. Results from Real-time PCR on triplicate pools of RNA for each treatment group were normalized to both Gapdh and β-actin and statistically analyzed with a two-tailed *t*-test on the treatment means. Results are presented as mean fold difference ± SEM versus PBS. Densitometry values taken from replicate samples run on Western blots were normalized to β-Actin then asbestos treated samples were analyzed for percent expression versus the PBS treatment group. A one-way ANOVA with a Newman-Keuls test for multiple comparisons was used to verify the significance of the mean percent expression values and results are presented as mean values ± SEM versus PBS. Inflammation scores were first averaged for each mouse, then treatment groups

analyzed by one-way ANOVA with a Bonferroni test for multiple comparisons. In all cases, significant results were determined by $p < 0.05$.

Results

Immunohistochemisty was initially performed to determine if SPARC was potentially involved in the development of asbestosis. C57Bl/6 wild-type (WT) mice were intratracheally instilled with phosphate buffered saline (PBS) as a control, crocidolite asbestos (CRO), or Libby amphibole (LA). Mice were sacrificed after one month and the lungs were removed and fixed for immunohistochemistry. Seven-micrometer thick sections taken from the lungs of these mice were fluorescently labeled with antibodies against SPARC protein (Figure 11). Examination of the fluorescence levels indicated that SPARC expression was increased in the lungs of mice exposed with asbestos (Figure 11B and 11C) when compared to the PBS treatment group (Figure 11A). These initial results indicated that SPARC may be involved in the development of fibrosis after asbestos exposure and was therefore worthy of further investigation.

Figure 11: **1 Month WT SPARC Immunohistochemistry**

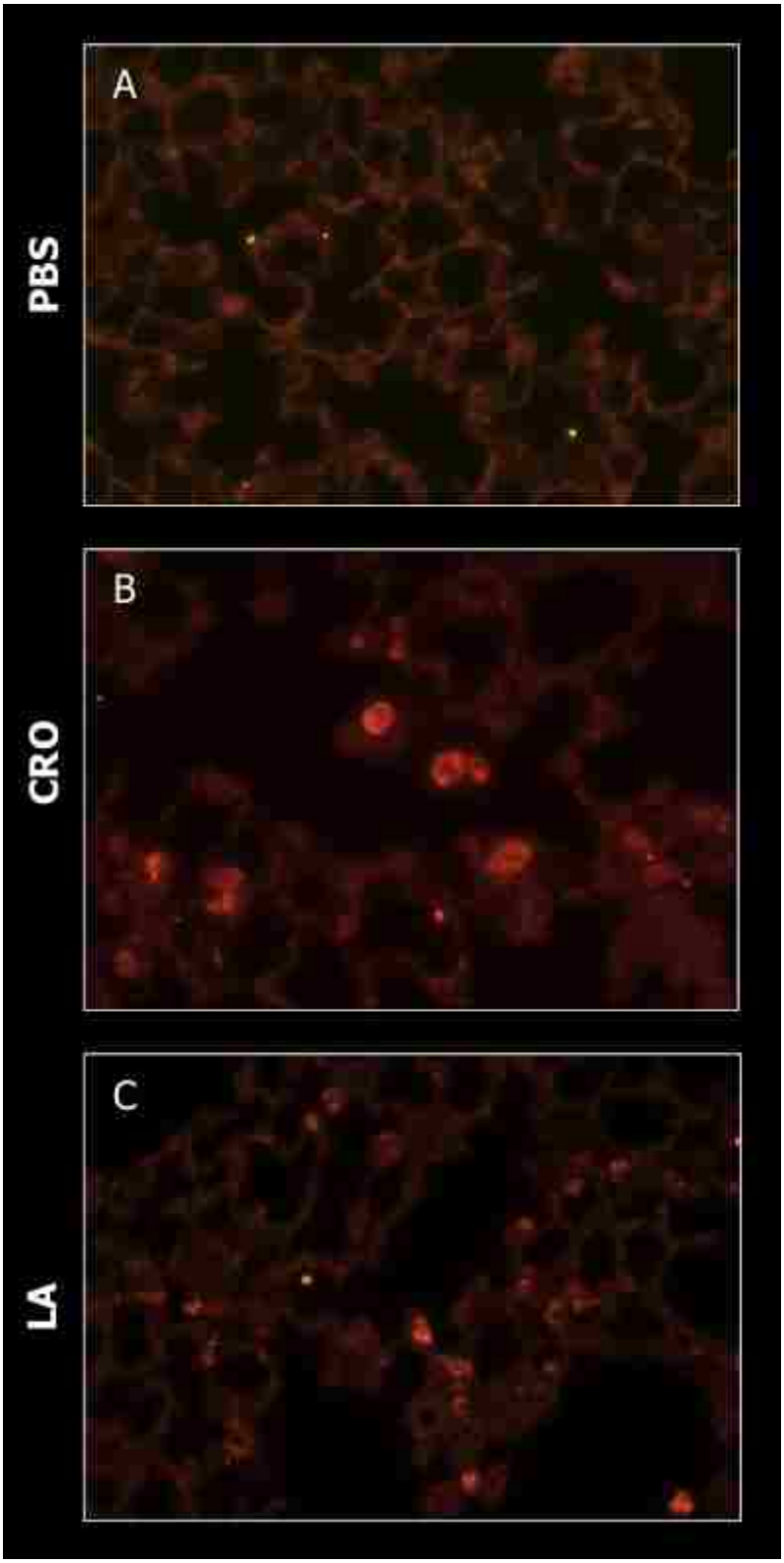

Figure 11 Legend: Immunohistochemical analysis of WT mouse lungs revealed that animals exposed to asbestos showed increased SPARC expression. Though both amphibole treatment groups showed heightened SPARC expression, it appeared as though CRO treated lungs had slightly more expression than LA treated lungs. This observation must be verified via immunoblotting.

Quantitative real-time PCR was utilized to determine if the initial protein expression level changes were also occurring at the mRNA level. Equal quantities of the total cellular mRNA from eight to ten mice were pooled for each treatment group and reverse-transcribed into cDNA for real-time analysis (Figure 12). No significant fold differences in *Sparc* mRNA were detected at either the one week or three month treatment time points. However, at the one month time point, the level of *Sparc* mRNA was significantly increased in both the CRO treatment group and the LA treatment group relative to the PBS control. The increase in *Sparc* mRNA in response to asbestos exposure at one month further implicates the role of SPARC in asbestosis development.

Figure 12: Wild-Type SPARC qRT-PCR

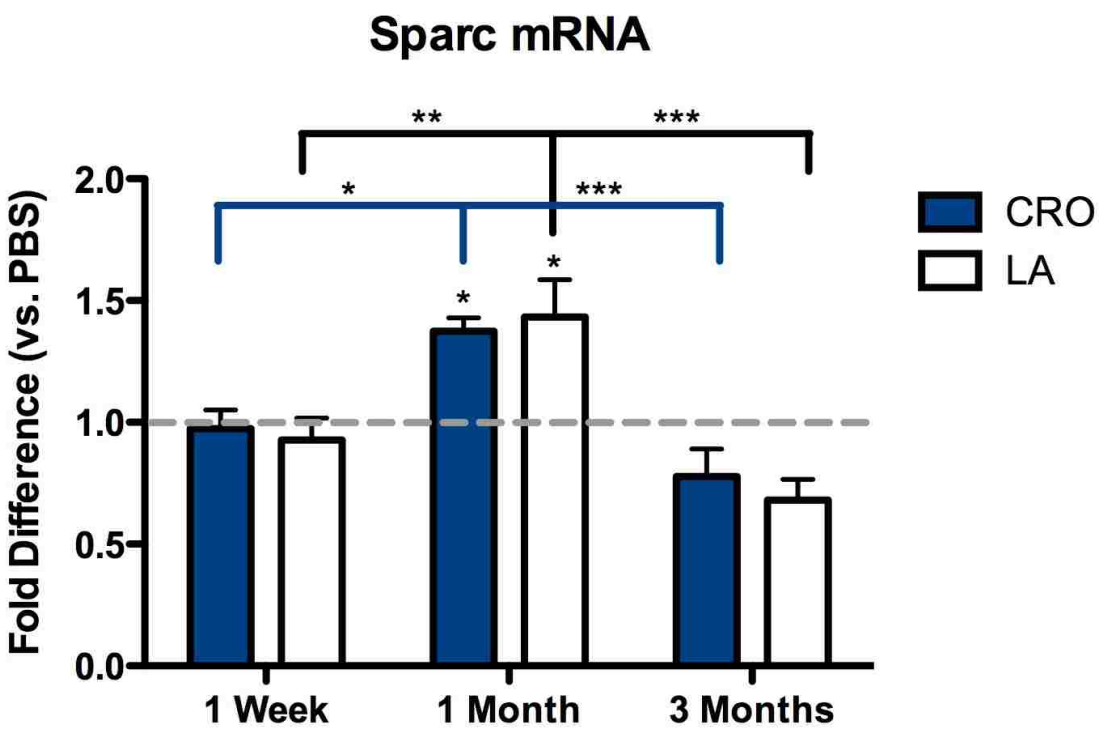

Figure 12 Legend: Real-Time PCR of *Sparc* mRNA from the lungs of C57Bl/6 mice exposed to PBS, CRO, or LA. Each experiment was repeated three times. Results on triplicate pools of RNA for each treatment group (n = 10 – 12 per group) were normalized to both Gapdh and β-actin and are presented as mean fold difference ± SEM. Both the CRO and LA treatment groups had a significantly increased amount of *Sparc* mRNA compared to the PBS treatment group at one month. When looking at changes over time, both LA and CRO treated groups had significantly more *Sparc* mRNA at one month than at one week or three months post exposure. (* = $p < 0.05$, ** = $p < 0.01$, *** = $p < 0.001$)

Western immunoblotting was necessary to confirm the increase in SPARC protein expression seen via immunohistochemistry. Equivalent quantities of total cellular protein isolated from the lungs of eight to ten WT mice per treatment group were pooled and analyzed for levels of SPARC (Figure 13). The level of SPARC protein was significantly increased at one week for both asbestos exposure groups. By one month the expression of SPARC in the LA treatment group was still significantly increased when compared to the PBS treatment group but there was no longer any measurable difference in the CRO treatment group. This difference in the LA treatment group was no longer detectable by three months. The increased levels of both SPARC protein and mRNA provide strong evidence that SPARC could play a role in the development of asbestosis-induced fibrosis, especially at one week and one month after exposure.

Figure 13: Wild-Type SPARC Protein Expression

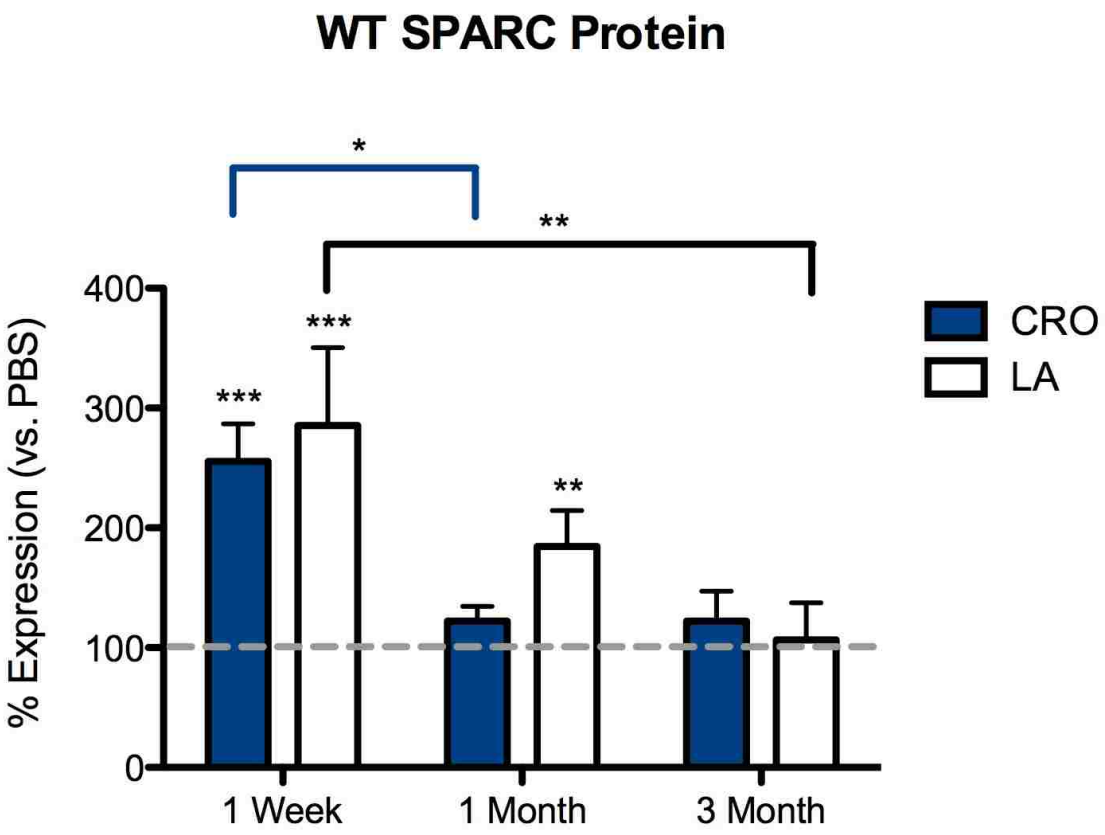

Figure 13 Legend: Immunoblotting of SPARC protein from the lungs of C57Bl/6 mice exposed to PBS, CRO, or LA. Each blot was repeated three times. Results on triplicate pools of RNA for each treatment group (n = 10 – 12 per group) were normalized to β-actin and are presented as the mean percent expression versus PBS ± SEM. Both the CRO and LA treatment groups had a significantly increased amount of SPARC protein compared to the PBS treatment group at one week after exposure. By one month post-exposure only the LA treated group had significantly more SPARC than PBS and by three months SPARC levels for both treatment groups return to PBS levels. When looking at changes over time, CRO treated lungs had significantly more SPARC at one week than one month and LA treated lungs had significantly more SPARC at one week than at three months. (* = $p < 0.05$, ** = $p < 0.01$, *** = $p < 0.001$)

SPARC-null (SP-null) mice were utilized to determine more specifically what role SPARC is playing in the induction of asbestosis. Eight to ten WT and SP-null mice were again given asbestos (CRO and LA) or PBS via intratracheal instillation, sacrificed at one week, one month, and three months after exposure, and fixed for histology (Figure 14 to Figure 16). When compared to their PBS treated counter parts (Figures 14, 15, and 16 A and D), the CRO and LA treated WT (Figures 14, 15, and 16 B and C) and SP-null (Figures 14, 15, and 16 E and F) mice appeared to develop fibrosis at all time points, as evident by the ensuing inflammation.

After one week of exposure, histological examination revealed similar fibrosis development between the WT (Figure 14A to 14C) and SP-null (Figure 14D to 14F) treatment groups with the exception of the amount of collagen being deposited around the airways of the CRO treated WT mice (Figure 14B: arrows, blue stain) and LA treated WT mice (Figure 14C). This was also apparent at one month after exposure with much more collagen being deposited around the airways of asbestos treated WT mice (Figure 15B and 15C) than the airways of SP-null mice (Figure 15D to 15F) and the WT PBS treated mice (Figure 15A). By three months post exposure, the difference in collagen deposition was still apparent in the LA treated WT (Figure 16C) mice and the WT CRO exposed animals (Figure 16B) who still had much greater levels of collagen being deposited around the airways than their SP-null LA (Figure 16F) and CRO (Figure 16E) exposed counter parts.

Figure 14: 1 Week Wild-Type/SPARC-null Lung Histology

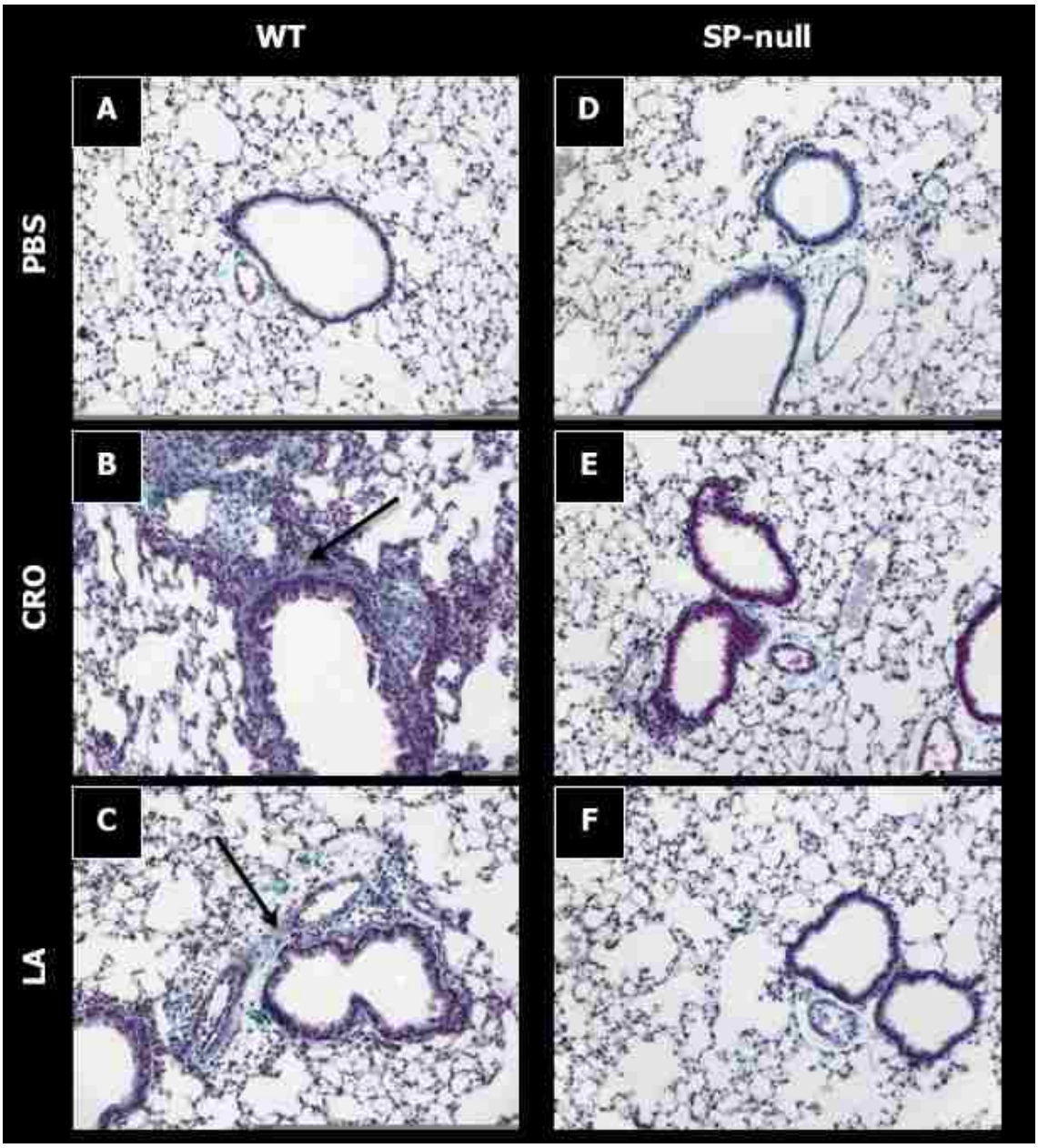

Figure 14 Legend: Gomori Trichrome-stained 7 μM sections of mouse lungs from C57Bl/6 WT and SP-null mice instilled for one week with crocidolite asbestos (CRO), Libby amphibole (LA), or sterile saline (PBS) as a vehicle control for comparison (200X original magnification). Blue-green staining indicates collagen deposition and arrows point to areas of increased accumulation. The airways of the amphibole exposed WT mice showed much higher levels of collagen accumulation than the SP-null mice, though both mouse strains showed signs of increased inflammation.

Figure 15: 1 Month Wild-Type/SPARC-null Lung Histology

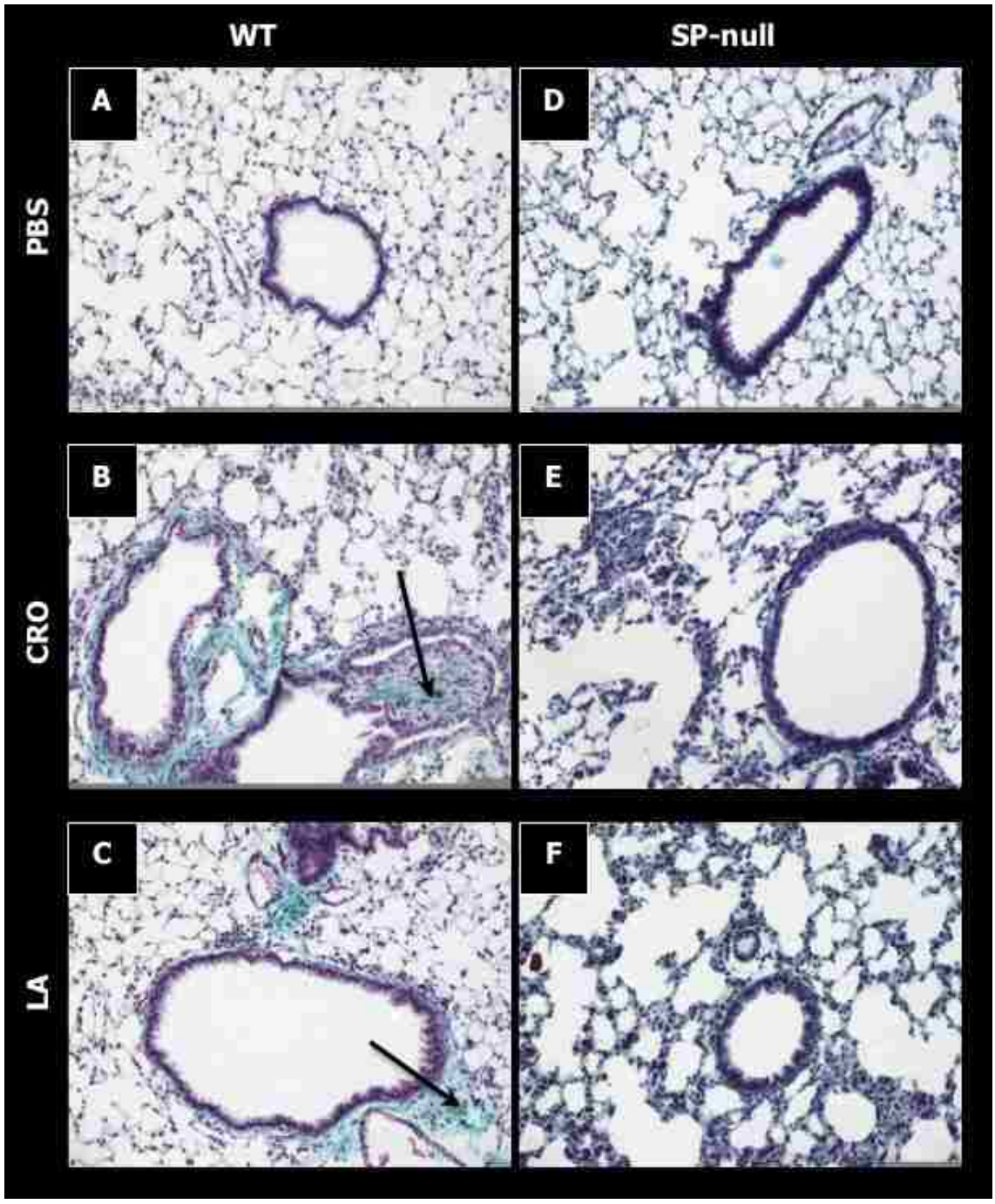

Figure 15 Legend: Gomori Trichrome-stained 7 μM sections of mouse lungs from C57Bl/6 WT and SP-null mice instilled for one month with crocidolite asbestos (CRO), Libby amphibole (LA), or sterile saline (PBS) as a vehicle control for comparison (200X original magnification). Blue-green staining indicates collagen deposition and arrows point to areas of increased accumulation. As at one week, the airways of the amphibole exposed WT mice showed much higher levels of collagen accumulation than the SP-null mice, and both mouse strains showed signs of increased inflammation.

Figure 16: 3 Month Wild-Type/SPARC-null Lung Histology

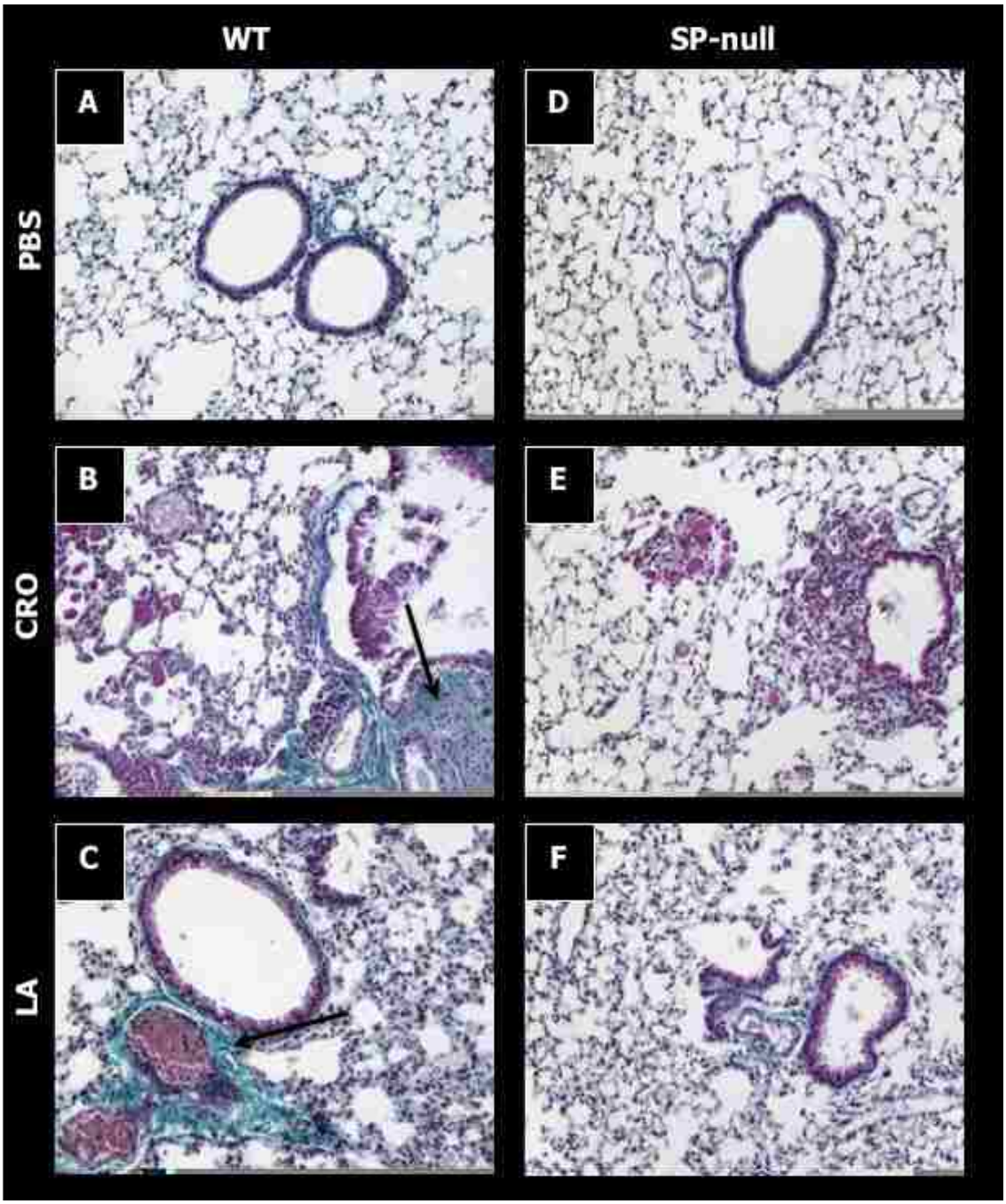

Figure 16 Legend: Gomori Trichrome-stained 7 μM sections of mouse lungs from C57Bl/6 WT and SP-null mice instilled for three months with crocidolite asbestos (CRO), Libby amphibole (LA), or sterile saline (PBS) as a vehicle control for comparison (200X original magnification). Blue-green staining indicates collagen deposition and arrows point to areas of increased accumulation. As with both previous time points, airways of the amphibole exposed WT mice showed much higher levels of collagen accumulation than the SP-null mice, and again both mouse strains showed signs of increased inflammation.

Histology sections were also scored on a scale of inflammation to further determine if the lack of SPARC altered the development of fibrosis after asbestos exposure (Table 3). Dr. Donald Gardner, a pathologist at Rocky Mountain Laboratories, performed the scoring. No significant differences were found when comparing WT and SP-null mice for each time and treatment. The similar inflammation scores between the WT and SP-null mice indicated that the mice lacking SPARC still develop the inflammatory response, regardless of the difference in the levels of collagen deposition.

Table 3: Inflammation Scoring of Wild-Type/SPARC-null Lung Tissue

TIME POINT	TREATMENT	INFLAMMATION SCORE[1]		# OF MICE		# OF SECTIONS	
		WT	SP-null	WT	SP-null	WT	SP-null
1 Week	PBS	0.0	0.0	4	3	48	27
1 Week	CRO	1.2	1.0	6	3	60	27
1 Week	LA	0.9	0.3	5	3	81	27
1 Month	PBS	0.1	0.0	4	6	36	54
1 Month	CRO	1.8	1.6	5	7	39	63
1 Month	LA	0.7	0.5	4	9	36	78
3 Month	PBS	0.0	0.0	3	3	27	27
3 Month	CRO	1.8	1.8	3	3	27	27
3 Month	LA	0.4	0.6	3	4	27	36

[1]Inflammation scoring values are as follows: 0.0 = absent, 1.0 = minimal, 2.0 = mild, 3.0 = moderate, and 4.0 = severe. There were no significant differences found between WT and SP-null mice for each treatment group at any time point.

Quantitative real-time PCR was used to verify that the differences in collagen levels seen in the trichrome stained lung sections also occurred at the mRNA level. Specifically the levels of collagen types I and III were evaluated. As before, equal quantities of total cellular mRNA from eight to ten mice were pooled for each treatment group for the SP-null mice and reverse-transcribed into cDNA for real-time PCR analysis (Figures 17). When evaluating only the SP-null animals, it was concluded that there were no apparent differences in the levels of Col1A1 mRNA in the SP-null mice exposed to asbestos compared to the PBS exposed controls (Figure 17A). There were, however, significant decreases in the expression of Col1A2 in the SP-null mice exposed to LA at both the one week and three month time points (Figure 17B). Finally, evaluation of type III collagen identified that expression in SP-null mice was significantly increased for the CRO treatment group at the one month time point and increased, though not significantly so, the three month time point (Figure 17C). Also when comparing differences between time points, expression of type III collagen mRNA was significantly increased at one month post-exposure compared to one week.

Figure 17: SP-null Collagen qRT-PCR

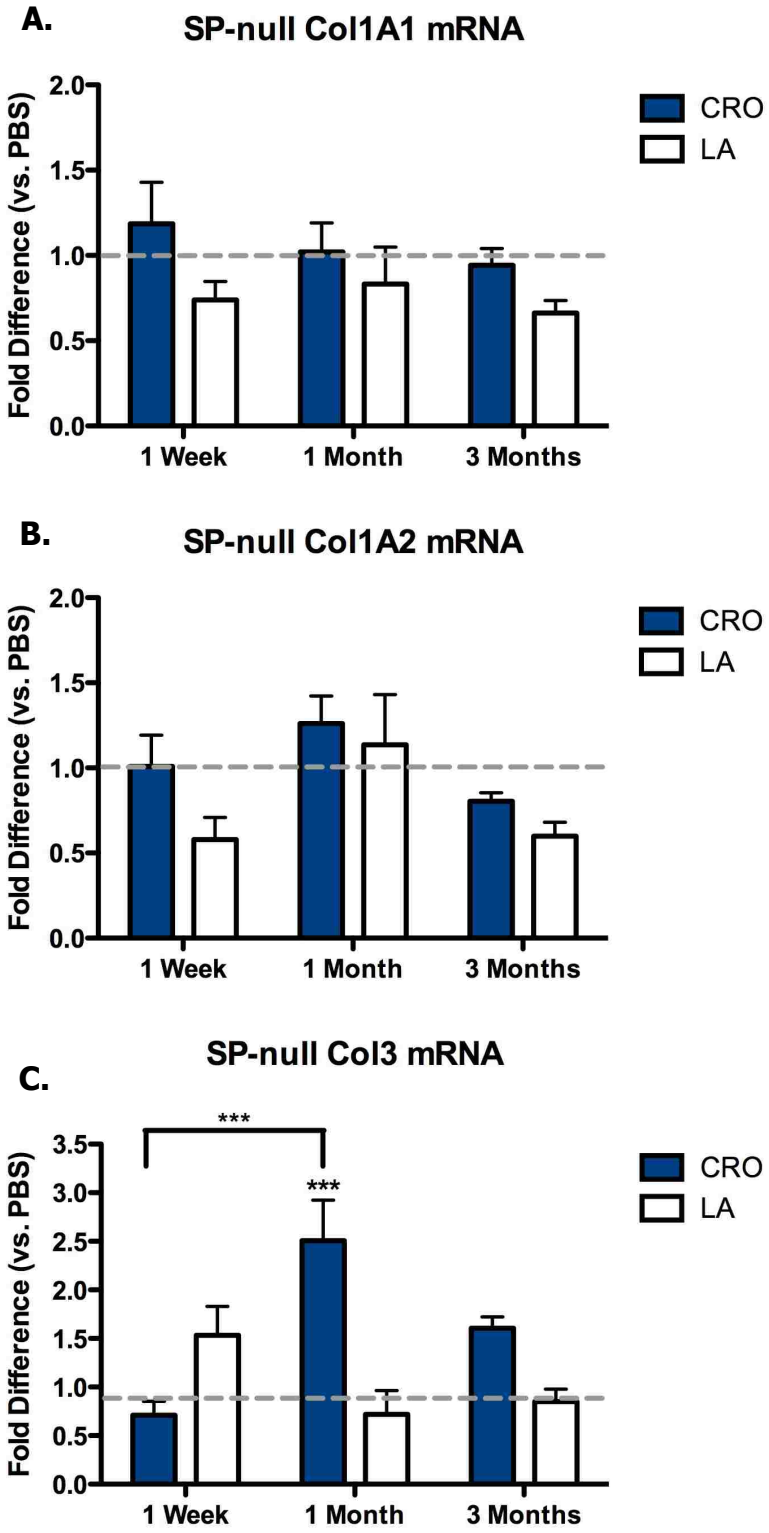

Figure 17 Legend: Real-Time PCR of Collagen mRNA from the lungs of SP-null mice exposed to PBS, CRO, or LA. Each experiment was repeated three times. Results on triplicate pools of RNA for each treatment group (n = 10 – 12 per group) were normalized to both Gapdh and β-actin and are presented as mean fold difference ± SEM. Significant differences in collagen mRNA expression occur in the CRO treatment group at one month post-exposure where there was a significant increase in type III collagen mRNA when compared to the PBS treatment group. When looking at changes over time, CRO exposed animals had significantly more type III collagen mRNA at one month than at one week. (* = $p < 0.05$, ** = $p < 0.01$, *** = $p < 0.001$)

The SP-null results were also compared with data from the exposure of wild-type mice previously presented in Chapter 1 for both the CRO and LA treatment groups (Figure 18). The expression levels of collagen type I alpha 1 (Col1A1) mRNA was significantly higher in WT mice exposed to either CRO or LA relative to their SP-null counterparts at both the one week and one month time points (Figure 18A and 18B). The expression levels of collagen type I alpha 2 (Col1A2) mRNA were also significantly increased in the WT mice versus the SP-null mice at the one week time point in the LA treatment group (Figure 18D). There were no differences in Col1A2 expression between the WT and SP-null mice in the CRO treatment group at any time point (Figure 18C). Expression of type III collagen (Col3) in WT mice was significantly increased when compared to the SP-null mice for the LA treatment group at the one month time point (Figure 18F). Again there were no significant differences in the CRO treatment group between the two strains for type III collagen mRNA expression (Figure 18E). The lack of a change in Col3 mRNA in the CRO exposed mice may indicate that another protein is compensating for the lack of SPARC in the SP-null animals. The differences in type I collagen between the WT and SP-null mice further demonstrated that SPARC plays an important role in asbestosis development, and this role appears to center around the presence of collagen.

Figure 18 Wild-Type vs SPARC-null Collagen qRT-PCR

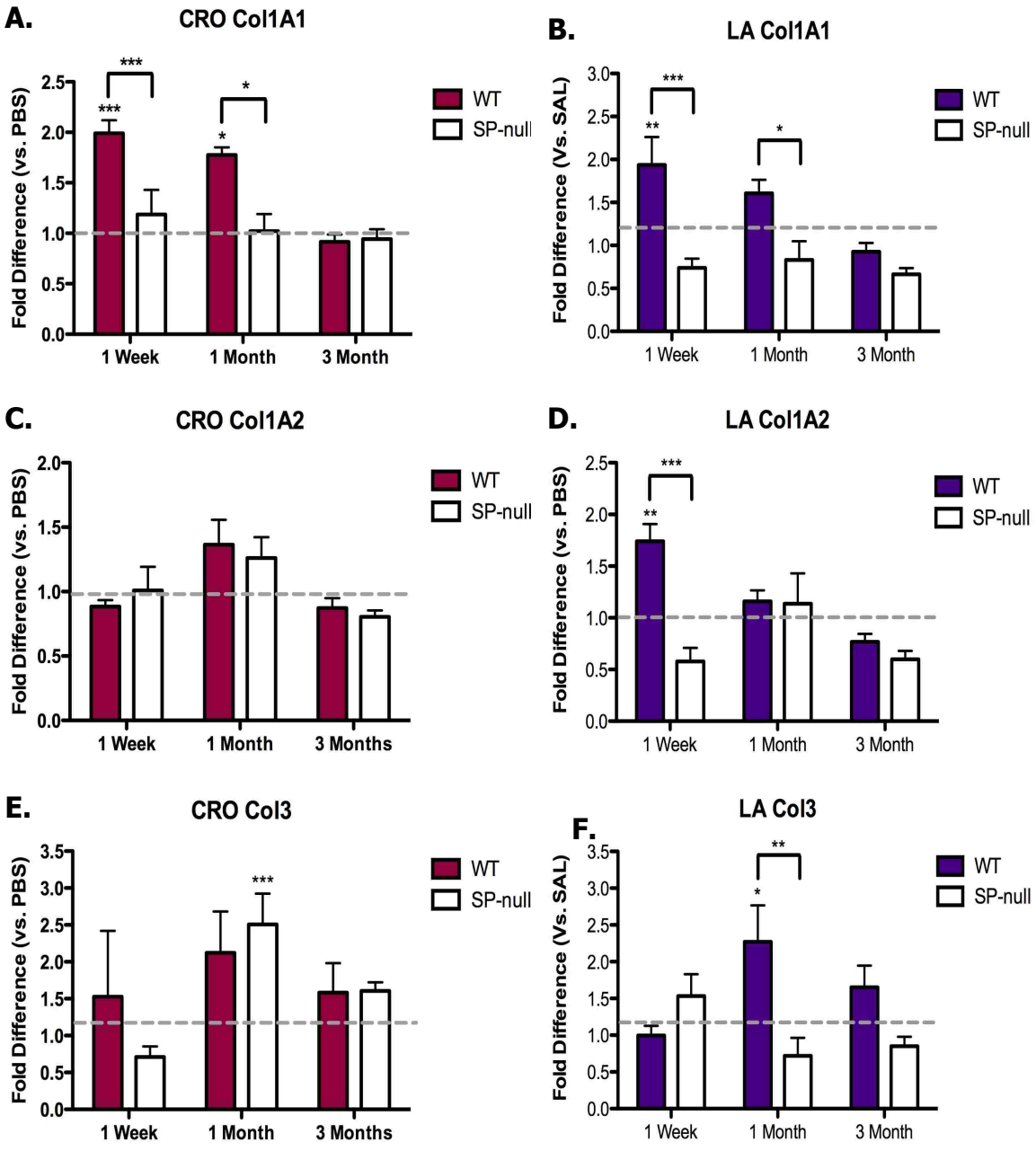

Figure 18 Legend: Real-Time PCR of Collagen mRNA from the lungs of SP-null mice versus WT mice exposed to PBS, CRO, or LA. Data were previously presented in Figures 9 (WT) and 17 (SP-null). There were significant decreases in type I alpha1 collagen mRNA expression in the SP-null mice of both amphibole treatment groups when compared to their WT counterparts at both one week and one month time points. There was also a significant decrease in type I alpha2 collagen mRNA expression at one week and type III collagen expression at one month in the SP-null versus WT mice of the LA treatment group. (* = $p < 0.05$, ** = $p < 0.01$, *** = $p < 0.001$)

To further confirm the role of SPARC as a regulator of collagen deposition in the lung after asbestos exposure, the hydroxyproline assay was utilized to quantify the total amount of collagen protein present in the lung (Figure 19). The levels of total collagen in the SP-null mice were for the most part constant regardless of treatment. The only difference occurred at one month post-exposure. At this time point, lungs from the CRO treated animals had significantly more total hydroxyproline content than the PBS controls. In addition lungs from the CRO treatment group demonstrated a significant increase in total hydroxyproline content from the one week to one month time points. However, hydroxyproline levels returned to baseline by three months after exposure. Compared to WT mice, it appeared that less collagen accumulated in the SP-null lung after asbestos exposure, further implicating SPARC for a role in the development of asbestos-induced fibrosis through the modulation of collagen deposition in the lung.

Figure 19: SPARC-null Hydroxyproline Assay

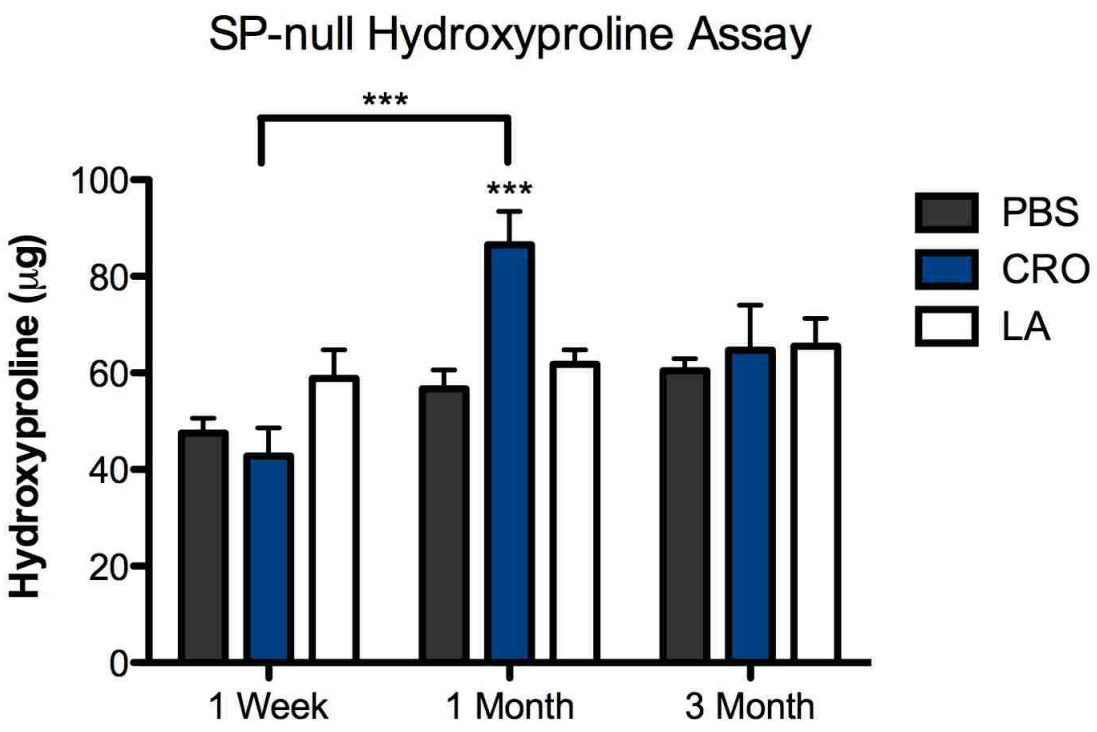

Figure 19 Legend: Total hydroxyproline content from the lungs of SP-null mice exposed to PBS, CRO, or LA. Mice were intratracheally instilled for 1 week, 1 month, or 3 months and collagen content of the left lung was determined by measuring hydroxyproline levels in replicate animals. All experiments were done in triplicate. Results are presented as mean values ± SEM for each treatment/time (all groups have n = 9-10). Only the one month CRO exposed mice had significantly more hydroxyproline content than the PBS controls. (*** = $p<0.001$). There was also a significant increase in total hydroxyproline in the CRO treatment group at the one month time point compared to one week.

To confirm that less collagen accumulated in the SP-null lungs, analysis was performed on the differences between total hydroxyproline in the WT and SP-null lungs. The WT data were previously presented in Chapter 1. At all three time points the levels of total collagen were significantly lower in the SP-null mice compared to the WT mice in both the CRO and LA treatment groups (Figure 20). This evidence in addition to the trichrome staining and decreased levels of type I collagen mRNA demonstrated that SPARC plays a significant role in the deposition of collagen in the lung in response to asbestos exposure. Mice lacking SPARC still developed fibrosis in response to amphiboles though it may be less severe due to less collagen in the lung, thereby making respiration easier.

Analysis was also performed on no-treatment (NT) controls to determine if the lungs were reacting to the PBS vehicle control. No significant differences were found between these groups and their PBS treated counterparts. However, a significant decrease was seen in the NT group at three months in the SP-null mice compared to WT mice, further demonstrating the decreased ability of the SP-null lung to accumulate collagen.

Figure 20: Wild-Type vs. SPARC-null Hydroxyproline Assay

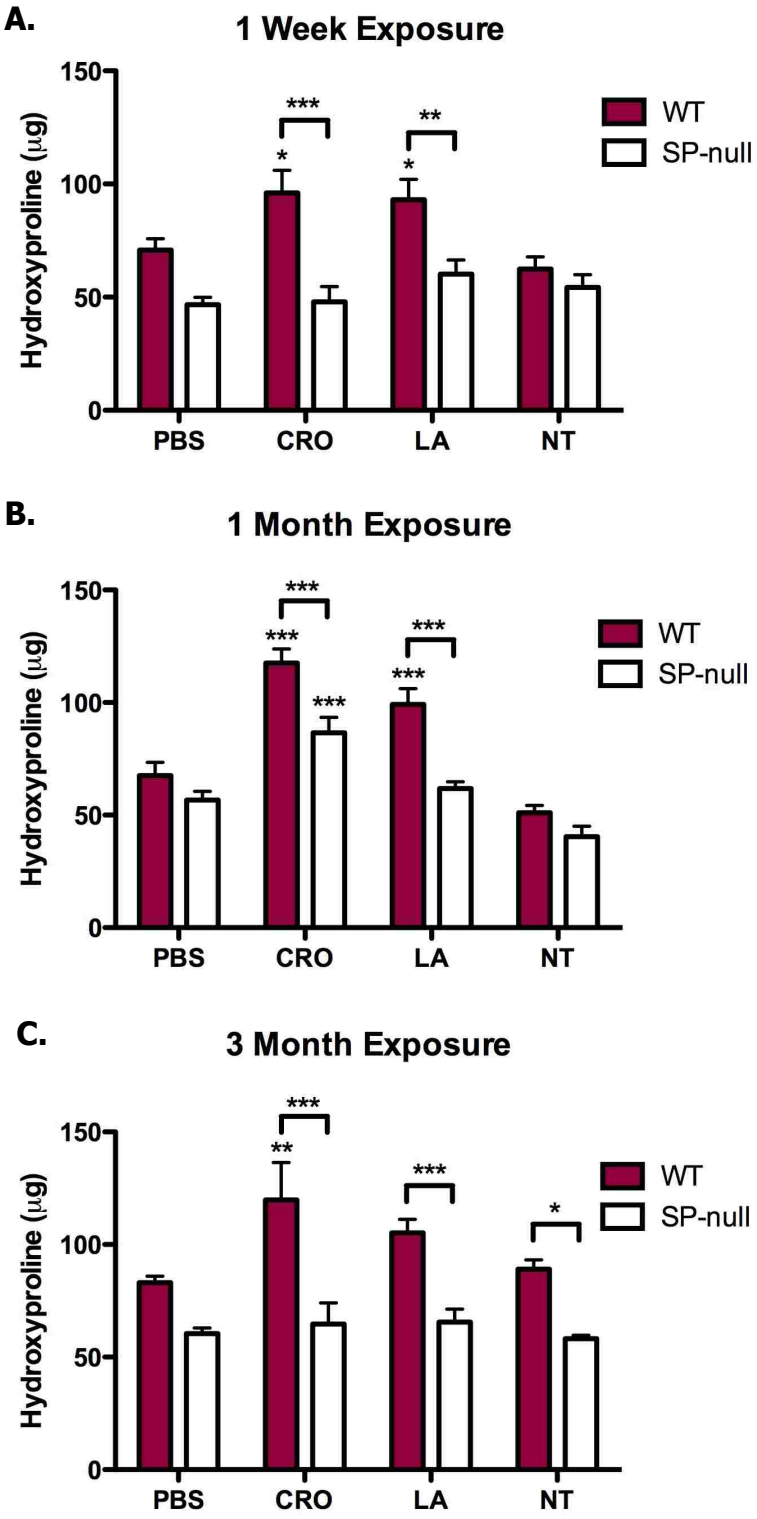

Figure 20 Legend: Total hydroxyproline content from the lungs of SP-null mice versus WT mice exposed to PBS, CRO, or LA. Data were previously presented in Figures 10 (WT) and 19 (SP-null). Results are presented as mean values ± SEM for each treatment/time (all groups have n = 8-10). At all time points there was a significant decrease in total hydroxyproline in the amphibole treated SP-null mice versus their WT counterparts. (* = $p<0.05$, ** = $p<0.01$, *** = $p<0.001$).

Discussion

The data presented in Chapter 1 demonstrated that intratracheal instillations of asbestos cause asbestosis *in vivo*, thereby providing a model of fibrosis for further study. Initial exploration into this model of disease identified SPARC as a candidate protein based on its involvement in cell-matrix interactions. I have demonstrated that SPARC mRNA and SPARC protein are induced in an asbestos model of pulmonary fibrosis. The known function of SPARC as a regulator of the extracellular matrix in remodeling tissues (Lane, 1994; Reed, 1996) as well as the previously reported increase in total collagen (Smartt, 2008: Chapter 1), implied that SPARC may be playing a substantial role in fibrosis development in terms of collagen accumulation. Here, I show that lack of SPARC may decrease the severity of fibrosis since significantly less collagen is deposited around the airways of asbestos exposed SP-null mice compared to their WT counterparts.

Even though its specific role in response to asbestos in the lung is not fully understood, previous studies implying the ability of SPARC to alter collagen deposition in the bleomycin-induced fibrotic lung make it a candidate for study in the development of asbestosis. My results showed that SPARC expression was increased in lungs exposed to asbestos. Initially it appeared that the levels of SPARC protein were increased via immunostaining of fibrotic lung sections. This was later confirmed at one week post exposure by immunoblotting. I also found that the expression of *Sparc* mRNA was increased at one month in asbestos exposed animals. Therefore it appeared that the initial response to the presence of asbestos was a decrease in the rate of SPARC protein elimination. By one month after amphibole exposure, more *Sparc* mRNA was being

transcribed but a correlating increase in the translation into SPARC protein was not observed in the CRO exposed mice. A possible explanation for this could be that there was a higher turnover rate of SPARC protein, or that there could be an increase in posttranscriptional regulation.

Because of the increase in protein expression after one week post-exposure, more SPARC may be bound to the TGF-β receptor complex, which could account for the increase in collagen expression observed in Chapter 1. Previous studies have found that TGF-β plays a significant role in the development of pulmonary fibrosis (Broekelmann, 1991; Denis, 1994; Toti, 1997). Several studies have also shown that levels of TGF-β are increased as well as activated in the presence of asbestos (Liu, 2001; Sullivan, 2008; Pociask, 2004), meaning that TGF-β is bound to its receptor complex and initiates one of several signaling cascades. The binding of SPARC to this receptor complex in addition to TGF-β may have the ability to activate the TGF-β signaling cascades responsible for the induction of collagen transcription (Francki, 2004). Therefore, it may be prudent for future studies to determine the extent to which SPARC is bound to the TGF-β receptor complex.

The data presented in Chapter 1 (Smartt, 2008) indicated that both the expression of type I collagen mRNA and total lung collagen protein content were significantly increased in C57Bl/6 WT lungs exposed to amphibole asbestos. This mirrors similar results in rats and hamsters exposed to bleomycin (Phan, 1980; Quinones, 1986; Clark, 1980). This trend does not occur in SP-null animals on a C57Bl/6 background. I found that SP-null animals exposed to asbestos did not exhibit a significant increase in total collagen content, as measured by hydroxyproline content, when compared to PBS controls. The only exception to this was the crocidolite treatment group at one month. It

is apparent that at one month, the SP-null lung was responding to the presence of CRO asbestos through the synthesis of collagen, however, when compared with their WT counterparts, SP-null mice had significantly less collagen accumulation in the lung after exposure to asbestos at all time points. This decrease was similar to that seen after low-dose bleomycin exposure in SP-null mice on a C57Bl/6 x 129 background (Strandjord, 1999). It may be interesting to determine if this same study repeated in a SP-null mice on a 129 background would produce results similar to the high-dose bleomycin exposure investigation (Savani, 2000).

Type I collagen is the form of collagen found in most connective tissues. It is a triple-stranded molecule used to strengthen and support many bodily tissues such as cartilage, bone, and skin. There are two main components that make up this type of collagen and they are pro-alpha1 and pro-alpha2 encoded by the genes Col1A1 and Col1A2 respectively. Pro-alpha1 is the major component of type I collagen and is present in a 2:1 ratio with its pro-alpha 2 counterpart. Type III collagen is also found in connective tissues, often in conjunction with type I collagen. The different responses in the expression of these collagen mRNAs, especially Col1A2 and Col3, between the CRO asbestos exposure group and LA exposure group, regardless of WT or SP-null strain, further demonstrated the differences between the two amphibole forms. Much more research is needed to determine why these differences are occurring. Several possibilities exist including differences in fiber size, surface charge, and composition. To begin to try to answer some of these questions, I evaluated total collagen content in both WT and SP-null lungs exposed to the elutriated, shorter LA fibers. These results are presented in Appendix A.

Overall, the reduction of the fibrotic response in the SP-null mice could be due to either a decreased synthesis of collagen, an increased degradation of collagens, or maybe both. It could also be that the collagen synthesized in the SP-null mouse is much more fragile than WT collagen. Also, it has been shown that SPARC plays a role in the cellular remodeling of collagen (Iruela-Arispe, 1996). Therefore, in mice lacking SPARC, failed remodeling or fragile proteins would facilitate collagen degradation. This could explain the significant collagen decrease seen in the SP-null mice compared to WT mice after asbestos exposure, along with the decrease in collagen mRNA transcription. If the cells in the lungs of SP-null animals have a hindered ability to deposit collagen around the intruding asbestos fibers, decreased scar tissue formation would result and therefore oxygen transfer would improve regardless of the level of inflammation.

Though SPARC is important to the deposition of collagen in the fibrotic response, there was still an increase in lung collagen content seen at one month post CRO exposure in the SP-null mice. It has previously been shown that the morphology of the SP-null mouse lungs are normal (Strandjord, 1999) even though SPARC is known to play a role in pulmonary development (Sage, 1989; Strandjord, 1995). Aside from any subtle differences that may exist in the SP-null lung, it is apparent that another protein or proteins may compensate for SPARC in lung development. These proteins could include some of those with a high degree of homology to SPARC such as QR-1 (Casado, 1996) or Hevin (Girard, 1995; Soderling, 1997) also known as SC-1 or SPARC-like protein 1. Several studies have experimented with Hevin in particular and found that it functions similar to SPARC in the inhibition of cell attachment and spreading (Girard, 1996) and also that its expression is increased in the developing SPARC-null lung (Soderling, 1997). In order to determine if Hevin was compensating for SPARC in the SP-null lung exposed

to asbestos, I investigated Hevin expression levels in exposed lungs. These results can be found in Appendix B.

I have shown that in the response to a fibrosis-inducing insult like asbestos in the lung, WT C57Bl/6 present with significant increases not only in collagen synthesis and accumulation but also in SPARC expression. In the absence of this expression I have found that the fibrotic response of the lung after asbestos exposure is muted in terms of collagen deposition around the airways. However, the lack of SPARC does not reduce the level of inflammation in the lung. It may therefore be prudent to not only diminish SPARC expression in animals exposed to asbestos, but to also treat them with an anti-inflammatory agent to reduce the immune response as well.

Conclusion

Exposure to asbestos causes an increase in collagen accumulation in response to the presence of foreign fibers in the lung. A lack of SPARC in mice treated with CRO or LA decreased the amount of collagen accumulation in the lung, further supporting the idea that SPARC plays a significant role in the development of pulmonary fibrosis. Therefore, SPARC is a potential therapeutic target in humans suffering from fibrotic diseases. The next step will be to determine if the silencing of SPARC after an individual has been exposed to an insult like asbestos will reverse collagen accumulation in the lung or just slow future deposition. This is explored in the following Chapter.

References

Adamson IY and Bowden DH. Response of mouse lung to crocidolite asbestos. *J. Pathol.* 152(2): 109-117, 1987.

American Thoracic Society. Diagnosis of nonmalignant diseases related to asbestos. *Am. Rev. Respir. Dis.* 134(2): 363-368, 1986.

Asbestosis: A Medical Dictionary, Bibliography, And Annotated Research Guide To Internet References. San Diego, Calif: Icon Health Publications, 2004.

ATSDR. Health Consultation on Mortality from Asbestosis in Libby, Montana. Atlanta, GA: US Dept. of Health and Human Services. 2000.

Becklake MR. Asbestos-related diseases of the lung and other organs: their epidemiology and implications for clinical practice. *Am. Rev. Respir. Dis.* 114(1): 187–227, 1976.

Bienkowski RS and Gotkin MG. Control of collagen deposition in mammalian lung. *Proc. Soc. Exp. Biol. Med.* 209(2): 118-140, 1995.

Blake DJ, Bolin CM, Cox DP, Cardozo-Pelaez F, Pfau JC. Internalization of Libby amphibole asbestos and induction of oxidative stress in muring macrophages. Toxicol. Sci. 99(1): 277-288, 2007.

Bornstein P. Diversity of function is inherent in matricellular proteins: an appraisal of thrombospondin 1. *J. Cell. Biol.* 130: 503–506, 1995.

Bradshaw AD, Sage EH, SPARC, a matricellular protein that functions in cellular differentiation and tissue response to injury. *J Clin Invest.* 107(9):1049-54. 2001

Broekelmann TJ, Limper AH, Colby TV, McDonald JA. Transforming growth factor beta 1 is present at sites of extracellular matrix gene expression in human pulmonary fibrosis. *Proc. Natl. Acad. Sci. USA.* 88: 6642-6646. 1991.

Casado FJ, Pouponnot C, Jeanny JC, Lecoq O, Calothy G, Pierani A. QR1, a retina-specific gene, encodes an extracellular matrix protein exclusively expressed during retina differentiation. Mech. Dev. 54: 237-250. 1996.

Clark JG, Overton JE, Marino BA, Uitto J, Starcher BC. Collagen biosynthesis in bleomycin-induced pulmonary fibrosis in hamsters. *J. Lab. Clin. Med.* 96: 943-953. 1980.

Craighead JE, Abraham JL, Churg A, Green FH, Kleinerman J, Pratt PC, Seemayer TA, Vallyathan V, Weill H. The pathology of asbestos-associated diesaseas of the lungs and pleural cavities: diagnostic criteria and proposed grading schema. Report of the Pneumoconiosis Committee of the College of American Pathologists and the National Institute for Occupational Safety and Health. *Arch. Pathol. Lab. Med.* 106(11): 544-596, 1982.

Denis M. Neutralization of transforming growth factor-β1 in a mouse model of immune-induced lung fibrosis. *Immunology.* 82: 584-590. 1994.

Framson PE, Sage EH. SPARC and tumor growth: Where the seed meets the soil? *J Cell Biochem.* 92:679-90. 2004.

Francki A, McClure TD, Brekken RA, Motamed K, Murri C, Wang T, Sage EH. SPARC regulates TGF-beta-1-dependent signaling in primary glomerular mesangial cells. *J. Cell. Biochem.* 91: 915-925. 2004.

Girard JP, Springer TA. Modulation of endothelial cell adhesion by hevin, an acidic protein associated with highendothelial venules. *J. Biol. Chem.* 271: 4511-4517. 1996.

Girard JP, Springer TA. Cloning from purified high endothelial venule cells of hevin, a close relative of the antiadhesive extracellular matrix protein SPARC. Immunity. 2: 113-123. 1995.

Gunter ME, Dyar DM, Twamley B, Foit FF, and Cornelius S. Composition, Fe+3/Fe and crystal structure of non-abestiform and asestiform amphiboles from Libby, Montana, USA. *Am. Mineral.* 89:1579. 2003.

Iruela-Arispe ML, Vernon RB, Wu H, Jaenisch R, Sage EH. Type I collagen-deficient Mov-13 mice do not retain SPARC in the extracellular matrix: implications for fibroblast function. *Dev. Dyn.* 207: 171-183. 1996.

Jendraschak E and Sage EH. Regulation of angiogenesis by SPARC and angiostatin: implication for tumor cell biology*. Semin. Cancer Biol.* 7: 139-146, 1996.

Kuhn C and Mason RJ. Immunolocalization of SPARC, tenascin, and thrombospondin in pulmonary fibrosis. *Am. J. Pathol.* 147:1759-1769, 1995.

Lane TF, Sage EH. The biology of SPARC, a protein that modulates cell-matrix interactions. *FASEB J.* 8:163–173. 1994.

Latvala T, Puolakkainen P, Vesaluoma M, Tervo T. Distribution of SPARC protein (osteonectin) in normal and wounded feline cornea. *Exp. Eye Res.* 63: 579-584. 1996.

Liu JY, Brody AR. Increased TGF-beta1 in the lungs of asbestos-exposed rats and mice: reduced expression in TNF-alpha receptor knockout mice. *J. Environ. Pathol. Toxicol. Oncol.* 20: 97-108. 2001.

Meeker GP, AM Bern, IK Brownfield, HA Lowers, SJ Sutley, TM Hoefen, and JS Vance. The composition and morphology of amphiboles from the Rainy Creek complex, near Libby, Montana. *Am Mineral* 88:1955-1969. 2003.

Meeker GP, Brownfield IK, Clark RN, Vance JS, Hoefen TM, Sutley SJ, and Gent CA. The Chemical Composition and Physical Properties of Amphibole from Libby, Montana: A Progress Report, Abstract, 2001 health Effects of Asbestos, Oakland, CA. 2001.

Phan SH, Thrall RS, Ward PA. Bleomycin-induced pulmonary fibrosis in rats: biochemical demonstration of increased rate of collagen synthesis. *Am. Rev. Respir. Dis.* 121: 501-506. 1980.

Pociask DA, Sime PJ, Brody AR. Asbestos-derived reactive oxygen species activate TGF-beta1. *Lab. Invest.* 84: 1013-1023. 2004.

Porter PL, Sage EH, Lane TF, et al. Distribution of SPARC in normal and neoplastic human tissue. *J. Histochem. Cytochem.* 43:791-800. 1995

Puolakkainen P, Reed M, Vento P. et al. Expression of SPARC (Secreted Protein, Acidic and Rich in Cysteine) in healing intestinal anastomoses and short bowel syndrome in rats. *Dig. Dis. Sci.* 44: 1554-1564. 1999.

Putnam EA, Smartt A, Groves A, Schwanke C, Brezinski M, Pershouse MA. Gene expression changes after exposure to six-mix in a mouse model. *J. Immunotoxicol.* 5: 139-144. 2008.

Quinones F, Crouch E. Biosynthesis of interstitial and basement membrane collagens in pulmonary fibrosis. *Am. Rev. Respir. Dis.* 134: 1163-1171. 1986.

Reed MJ and Sage EH. SPARC and the extracellular matrix: implications for cancer and wound repair. *Curr. Top. Microbiol. Immunol.* 213: 81-94, 1996.

Reed MJ, Puolakkainen P, Lane TF, et al. Differential expression of SPARC and Thrombospondin 1 in wound repair: immunolocalization and in situ hybridization. *J. Histochem. Cytochem.* 41: 1467-1477. 1993.

Sage EH and Bornstein P. Extracellular proteins that modulate cell-matrix interactions. SPARC, tenascin, and thrombospondin. *J. Biol. Chem.* 266(23): 14831-14834, 1991.

Sage H, Vernon RB, Runk SE, Everitt EA, Angello J. Distribution of the calcium-binding protein SPARC in tissues of embryonic and adult mice*. J. Histochem. Cytochem.* 37: 819-829. 1989.

Savani RC, Zhou Z, Arguiri E, Wang S, Vu D, Howe CC, DeLisser HM. Bleomycin-induced pulmonary injury in mice deficient in SPARC. *Am. J. Physiol. Lung Cell. Mol. Physiol.* 279(4): 743-750, 2000.

Schiemann BJ, Neil JR, Schiemann WP. SPARC inhibits epithelial cell proliferation in part through stimulation of the transforming growth factor-b-signaling system. *Mol Biol Cell.* 14:3977-88. 2003.

Schulz A, Jundt G, Berghauser KH, Gehron-Robey P, Termine JD. Immunohistochemical study of osteonectin in various types of osteosarcoma. *Am. J. Pathol*. 132: 233–23, 1988.

Siddiq F, Sarkar FH, Wali A, Pass HI, Lonardo F. Increased osteonectin expression is associated with malignant transformation and tumor associated fibrosis in the lung. *Lung Cancer*. 45:197-205. 2004.

Smartt AM, Brezinski M, Trapkus M, Gardner D, Putnam EA. Collagen accumulation over time in the murine lung after exposure to crocidolite asbestos or Libby amphibole. *Environmental Toxicology.* In Press. 2008.

Soderling JA, Reed MJ, Corsa A, Sage EH. Cloning and expression of murine SC1, a gene product homologous to SPARC. J. Histochem. Cytochem. 45: 823-835. 1997.

Strandjord TP, Madtes DK, Weiss DJ, Sage EH. Collagen accumulation is decreased in SPARC-null mice with bleomycin-induced pulmonary fibrosis. *Am. J. Physiol.* 277: 628-635, 1999.

Strandjord TP, Sage EH, Clark JG. SPARC participates in the branching morphogenesis of developing fetal rat lung. *Am. J. Respir. Cell. Mol. Biol.* 13: 279-287. 1995.

Sullivan DE, Ferris M, Pociask D, Brody AR. The latent form of TGFbeta(1) is induced by TNFalpha through an ERK specific pathway and is activated by asbestos-derived reactive oxygen species in vitro and in vivo. *J. Immunotoxicol.* 5: 145-149. 2008.

Toti P, Buonocore G, Tanganelli P, Catella AM, Palmieri MLD, Vatti R, Seemayer TA. Bronchopulmonary dysplasia of the premature baby: an immunohistochemical study. *Pediatr. Pulmonol.* 24: 22-28. 1997.

Wang H, Workman G, Chen S, Barker TH, Ratner BD, Sage EH, Jiang S. Secreted protein acidic and rich in cysteine (SPARC/osteonectin/BM-40) binds to fibrinogen fragments D and E, but not to native fibrinogen. *Matrix Biol.* 25:20-6. 2006.

Woessner JF Jr. The determination of hydroxyproline in tissue and protein samples containing small proportions of this imino acid. Arch. Biochem. Biophys. 93: 440-447, 1961.

Wrana JL, Overall CM, Sodek J. Regulation of the expression of a secreted acidic protein rich in cysteine (SPARC) in human fibroblasts by transforming growth factor beta. Comparison of transcriptional and post-transcriptional control with fibronectin and type I collagen. *Eur. J. Biochem.* 197:519–528, 1991.

Wylie AG and Verkouteren JR. Amphibole asbestos from Libby, Montana, aspects of nomenclature. *Am. Mineral.* 85:1540-1542. 2000.

CHAPTER THREE

The Effect of SPARC Knockdown on Collagen Production in an Asbestos-Induced Model of Pulmonary Fibrosis

Abstract

Pulmonary fibrosis is a disease that affects millions of people worldwide. As of yet, treatments for the disease only help to improve quality of life but do not cure the disease itself. In order to begin to develop a cure, the process by which the disease is manifested must be interrupted. Specifically, both the inflammatory process and scar tissue formation must be inhibited. One step in that direction is the inhibition of the production of the matricellular protein SPARC (secreted protein acidic and rich in cysteine). I have previously shown that SPARC-null mice exposed to the fibrosis-inducing agent asbestos do not have the same increased level of collagen deposition in the lung as wild-type mice. The purpose of this investigation was to discover if the inhibition of SPARC in wild-type mice already demonstrating fibrosis will cause a similar reduction in collagen accumulation. Through the use of RNA interference, I have found that administration of SPARC small interfering RNA (siRNA) to animals with fibrosis decreased total collagen. However, the results of this study are preliminary and this topic needs further research before the true therapeutic potential of SPARC siRNA as a therapy can be determined.

Introduction

Asbestosis is a form of progressive pulmonary fibrosis induced by the inhalation of asbestos fibers (American Thoracic Society, 2004). Characteristics of the disease include both an inflammatory reaction with an infiltration of lymphocytes and macrophages as well as the increased proliferation of fibroblasts and increased accumulation of interstitial collagen and scar tissue in the alveoli (Ziesche, 1999). The development of scar tissue is caused by the overproduction and deposition of types I and III collagen by fibroblasts (Oriente, 2000).

Fibroblasts play crucial roles in the generation, deposition, and remodeling of the extracellular matrix during fibrosis development (Clark, 1995). After asbestos exposure, fibroblasts are recruited to the lung by the release of inflammatory mediators, TGF-β, and Platelet Derived Growth Factor (PDGF). Here they are stimulated by growth factor release to produce extracellular matrix components such as collagen and fibronectin (Clark, 1995; Singer, 1999). Typically, once an insult is destroyed through phagocytosis, the excess collagen is degraded by proteolytic enzymes such as MMPs (matrix metalloproteinases) secreted by both fibroblasts and macrophages (Mignatti, 1995). Unfortunately, asbestos trapped in the lung cannot be degraded so collagen continues to accumulate and cause scar tissue formation. It is therefore necessary to discover a mechanism to slow or stop collagen accumulation in the lung after asbestos exposure. One gene with the ability to alter levels of collagen deposition in the fibrotic lung is *Sparc* (Chapter 2; Strandjord, 1999; Savani 2000).

SPARC (secreted protein acidic and rich in cysteine), a matricellular protein involved in extracellular matrix regulation, has been shown to play a significant role in

fibrosis development. Studies have found SPARC to be over expressed in several fibrotic disorders including asbestosis (Smartt, 2008), scleroderma (Zhou, 2002), pulmonary fibrosis (Kuhn, 1995), renal interstitial fibrosis (Pichler, 1996), hepatic cirrhosis (Frizell, 1995), and atherosclerotic vascular lesions (Dhore, 2001). Though the role of SPARC in these disorders is not clear, it may be that SPARC is stimulating the TGF-β signaling pathways involving Smad2/3 or JNK (Schiemann, 2003; Francki, 2004). This would cause an increased transcription of collagen, a key component of the fibrotic response.

Using SPARC-null mice, previous studies have indicated that lack of SPARC in the lung leads to a diminished amount of collagen deposition in several models of pulmonary fibrosis (Chapter 2; Strandjord, 1999). SPARC-null mesangial cells have also been shown to display a decreased expression of both TGF-β1 and type I collagen until exogenous SPARC is added (Francki, 1999). Based on these observations, SPARC appears to have the ability to indirectly regulate collagen expression through its influence on the TGF-β signaling system in addition to its ability to directly bind collagen. Therefore, based on its ability to regulate collagen deposition in fibrotic disorders, SPARC is a candidate to target for the treatment of fibrosis.

In order to use the ability of SPARC to alter the expression of collagen for the treatment of fibrotic disorders, it must be determined if SPARC inhibition will can prevent or even reverse excess collagen deposition in those already suffering from fibrosis. Essentially the question becomes: can the inhibition of SPARC expression in a fibrotic model change the existing excess levels of collagen? Here I examine whether the inhibition of SPARC expression with small interfering RNA (siRNA) can influence the level of collagen deposition after asbestos exposure both *in vitro* using primary mouse lung fibroblasts and *in vivo* using C57Bl/6 wild-type mice.

Materials and Methods

Asbestos: Crocidolite asbestos was obtained from the Research Triangle Institute (Research Triangle Park, NC). The fiber size distribution of the asbestos has been previously reported (Blake, 2007). For reference, size parameters of the crocidolite were 0.16 μm in diameter and 4.59 μm in length, with a 34.05 aspect ratio. Samples were freshly prepared in sterile phosphate-buffered saline (PBS, pH 7.4) and sonicated before *in vivo* instillation (Putnam, 2008). CRO fibers were sterilized under UV light, suspended in sterile PBS, and triturated twenty times through a 22-gauge needle for *in vitro* studies.

Lentivirus Generation: Pre-designed SPARC siRNA plasmids contained in bacterial glycerol stocks were obtained from Sigma Adrich (Saint Louis, Missouri). Agar plates containing ampicillin as a selection agent were streaked with a small amount of the siRNA glycerol stocks. LB broth, also containing ampicillin, was inoculated with one colony selected from the agar plate. After incubation, plasmid DNA was isolated from the broth using a Qiagen Plasmid Midi Kit (Valencia, CA) and following the manufacturer's instructions. The plasmid DNA was then co-transduced with a ViraPower Packaging Mix in 293FT cells again following the manufacturer's instructions (Invitrogen, Carlsbad, CA). Virus was harvested from the media of the 293FT cells 72 hours post-transduction and stored at -80°C until ready for use.

Isolating Primary Fibroblasts: Fibroblasts were isolated from C57Bl/6 wild-type mice according to the procedure published in Migliaccio et al., 2005. Briefly, the lungs were

harvested from the mice and minced, then treated with collagenase. Digestion was stopped after the addition of serum and the cell suspension was layered on to a discontinuous Percoll gradient. Following centrifugation, the fibroblast/epithelial cell layer was removed and the cells washed in complete DMEM. The pellet was then resuspended in complete DMEM cultured at 37°C in 5% CO_2. Cells were subcultured at a 1:3 dilution when they were approximately 90% confluent.

Cell Culture: Primary fibroblasts were cultured in complete Dulbecco's Modified Eagle Medium (high glucose DMEM, 10% Fetal Bovine Serum, 1% Antibiotic/Antimycotic, and 1% sodium pyruvate: VWR, West Chester, PA) at 37°C in 5% CO_2. Primary cultures used were between passages 2 and 10 and typically the cells would double every 24 hours. 293FT cells were grown according to the manufacturer's instructions (Invitrogen, Carlsbad, CA).

Determining MOI: All 5 viruses used were titered according to the manufacturer's protocol (Invitrogen, Carlsbad, CA). Primary mouse lung fibroblasts at 60% confluence were grown in 6-well plates and treated with 2000, 4000, 6000, 8000, or 10,000 titered units (TU) of one of four SPARC siRNA viruses: 349, 350, 351, and 352. After 24 hours the viruses were removed and cells cultured for another 24 hours in complete media. Protein was harvested at the completion of the final incubation and analyzed for percent expression versus no virus treatment.

In vitro Virus Treatment: Primary mouse lung fibroblasts were cultured to 60% confluency then exposed to 5$\mu g/cm^2$ CRO or an equivalent volume of PBS for 6, 12, or 24 hours. Upon completion of the asbestos incubation, the media was replaced and no

virus (NV), non-target virus (-CNT), or virus 350 (833.33 TU/cm^2 – as determined by the MOI) was added to the new media. 24 hours later the virus containing media was removed and replaced with fresh media. Cells were harvested 24 hours later.

Sircol Assay: The Sircol Assay was performed according to the manufacturer's instructions (Biocolor, Carrickfergus, Northern Ireland). Briefly, treated fibroblasts were harvested by scraping in sterile PBS. The cells were sonicated for 30 seconds, mixed with the dye reagent, and centrifuged. Unbound dye was decanted and the remaining collagen bound dye was treated with the dye release reagent. Absorbance was then measured at 540nm.

Immunocytochemistry: Primary mouse lung fibroblasts were cultured on sterile coverslips for immunocytochemical analysis. At the completion of the experiment, the cells were fixed in 3% hydrogen peroxide in ice cold methanol. Cells were blocked in 4% Normal Rabbit Serum. SPARC expression was detected by incubation with anti-SPARC antibodies (R & D Systems, Minneapolis, MN) followed by labeling with Rabbit anti-Goat Alexa Fluor 568. Original magnification was 200X.

Mouse Treatment: All animal protocols were approved by the Institutional Animal Care and Use Committee. Mice were exposed to crocidolite according to methods previously described (Adamson, 1987). Briefly, pathogen-free 6-8 week old female and male C57Bl/6 WT mice were instilled intratracheally with 100 μg of crocidolite asbestos in 30μl PBS. Control mice received only PBS. Two months after asbestos instillation, mice were intratracheally instilled with 150,000 titered units of virus in 30μl complete media. Mice

were euthanized 3 months after asbestos instillation. The lungs of treated mice were then divided for RNA isolation, histology, protein isolation, and for the hydroxyproline assay. The section of lung used for each analysis was held constant.

Histology: Lungs were perfused and immersed in Histochoice (Amresco, Solon, OH) as a fixative. Fixed lungs were then embedded in paraffin and sliced into 7μm sections. Routine Gomori's trichrome staining was performed in order to visualize fibrillar collagen localization in the lung, and the sections examined under light microscopy.

RNA Isolation: Lung tissue samples were homogenized in 1ml of TRIZOL and RNA isolated following the manufacturer's protocol (Invitrogen, Carlsbad CA). The resulting RNA was purified using the RNeasy kit (Qiagen, Valencia, CA) and subsequently treated with DNAse (Qiagen, Valencia, CA).

Protein Isolation: Upon removal from the mouse, lung samples were snap frozen in liquid nitrogen. Lung tissue was then homogenized in lysis buffer (0.1% Triton X-100, 12.6mM sodium desoxycholate, 3.47mM sodium dodecyl sulfate, 1mM EDTA, 2mM phenylmethylsulphonylfluride, and protease inhibitor in PBS; Roche, Indianapolis, IN) and centrifuged to isolate protein. For in vitro isolation, cells were immersed in lysis buffer and scraped from the flask bottom. Total protein concentration was measured with the Lowry-like DC Protein Assay (Bio-Rad, Hercules, CA).

Western Blotting: Lung protein samples were separated by electrophoresis through 4-12% Bis-Tris NuPAGE gels (Invitrogen, Carlsbad, CA) then transferred to PVDF

membrane (Millipore, Billerica, MA). Membranes were blocked in a 5% milk in PBS-Tween20. Specific antibodies for both SPARC (R & D Systems, Minneapolis, MN) and β-Actin (Santa Cruz Biotechnology, Santa Cruz, CA) were used to detect protein levels, which were quantified using chemiluminescence on a Fuji gel documentation system (Fujifilm Life Sciences, Stamford, CT).

Hydroxyproline Assay: Quantitation of lung collagen content from exposed and control mice was determined by an assay for hydroxyproline content according to methods previously described (Woessner, 1961) with some modifications. The caudal lobe of the left lung was rinsed in PBS, minced and hydrolyzed in 1.5ml of 6N HCl overnight at 110°C. To 5µl of the hydrolysate were added 10µl of 0.02% methyl red and 2µl of 0.04% bromothymol blue. Sample volume was adjusted to 200µl with assay buffer (0.024M Citric Acid, 0.02M Glacial Acetic Acid, 0.088M Sodium Acetate, and 0.085M NaOH). The colorimetric assay was performed by the addition of 100µl of chloramine T solution and incubation at room temperature for 20 minutes. Following incubation, 100µl of dimethyl benzaldehyde solution was added and the solution incubated in a 60°C water bath for 15 minutes. Absorbance was measured at 550nM for each lung sample in a 96-well plate and quantitation of hydroxyproline was determined by comparison to a standard curve.

Statistical Analysis: Mean values for the hydroxyproline and Sircol assays were compared by one-way ANOVA with a Newman-Keuls test for multiple comparisons. Results are presented as mean values ± SEM. Densitometry values taken from replicate samples run on Western blots were normalized to β-Actin, then asbestos treated samples were

analyzed for percent expression versus the PBS treatment group. A one-way ANOVA with a Newman-Keuls test for multiple comparisons was used to verify the significance of the mean percent expression values and results are presented as mean values ± SEM versus PBS. Significant results were determined by $p < 0.05$.

Results

Lentivirus, a retrovirus commonly utilized as a gene delivery vector, was used to transduce cells with small interfering RNA (siRNA) directed against SPARC. These viruses have the ability to deliver genetic information directly into the nucleus of the host cell. The siRNA then are integrated into the host's DNA. The small hairpin RNA (shRNA) lentiviral vectors I used to inhibit *Sparc* expression were packaged into the pLKO.1-puro plasmid (Figure 21). This plasmid is capable of establishing either stable or transient transductions of shRNA as well as lentiviral particle production. pLKO.1-puro is especially useful when attempting long-term knockdown in sensitive cell lines such as primary cells. The sequences used for the shRNA inserts into the vectors can be found in Table 4 and the viruses containing these inserts will be referred to by the last three digits of the MISSION TRC No (Table 4 in blue).

Figure 21: MISSION RNAi pLKO.1-puro Vector Map

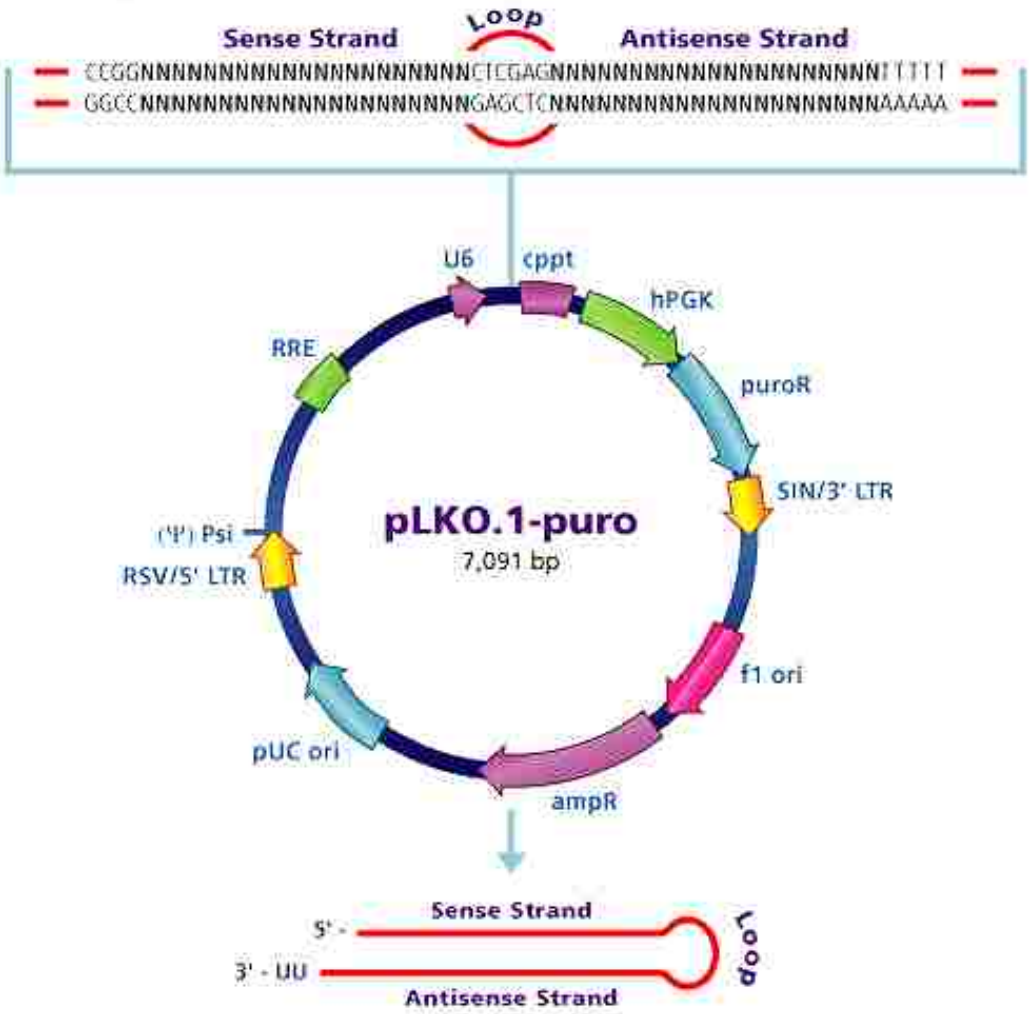

pLKO.1-puro vector description and features

Name	Description
cppt	Central polypurine tract
hPGK	Human phosphoglycerate kinase eukaryotic promoter
puroR	Puromycin resistance gene for mammalian selection
SIN/LTR	3' self inactivating long terminal repeat
f1 ori	f1 origin of replication
ampR	Ampicillin resistance gene for bacterial selection
pUC ori	pUC origin of replication
5' LTR	5' long terminal repeat
Psi	RNA packaging signal
RRE	Rev response element

Figure 21 Legend: This vector map of the Sigma-Aldrich MISSION RNAi pLKO.1-puro plasmid was provided by Sigma-Aldrich at http://www.sigmaaldrich.com/life-science/functional-genomics-and-rnai/shrna/library-information/vector-map.html. The sequences of the SPARC shRNA strands can be found in Table 4.

Table 4: SPARC shRNA Target Sequences

MISSION™ TRC No.	TRC shRNA Target Set Sequence
TRCN0000080349	CCGGCCTAGACAACGACAAGTACATCTCGAGATGTACTTGTCGTTGTCTAGGTTTTTG
TRCN0000080350	CCGGGAAGGTATGCAGCAATGACAACTCGAGTTGTCATTGCTGCATACCTTCTTTTTG
TRCN0000080351	CCGGCCATCATTGCAAACATGGCAACTCGAGTTGCCATGTTTGCAATGATGGTTTTTG
TRCN0000080352	CCGGCATCGGACCATGCAAATACATCTCGAGATGTATTTGCATGGTCCGATGTTTTTG

After each virus was made, the titer was verified following the manufacturer's protocols utilizing the puromycin resistance gene contained in the vector. The Non-Target (NT) Control contains 4 base pair mismatches within the short hairpin sequence to any known human or mouse genes and can therefore be used as a negative control. The GFP control contains TurboGFP, a variant of the green fluorescent protein copGFP, in place of shRNA and can therefore be used as a positive control to monitor transduction efficiency. The determined titers are listed in Table 5. Cells were infected with a serial dilution of titered units of each virus (Table 5), to determine the multiplicity of infection (MOI). The MOI was verified in order to determine the viral particle number of each virus. Next the knockdown ability of each virus was assayed by western blotting (Figure 22E). This would allow for selection of the proper virus for both the *in vitro* and *in vivo* portions of the study. The viruses were found to have the following maximum SPARC knockdown abilities: 349-50% (Figure 22A), 350-63% (Figure 22B), 351-38% (Figure 22C), and 352-36% (Figure 22D). From these results, virus 350 was used for *in vitro* studies and 352 for *in vivo* studies. Virus 352 was chosen for *in vivo* studies even though it had the least amount of SPARC knockdown because it had the highest titer and I could therefore instill more titered units into the mice without fear of them drowning, an adverse event that can occur during instillation. In order to enable the instillation of even more titered units (TU) *in vivo*, virus 352 was concentrated following the manufaturer's instructions. The final concentrated titer for virus 352 was 5×10^6 TU/ml.

Table 5: Lentivirus Titers

VIRUS	SAMPLE						TITER
	CNT	1	2	3	4	5	
349	0	2,000	4,000	6,000	8,000	10,000	2×10^5
350	0	2,000	4,000	6,000	8,000	10,000	2×10^4
352	0	2,000	4,000	6,000	8,000	10,000	1×10^5
352	0	2,000	4,000	6,000	8,000	10,000	5×10^5
NT Control	0	2,000	4,000	6,000	8,000	10,000	2×10^4
GFP Control	Direct from the manufacturer (Sigma Aldrich)						1×10^6

Figure 22: SPARC siRNA Virus Knockdown Ability

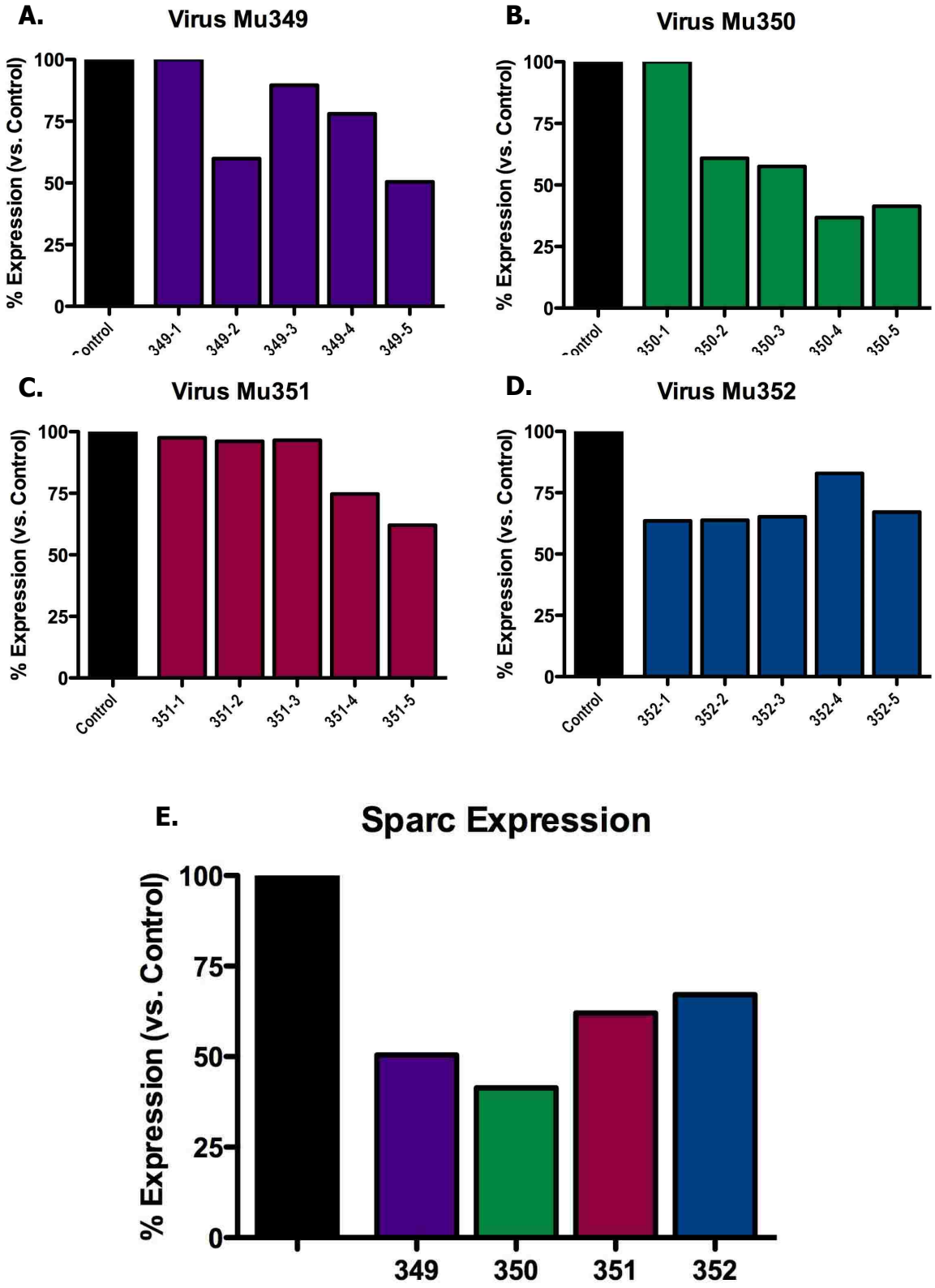

Figure 22 Legend: Primary mouse lung fibroblasts at 60% confluence were grown in 6-well plates and treated with equal titered units of one of four viruses containing siRNA directed against SPARC: 349, 350, 351, and 352. After 24 hours the viruses were removed and cells cultured for another 24 hours in complete media. The titered units used for each sample are listed on Table 5. Protein was harvested at the completion of the final incubation and analyzed by immunoblotting to determine the percent expression versus no virus treatment. Results are presented as percent expression versus a no virus control. All four viruses had decreases in SPARC protein expression ranging from 63% to 36%.

Primary mouse fibroblasts were isolated from the lungs of WT C57Bl/6 mice and cultured for *in vitro* analysis (Migliaccio, 2005). Cells were then exposed to 5μg/cm^2 of crocidolite (CRO) asbestos for 6, 12, or 24 hours. Initially, immunocytochemistry (ICC) was performed to visually determine if there were any differences in SPARC expression. ICC is also a useful tool to identify the cellular location of SPARC expression with or without asbestos treatment. After 6 hours of asbestos treatment, the CRO treated fibroblasts appeared to have higher SPARC expression than PBS treated cells (Figure 23). Transduction of either the NT control virus or virus 350 did not appear to change this. This trend continued at both 12 hours (Figure 24) and 24 hours (Figure 25) of asbestos exposure. However, it was difficult to find an area to image on slides covered in cells treated with both CRO and virus 350. Those cell clusters that stained for SPARC may not have received the virus. To be sure, western blotting is needed to quantify SPARC protein expression. No differences were seen over time. It is also interesting to note that it appears as though SPARC is localized to the cytoplasm until exposed to asbestos where it may be moving into the nucleus or localizing to the nuclear membrane. Confocal microscopy along with markers for nuclear membrane bound protein could be used to verify this.

Figure 23: 6 Hour SPARC Immunocytochemistry

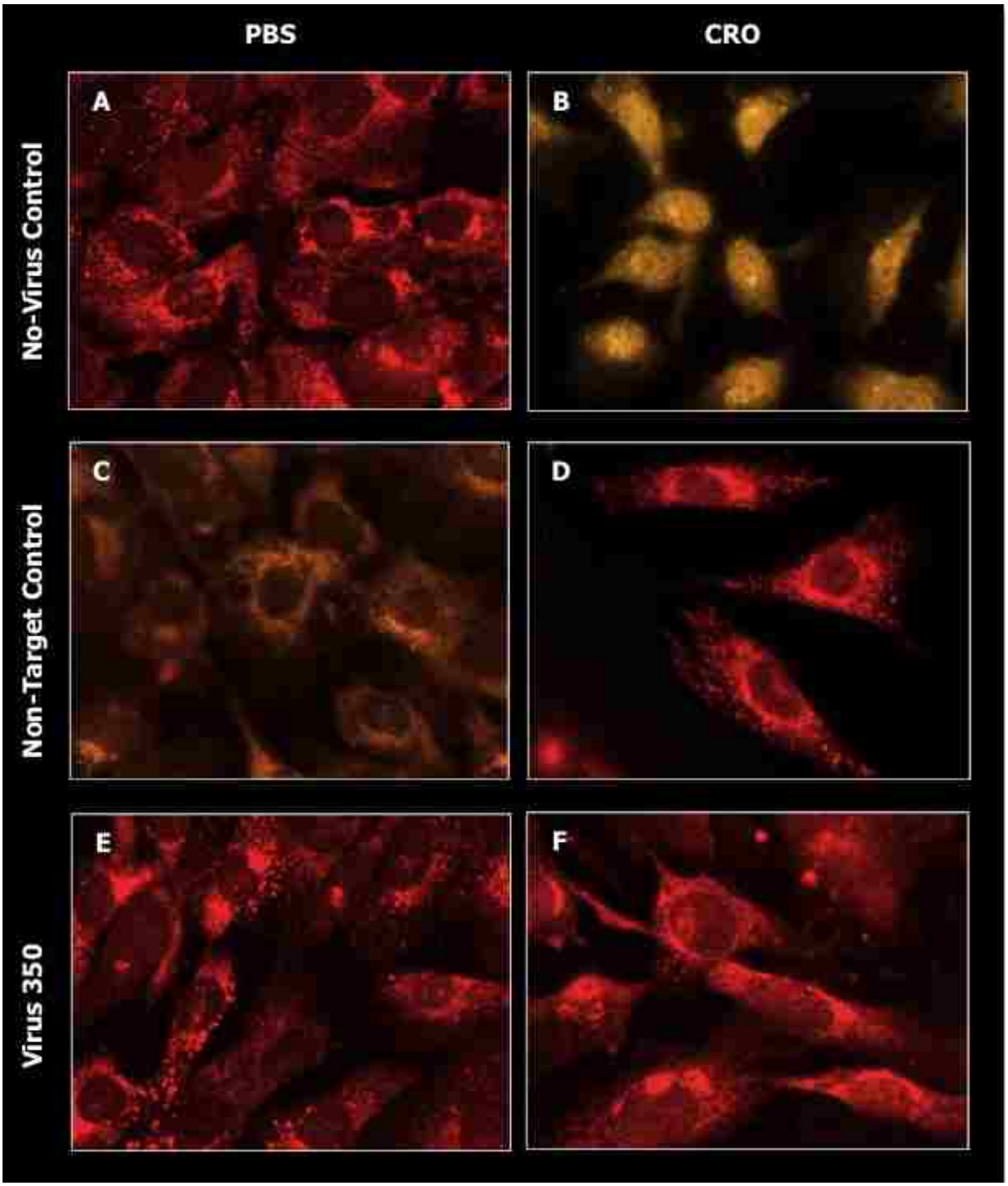

Figure 23 Legend: Primary mouse lung fibroblasts were plated at equal density on sterile coverslips in complete medium. Once they were approximately 50% confluent, CRO was added to the media. 6 hours later the asbestos containing media were removed, the cells quickly rinsed with sterile PBS and complete media containing either no virus (NV), a Non-Target virus (-CNT), or virus 350 was added. 24 hours post transduction, the virus containing media were removed and replaced with complete media for another 24 hours before the cells were fixed for detection of SPARC by immunostaining. Images are 200x.

Figure 24: 12 Hour SPARC Immunocytochemistry

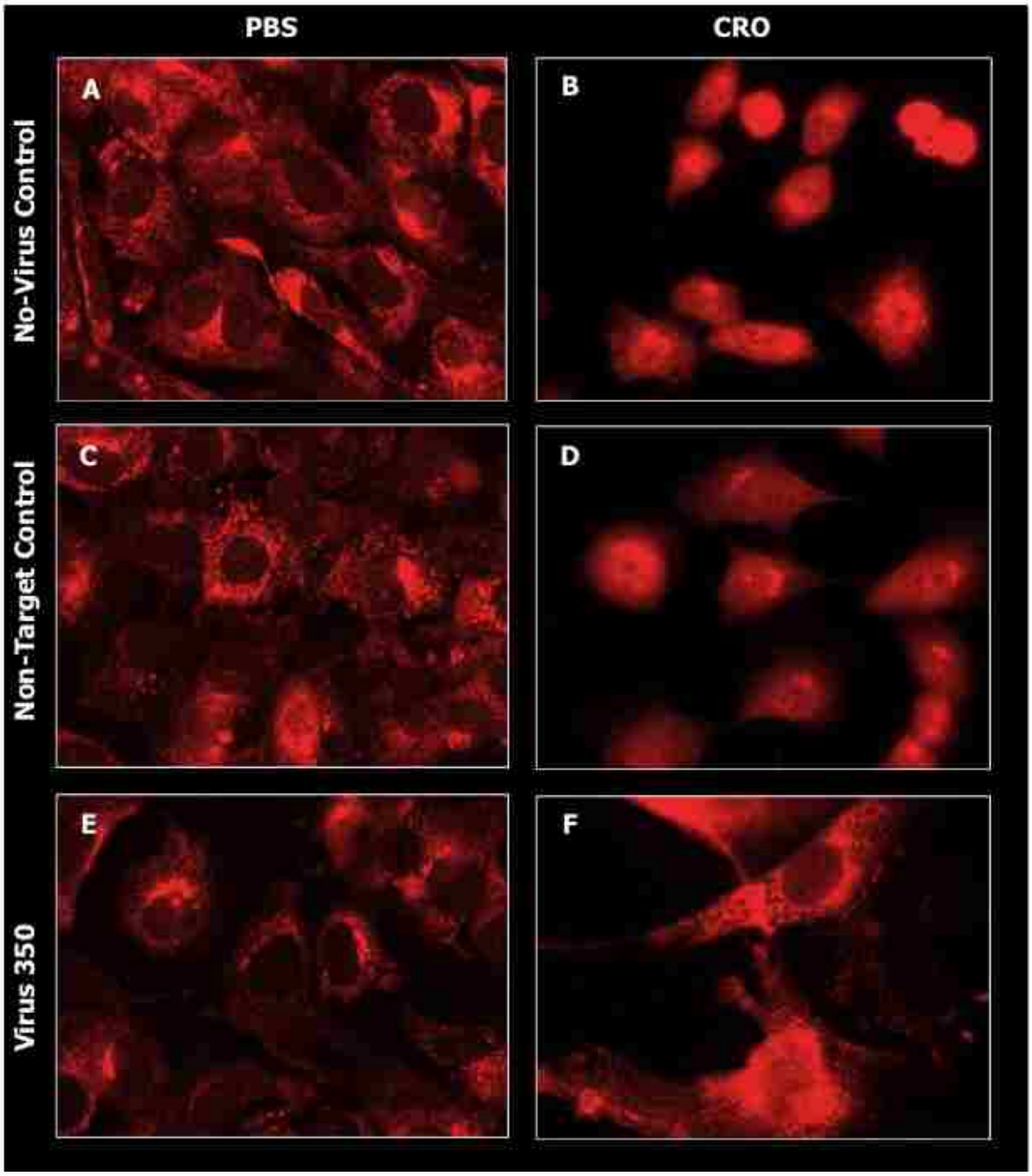

Figure 24 Legend: Primary mouse lung fibroblasts were plated at equal density on sterile coverslips in complete medium. Once they were approximately 50% confluent, CRO was added to the media. 12 hours later the asbestos containing media were removed, the cells quickly rinsed with sterile PBS and complete media containing either no virus (NV), a Non-Target virus (-CNT), or virus 350 was added. 24 hours post transduction, the virus media was removed and replaced with complete media for another 24 hours before the cells were fixed for immunostaining with antibodies directed against SPARC. Images are 200x.

Figure 25: 24 Hour SPARC Immunocytochemistry

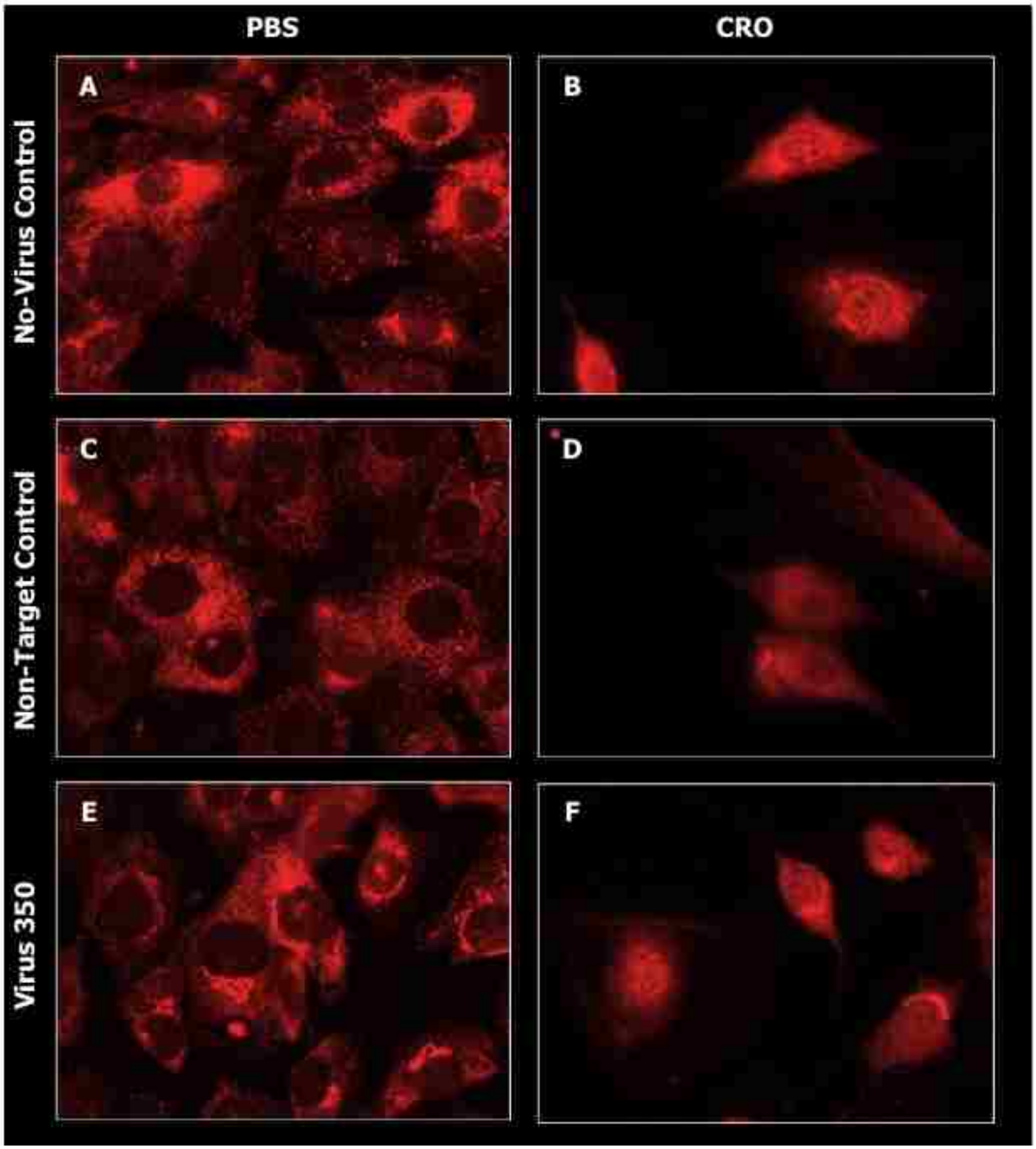

Figure 25 Legend: Primary mouse lung fibroblasts were plated at equal density on sterile coverslips in complete medium. Once they were approximately 50% confluent, CRO was added to the media. 24 hours later the asbestos containing media were removed, the cells quickly rinsed with sterile PBS and complete media containing either no virus (NV), a Non-Target virus (-CNT), or virus 350. 24 hours post transduction, the virus media was removed and replaced with complete media for another 24 hours before the cells were fixed for detection of SPARC by immunostaining. Images are 200x.

To verify if there were any quantifiable differences in SPARC expression in the treated fibroblasts, western blotting was performed on protein isolated from treated cells (Figure 26). The cells exposed to PBS alone (No virus – NV) or PBS in addition to –CNT virus or virus 350 show no significant differences in SPARC expression (Figure 26A). Compared to the NV and –CNT virus treatment groups, the cells treated with virus 350 show significant decreases in SPARC protein after CRO exposure but not after PBS exposure (Figures 26A and 26B). The virus was successful at reducing SPARC expression when determining the MOI (Figure 22) but was not successful at reducing the level of SPARC in cells treated with both virus 350 and PBS. This is most likely a result of the PBS treated cells in this experiment being too confluent at the time of virus transduction. Because these PBS treated cells were not replicating, the siRNA may not have incorporated into host DNA as efficiently as in the cells treated with CRO.

Figure 26: In Vitro SPARC siRNA Virus PBS and CRO Western Blots

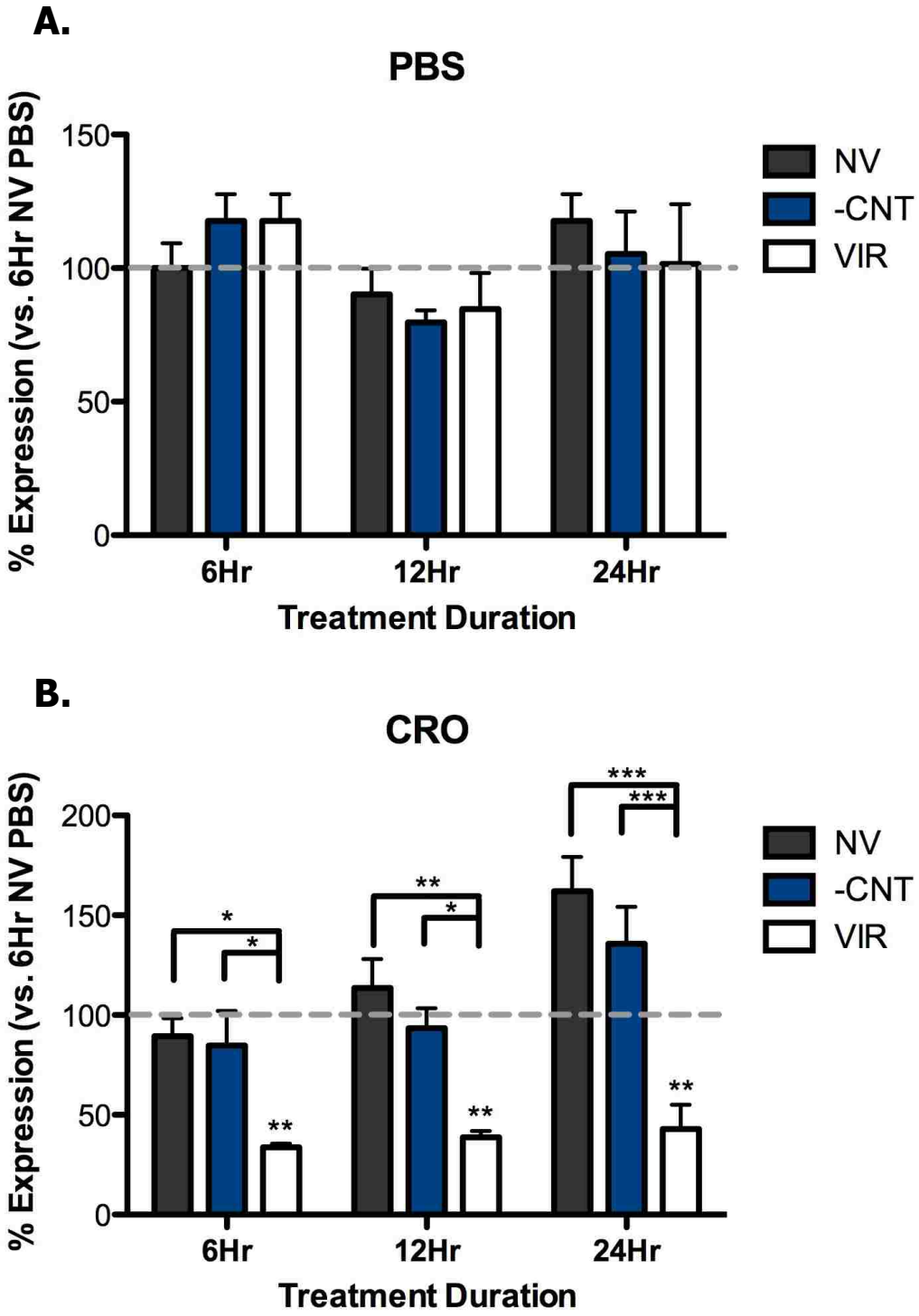

Figure 26 Legend: Primary mouse fibroblasts were plated at equal densities in T25 flasks and treated as described in Figure Legends 23-25. Upon treatment completion, protein was harvested, quantified, and run in equal amounts on western blots to determine SPARC protein expression. Results are presented as mean percent expression vs. 6Hr NV PBS ± SEM. No significant differences were detected in PBS treated cells at any time point (A). At all three time points there is significantly less SPARC protein in the 350 virus exposed cells than either NV or -CNT exposed cells after CRO treatment (B). Also there is significantly less SPARC expression in the cells exposed to both virus 350 and CRO at every time point compared to the cells exposed to no virus and PBS for 6 hours (B). * = $p < 0.05$, ** = $p < 0.01$, *** = $p < 0.001$

Changes in each viral treatment group were also analyzed to determine differences over time and between PBS and CRO exposure (Figure 27). When comparing cells infected with NV, those cells exposed to CRO versus those exposed to PBS show no differences in SPARC expression (Figure 27A). Though it does appear as though there is a slight increase in expression in the CRO treated cells at 24 hours when compared to PBS, and there is a significant increase in SPARC expression in the CRO treatment group from 6 to 24 hours. The results of SPARC expression analysis in the –CNT viral group directly mimic those of the NV viral group with the only significant difference being the increase in expression in the CRO treatment group from 6 to 24 hours (Figure 27B). The cells in the 350 virus treatment group have significantly less SPARC expression in CRO treated fibroblasts than PBS treated fibroblasts at every time point (Figure 27C). Again, this could be due to the PBS treated cells being too confluent at the time of virus transduction. No significant differences in the virus 350 exposure group were detected over time. Overall, treatment with the virus containing siRNA directed against SPARC was capable of significantly decreasing SPARC expression after CRO exposure.

Figure 27: In Vitro SPARC siRNA Virus, -CNT Virus, and No Virus Western Blot

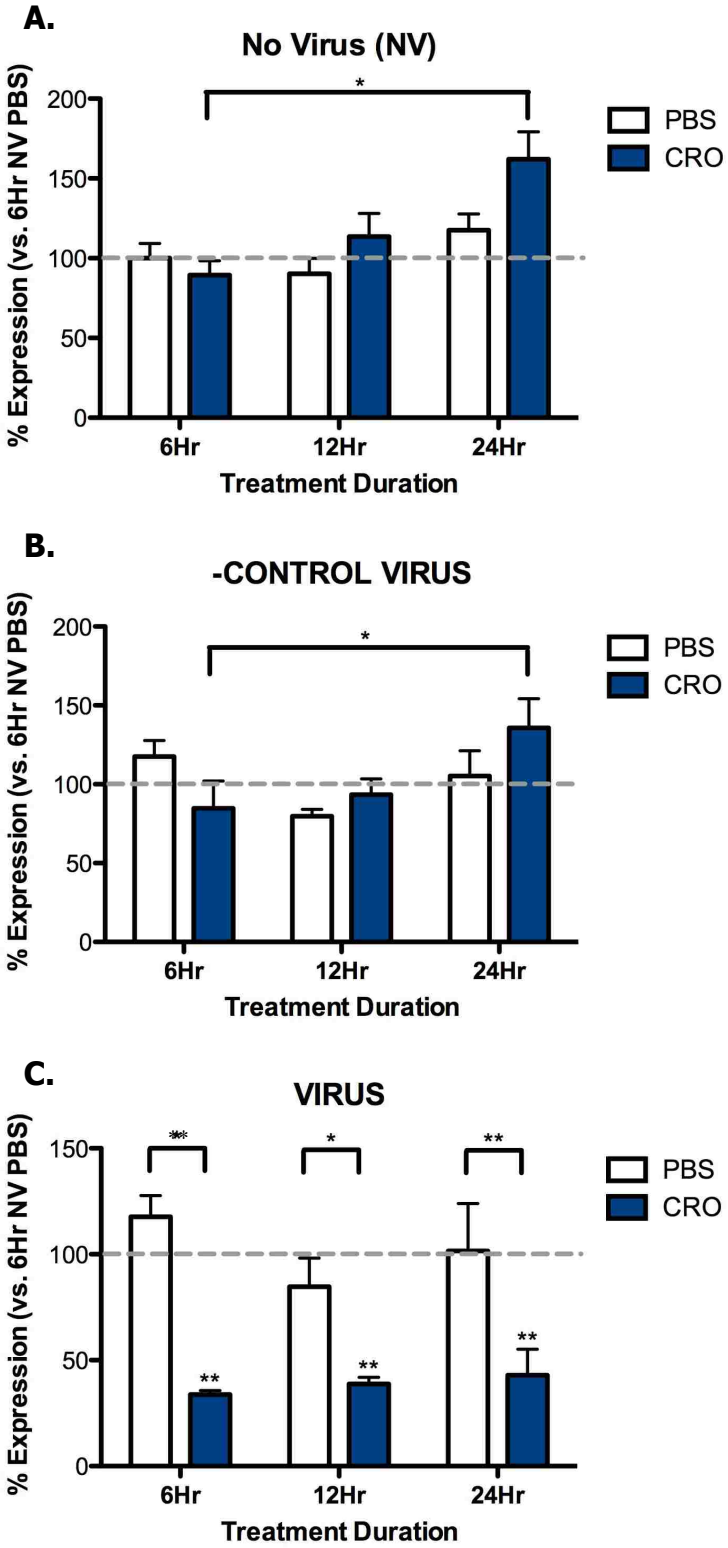

Figure 27 Legend: The data presented in Figure 26 was re-analyzed to compare PBS treatment to CRO treatment and to compare SPARC expression levels over time. Results are again presented as mean percent expression vs. 6Hr NV PBS ± SEM. In both the NV (A) and –CNT (B) groups exposed to CRO showed a significant increase in SPARC protein from 6 to 24 hours but no significant differences when comparing CRO exposure to PBS exposure. The 350 Virus treatment groups showed a significant decrease in SPARC expression after CRO treatment compared to PBS treatment (C). * = $p < 0.05$, ** = $p < 0.01$, *** = $p < 0.001$

The Sircol Assay was used to determine if the decreased SPARC protein expression in CRO exposed fibroblasts transduced with virus 350 has any effect on collagen deposition (Figure 28). The Sircol Assay is a quantitative method for the analysis of acid-soluble collagens both *in vivo* and *in vitro*. It is capable of measuring mammalian types I to IV collagen. Mouse primary lung fibroblasts were exposed to either PBS or CRO for 6, 12, or 24 hours and then to either a no-virus control (NV), non-target control (-CNT), or virus 350 (VIRUS) containing the siRNA directed against SPARC for 24 hours. Analysis of both the 6 hour and 12 hour exposure time points revealed no significant differences between cells exposed to PBS and cells exposed to CRO, though it appeared as if cells treated with CRO had slightly more collagen than their PBS treated counterparts in both NV and -CNT treated controls (Figures 28A and 28B). It also appeared as though cells treated with both CRO and virus 350 had less collagen content than either of the CRO treated viral control cells at both the 6 hour and 12 hour time points, however, the difference was again not significant. At 24 hours of exposure, an increase in collagen was seen in CRO exposed cells treated with either the NV or –CNT controls compared to their PBS exposed counterparts, this increase being significant in the –CNT treatment group (Figure 28C). No such increase was seen in the cells exposed to both CRO and virus 350 compared to their PBS exposed counterparts. In addition, a significant decrease was found in the cells exposed to both CRO and virus 350 compared to those exposed to CRO and the non-target control. At 24 hours of exposure, the siRNA directed against SPARC induced a significant decrease in collagen deposition in wild-type mouse lung fibroblasts.

Figure 28: In Vitro SPARC siRNA Virus Sircol Assay

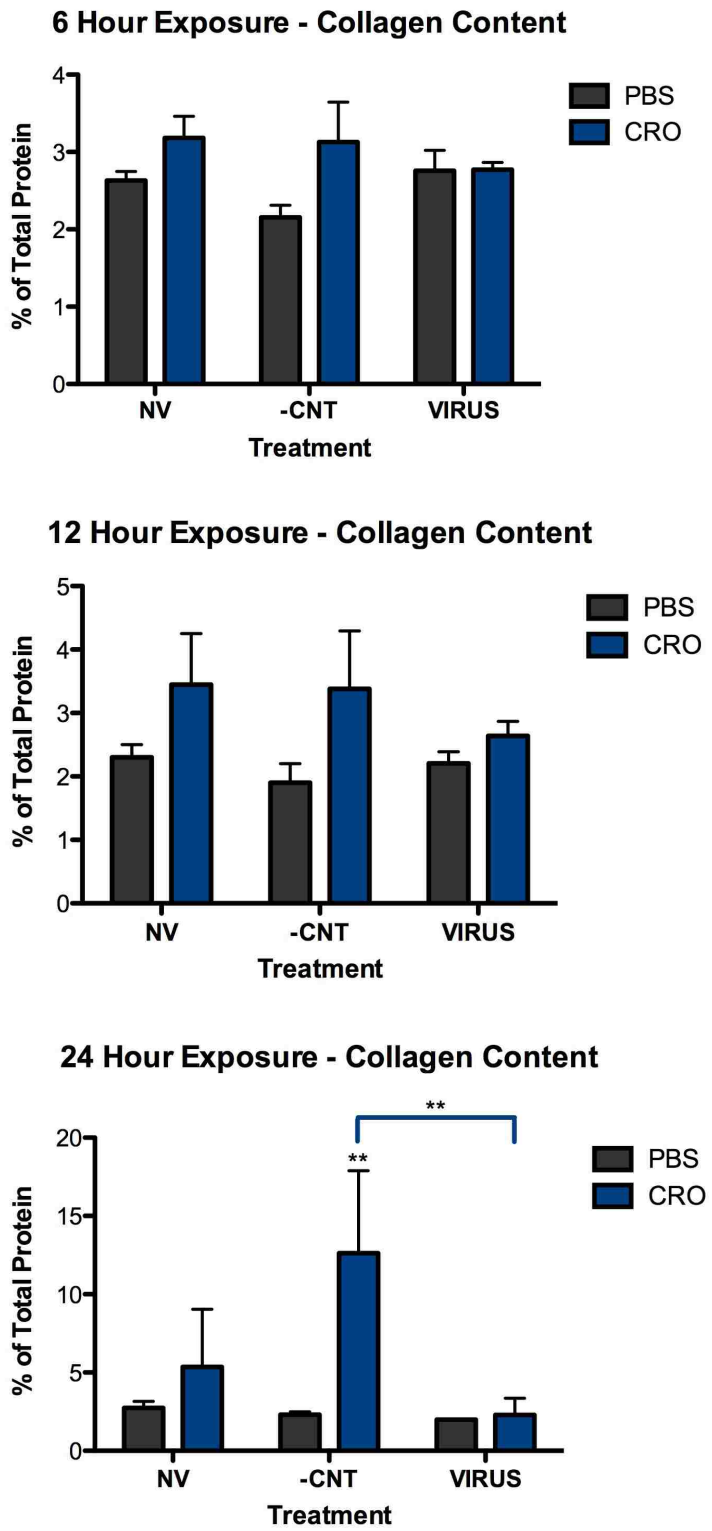

Figure 28 Legend: Primary mouse fibroblasts were plated at equal densities in 6-well plates and treated as described in Figure Legends 23-25. Upon treatment completion, cells were harvested with cell scrapers and total collagen content was quantified with the Sircol Assay. This value was normalized against the total protein concentration and results are presented at the mean percentage of collagen in the total protein ± SEM. No significant changes were detected at either 6 (A) or 12 (B) hours of CRO/PBS exposure. At 24 hours of CRO or PBS exposure (C), the cells exposed to the non-target control virus (-CNT) had significantly more collagen content if they were also treated with CRO than if they were treated with PBS. Furthermore, the cells treated both CRO and the –CNT virus had significantly more collagen content than the cells treated with both CRO and virus 350.

As a preliminary study with limited available mice, I next used WT C57Bl/6 mice who had already been exposed to CRO asbestos for two months to determine if siRNA directed against SPARC could also decrease SPARC expression *in vivo* and help to reduce some of the excess collagen deposited during the development of asbestosis. Virus 350 was intratracheally instilled after the two month asbestos exposure time and mice were sacrificed one month following virus instillation. Therefore, total asbestos exposure time was three months at the completion of the experiment. Unfortunately the negative non-target control virus was not ready when the mice were, so the GFP lentivirus was used instead as a control. This portion of experiments should be repeated using the –CNT virus.

Western blotting for SPARC protein revealed no significant differences between the GFP control group, media vehicle control group, or 352 Virus group (Figure 29). It does appear as though the mice exposed to CRO have slightly more SPARC than the PBS exposed mice in both the GFP and Media control groups, but the difference is not significant. This mimics the results seen in the previous 3 month WT study (Chapter 2) presented in Figure 13. SPARC was no longer suppressed at the completion of the incubation period; however, this may be because not enough virus was introduced into the lung to induce a detectable decrease in SPARC expression. However, collagen deposition could still have been altered if some of the SPARC present in the lung was silenced.

Figure 29: In Vivo SPARC siRNA Virus Western Blot

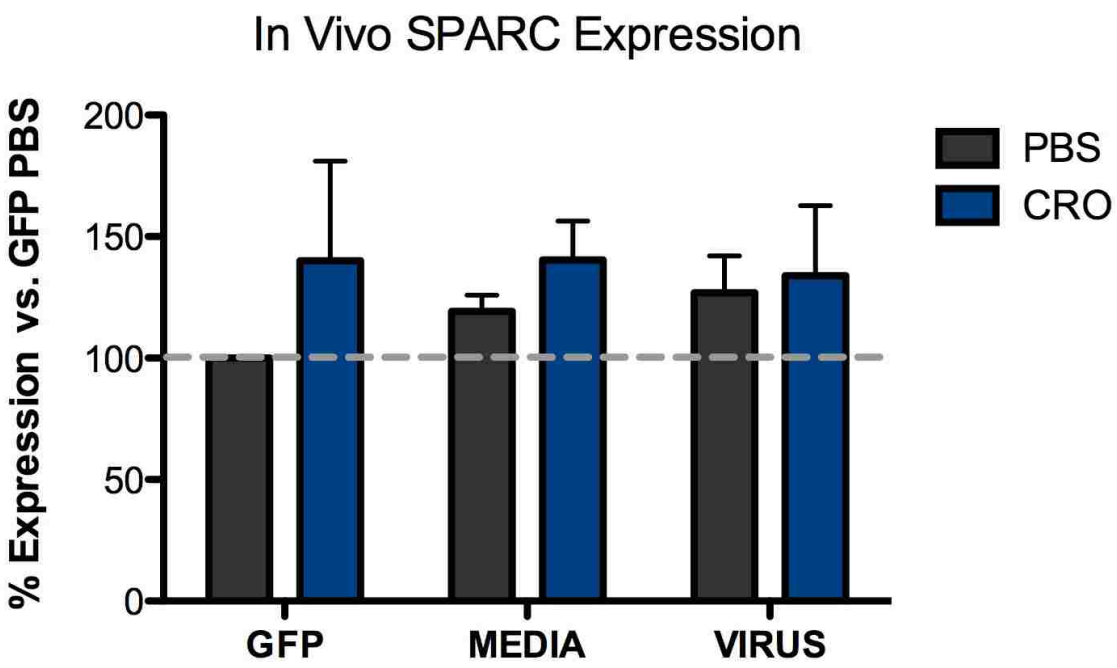

Figure 29 Legend: Immunoblotting of SPARC protein from the lungs of C57Bl/6 mice exposed to PBS or CRO for two months followed by GFP virus, virus 352, or media as a vehicle control for an additional month. Results for each treatment group (n = 5 – 8 per group) were normalized to β-actin and are presented as the mean percent expression versus GFP PBS ± SEM. No significant differences in SPARC protein expression were found.

Histological examination revealed that collagen deposition around the airways was increased in the crocidolite treated animals (collagen appears blue-green in Gomori Trichrome-stained sections, indicated by the arrows, Figure 30D, 30E, and 30F), which represented the typical pattern of fibrosis seen in animals exposed to crocidolite. Multi-nucleated giant cells and activated macrophages are also apparent in the CRO-exposed animals which resembles what was previously found for three month treated wild type mice (Figure 16), a further indication of the chronic inflammation and fibrosis. PBS treated mice did not show signs of excessive collagen deposition or inflammation which is also similar to the results previously presented for 3 month wild-type mice (Figure 30A, 30B, and 30C). Instillation of GFP control virus (GFP), no-virus (NV) or virus 352 did not appear to significantly alter the level of collagen deposition. However, it does appear that mice instilled with both CRO and virus 350 (Figure 30F) had a decreased level of collagen accumulation in comparison to the mice exposed to both CRO and GFP (Figure 30D) or CRO and NV (Figure 30F). In order to verify this, total collagen content of the lungs must be verified.

Figure 30: In Vivo SPARC siRNA Virus Histology

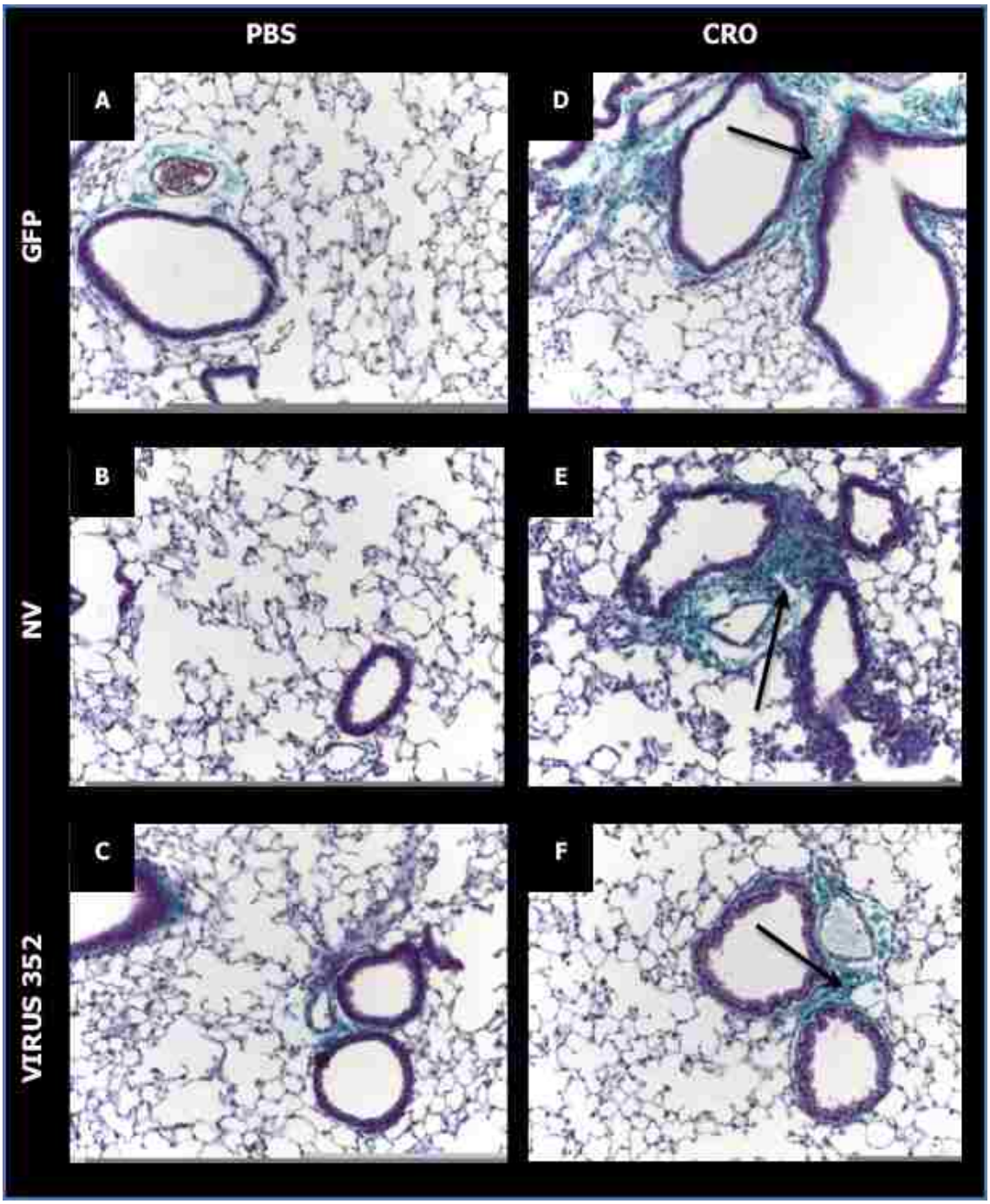

Figure 30 Legend: Gomori Trichrome-stained 7 μM sections of mouse lungs from C57Bl/6 WT mice instilled with CRO or PBS for two months followed by treatment with either GFP virus (GFP), no-virus (NV), or virus 352 for one additional month (200X original magnification). Blue-green staining indicates collagen deposition and arrows point to areas of increased accumulation. In every viral treatment group (GFP, NV, and 352), the airways of the amphibole exposed mice showed much higher levels of collagen accumulation and inflammation than PBS exposed mice. It does appear, however, that the level of collagen accumulation in the mice treated with both CRO and virus 350 (F) was less than that of the mice treated with CRO and either NV (E) or GFP (D).

The hydroxyproline assay was used to quantify total collagen content in the lungs of treated mice in order to determine if the SPARC siRNA virus had any effect on alleviating collagen deposition after animals had already been exposed to asbestos and developed fibrosis. No significant differences were found in total hydroxyproline between CRO and PBS exposed mice in either the GFP control group or the 350 virus group (Figure 31A). The media control group had significantly more hydroxyproline after CRO exposure than after PBS exposure. To analyze how this result compared to the previous results presented in Chapter 2 for the 3 month treated WT mice, the results were basically identical (Figure 31B). This indicates how consistent and reliable this assay is to determine total collagen. Even though there was no detectable decrease in SPARC protein expression in the mice exposed to the virus containing siRNA directed against SPARC, the virus was able to reduce collagen levels back to PBS baselines.

Figure 31: In Vivo SPARC siRNA Virus Hydroxyproline Assay

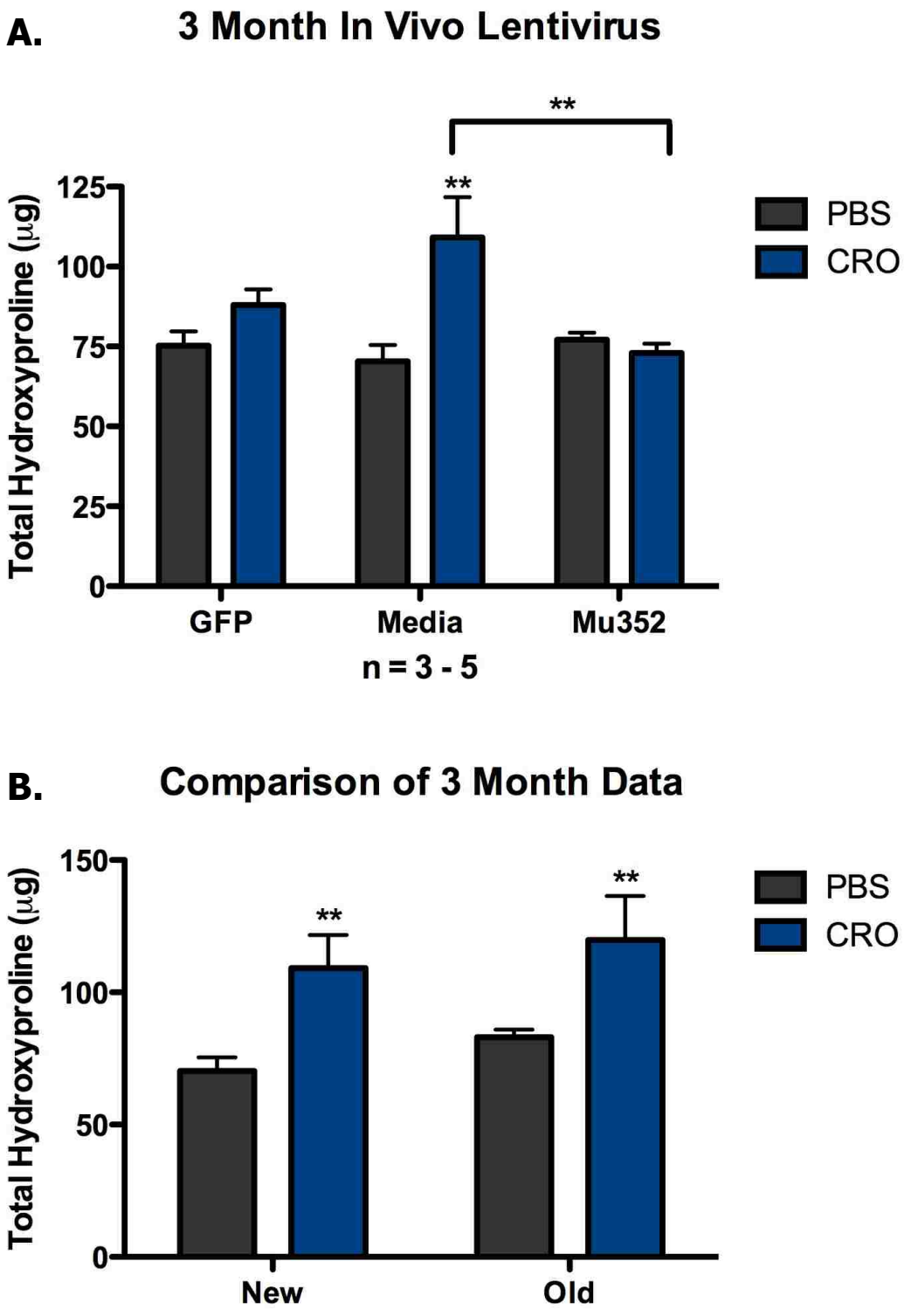

Figure 31 Legend: Total hydroxyproline content was determined from the lungs of C57Bl/6 mice exposed to PBS or CRO for two months followed by GFP virus, virus 352, or media as a vehicle control for an additional month. Collagen content was determined by measuring hydroxyproline levels in replicate animals. All experiments were done in triplicate. Results are presented as mean values ± SEM for each treatment/time (all groups have n = 4 - 5). Only the CRO exposed Media control group had significantly more hydroxyproline than the PBS exposed counterparts (A). There was also a significant decrease in the amount of hydroxyproline present in the lungs of CRO exposed 350 virus mice compared to the CRO exposed Media control mice. When comparing the data found for both the PBS and CRO exposed media control groups with the previously presented WT 3 month data from Figure 10, the results appear to be nearly identical (B). * = $p<0.05$, ** = $p<0.01$, *** = $p<0.001$.

Discussion

Fibroblasts are activated in fibrotic disorders where they are stimulated to produce extracellular matrix components such as collagens (Claman, 1991). The biosynthesis and deposition of these components are regulated by matricellular proteins and growth factors (Varedi, 1997). One such matricellular protein with the ability to regulate collagen deposition in fibrotic disorders is SPARC. It remains to be seen, however, if the reduction of SPARC in individuals already suffering from fibrosis can halt or even reverse the excess collagen accumulation.

The utilization of RNA interference for gene silencing and knockdown is common. It is an efficient method to facilitate the degradation of target mRNA and thus achieve the resulting gene silencing (Wall, 2003). The use of this technology has already been suggested for use therapeutically on genes like the tumor suppressor p53 and the Ras oncogene (Dykxhoorn, 2003). In this study I used RNAi to silence SPARC expression both *in vitro* and *in vivo* after asbestos exposure to evaluate the effect of the silencing on collagen accumulation.

In primary mouse fibroblasts isolated from the lungs of wild-type C57Bl/6 mice, lentiviral vector delivered SPARC siRNA was successful in reducing SPARC protein expression up to 63%. Once the cells were exposed to CRO asbestos, SPARC expression was slightly increased though not significantly so when compared to PBS. Transduction of the CRO exposed fibroblasts with SPARC siRNA virus caused a significant decrease in SPARC expression, though PBS exposed cells that were also transduced with the siRNA virus did not show a decrease in SPARC expression. The reduction of SPARC expression in the CRO treated cells resulted in less collagen accumulation, especially after 24 hours

of exposure, which is similar to a previous investigation where it was reported that the use of SPARC siRNA was associated with a decrease in type I collagen levels in human fibroblasts (Zhou, 2005).

The lack of a reduction in SPARC expression in the PBS treatment group was most likely due to the higher confluency of the PBS treated cells which may have hindered the ability of the siRNA plasmid to incorporate into the host DNA. It was apparent that cells exposed to CRO were much less viable than cells exposed to PBS for the experiment duration. Fibroblasts exposed to CRO were approximately 50% confluent at the completion of the experiment whereas the PBS exposed fibroblasts were almost fully confluent. The PBS treated cells were therefore no longer dividing as much as the CRO treated cells when the virus was administered. If the lentivirus did not incorporate effectively into the DNA of dividing cells, I would hypothesize that little virus made it into the PBS treated fibroblasts, which would result in less siRNA production and subsequently less SPARC knockdown.

Due to the ability of SPARC siRNA to decrease the expression of both SPARC and collagen in vitro, I decided to use the lentivirus in vivo after mice had already developed fibrosis. This would demonstrate the ability of SPARC siRNA to be used therapeutically in individuals with existing fibrotic conditions. Initially, it appeared that administration of the SPARC siRNA lentivirus to wild-type mice suffering from asbestos-induced fibrosis did not significantly decrease SPARC expression in the lung. However, CRO exposed mice who also received siRNA virus appeared to have less collagen accumulation than the mice exposed to both CRO and the GFP control virus or CRO and no-virus. This decrease in collagen deposition seen histologically was found to be significant after quantification of total lung collagen. This indicates that waiting a month after virus

application for sacrifice may have been too long to see the effects of the virus on SPARC expression. Regardless the siRNA was capable of not only halting collagen deposition but also reducing the already present levels back to baseline. The mechanism by which SPARC could be responsible for this reduction warrants further study.

The fibrotic mice instilled with the GFP lentivirus did not show the same significant increase in total collagen as the media vehicle control fibrotic mice. This may indicate that the significant decrease in collagen in the siRNA virus instilled animals was not a result of the SPARC siRNA but maybe an artifact of the viral vector. In order to confirm the results seen here, collagen content should be quantified from fibrotic mice instilled with the non-target (NT) negative control virus. This virus was not ready for use in the in vivo study when the mice were ready. Once the ability of SPARC siRNA to reduce collagen deposition in the fibrotic lung has been confirmed, it may be developed into a potential therapeutic agent for the treatment of not only pulmonary fibrosis but other fibrotic diseases as well.

Conclusion

Millions of people currently suffer from pulmonary fibrosis without any hopes of cure. It is already known that a complete lack of SPARC in mice treated with asbestos or bleomycin as a fibrosis-inducing agent decreases the amount of collagen accumulation in the lung. Here I show that the use of RNA interference to silence SPARC expression in mice already suffering from pulmonary fibrosis may have the ability to reverse collagen deposition in the lung. With more research, silencing SPARC with siRNA could be used as therapy to treat the millions of people suffering from fibrotic diseases.

References

American Thoracic Society. Diagnosis and initial management of nonmalignant diseases related to asbestos. Am. J. Respir. Crit. Care Med. 170: 691-715. 2004.

Claman HN, Giorno RC, Seibold JR. Endothelial and fibroblastic activation in scleroderma: the myth of the uninvolved skin. *Arthritis Rheum.* 34: 1495-501. 1991.

Clark RA, Nielsen LD, Welch MP, McPherson JM. Collagen matrices attenuate the collagen-synthetic response of cultured fibroblasts to TGF-beta. *J. Cell. Sci.* 108: 1251-1261. 1995.

Dhore CR, Cleutjens JP, Lutgens E, Cleutjens KB, Geusens PP, Kitslaar PJ, et al. Differential expression of bone matrix regulatory proteins in human atherosclerotic plaques. A*rterioscler. Thromb. Vasc. Biol.* 21: 1998-2003. 2001.

Dykxhoorn DM, Novina CD, Sharp PA. Killing the messenger: short RNAs that silence gene expression. *Nat. Rev. Mol. Cell. Biol.* 4: 457-67. 2003.

Francki A, McClure TD, Brekken RA, Motamed K, Murri C, Wang T, Sage EH. SPARC regulates TGF-beta-1-dependent signaling in primary glomerular mesangial cells. *J. Cell. Biochem.* 91: 915-925. 2004.

Francki A, Bradshaw AD, Bassuk JA, Howe CC, Couser WG, Sage EH. SPARC regulates the expression of collagen type I and transforming growth factor-1 in mesangial cells. *J. Biol. Chem.* 274: 32145-52. 1999.

Frizell E, Liu SL, Abraham A, Ozaki I, Eghbali M, Sage EH, et al. Expression of SPARC in normal and fibrotic livers. *Hepatology.* 21: 847-54. 1995.

Kuhn C, Mason RJ. Immunolocalization of SPARC, tenascin, and thrombospondin in pulmonary fibrosis. *Am. J. Pathol.* 147: 1759-69. 1995.

Mignatti P. Extracellular matrix remodeling by metalloproteinases and plasminogen activators. *Kidney Int. Suppl.* 49: S12-S14. 1995.

Oriente A, Fedarko NS, Pacocha SE, Huang SK, Lichtenstein LM, Essayan DM. Interleukin-13modulates collagen homeostasis in human skin and keloid fibroblasts. *J. Pharmacol. Exp. Ther.* 292: 988-994. 2000.

Pichler RH, Hugo C, Shankland SJ, Reed MJ, Bassuk JA, Andoh TF, et al. SPARC is expressed in renal interstitial fibrosis and in renal vascular injury. *Kidney Int.* 50: 1978-89. 1996.

Savani RC, Zhou Z, Arguiri E, Wang S, Vu D, Howe CC, DeLisser HM. Bleomycin-induced pulmonary injury in mice deficient in SPARC. *Am. J. Physiol. Lung Cell. Mol. Physiol.* 279(4): 743-750, 2000.

Schiemann BJ, Neil JR, Schiemann WP. SPARC inhibits epithelial cell proliferation in part through stimulation of the transforming growth factor--signaling system. *Mol. Biol. Cell.* 14: 3977-88. 2003.

Singer AJ, Clark RA. Cutaneous wound healing. *N. Engl. J. Med.* 341: 738-746. 1999.

Smartt AM, Brezinski M, Trapkus M, Gardner D, Putnam EA. Collagen accumulation over time in the murine lung after exposure to crocidolite asbestos or Libby amphibole. *Environmental Toxicology.* In Press. 2008.

Strandjord TP, Madtes DK, Weiss DJ, Sage EH. Collagen accumulation is decreased in SPARC-null mice with bleomycin-induced pulmonary fibrosis. *Am. J. Physiol.* 277: 628-635, 1999.

Varedi M, Ghahary A, Scott PG, Tredget EE. Cytoskeleton regulates expression of genes for transforming growth factor-1 and extracellular matrix proteins in dermal fibroblasts. *J. Cell. Physiol.* 172: 192-9. 1997.

Wall NR, Shi Y. Small RNA: can RNA interference be exploited for therapy? *Lancet.* 362: 1401-3. 2003.

Zhou X, Tan FK, Guo X, Wallis D, Milewicz DM, Xue S, Arnett FC. Small interfering RNA inhibition of SPARC attenuates the profibrotic effect of transforming growth factor β1 in cultured normal human fibroblasts. *Arthritis & Rheumatism.* 52: 257-261. 2005.

Zhou X, Tan FK, Reveille JD, Wallis D, Milewicz DM, Ahn C, et al. Association of novel polymorphisms with the expression of SPARC in normal fibroblasts and with susceptibility to scleroderma. *Arthritis. Rheum.* 46: 2990-9. 2002.

Ziesche R, Hofbauer E, Wittmann K, Petkov V, Block LH. A preliminary study of long-term treatment with interferon gamma-1b and low-dose prednisolone in patients with idiopathic pulmonary fibrosis. *N. Engl. J. Med.* 341: 1264-1269. 1999.

SUMMARY

Pulmonary fibrosis is a serious medical condition with no cure. It is caused by a variety of environmental and pharmaceutical agents. Here I used asbestos-induced fibrosis as a model to study the ability of SPARC to regulate collagen accumulation in a fibrotic lung. The matricellular protein SPARC had previously been implicated as a regulator of collagen accumulation in bleomycin-induced fibrosis. Expression of SPARC, a regulator of cell-matrix interactions, was also found to be upregulated in a fibrotic lung after both one year and six months of asbestos exposure and therefore was a candidate for further study.

Here I show that both collagen accumulation and SPARC expression are increased in a wild-type mouse lung using a short-term asbestos exposure to induce fibrosis. To confirm whether or not these observations were correlated, fibrosis was induced through asbestos exposure in SPARC-null mice. The SPARC-null mice exposed to asbestos did not show the significant increase in collagen deposition as the wild-type fibrotic mice did. These results corresponded with some previous investigations into bleomycin-induced models of pulmonary fibrosis by further demonstrating the ability of SPARC to regulate the collagen deposition and subsequent scar tissue formation in the lung. Therefore SPARC may be a potential therapeutic target in the treatment of many fibrotic diseases, aside from asbestosis and bleomycin-induced pulmonary fibrosis. A model of asbestos-induced pulmonary fibrosis including the role of SPARC as discovered throughout this project in collagen deposition can be found in Figure 32 (red arrows).

Figure 32: The Role of SPARC in Asbestos-Induced Pulmonary Fibrosis

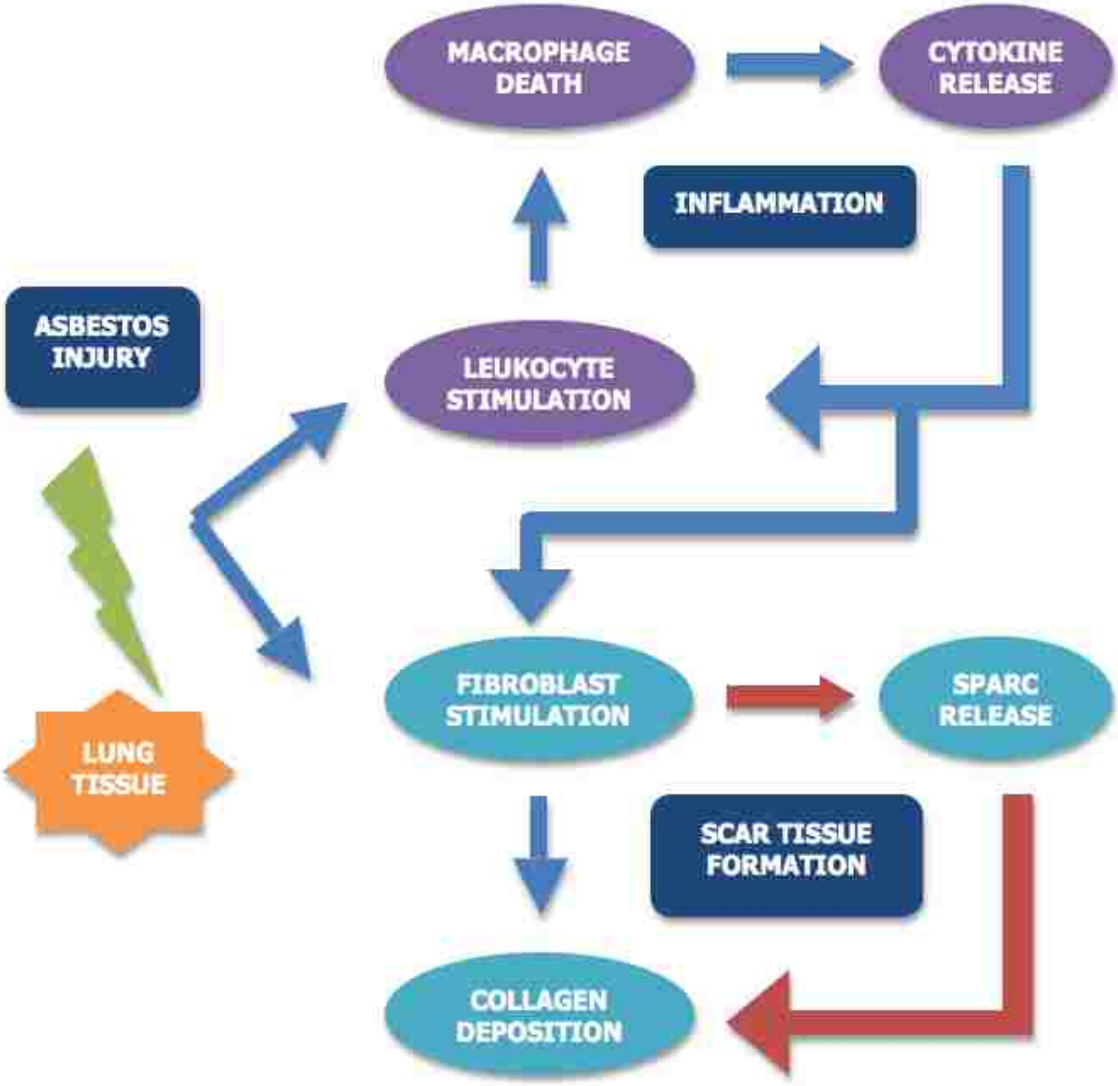

Figure 32 Legend: A model of asbestos-induced fibrotic disease. Blue arrows represent previously known routes of disease formation that include both inflammation and scar tissue formation. Briefly, after asbestos exposure to the lung, fibroblasts are stimulated by growth factors to deposit collagen around the foreign fibers and leukocytes, like macrophages, are stimulated to eradicate the foreign matter. However, due to the natural resistance of asbestos to phagocytic activity, the macrophages begin to die at which point they release cytokines to both recruit new macrophages to the area and stimulate fibroblasts to lay down more collagen. This perpetual stimulation of both the immune system and collagen deposition lead to the inflammation and scar tissue formation commonly associated with fibrosis. The red arrows represent the additional role of SPARC in this process as found in this dissertation project. I have found that the expression of SPARC is increased in fibroblasts after asbestos exposure (Chapter 3). This increase in expression leads to a significant increase in collagen deposition in the lung (Chapters 1 and 2).

To explore the therapeutic potential of SPARC knockdown, I used siRNA directed against SPARC mRNA to silence SPARC expression in a model of fibrosis both *in vitro* and *in vivo*. Primary mouse lung fibroblasts exposed to asbestos showed an increase in collagen levels at 24 hours post-exposure that was mitigated after transduction of the cells with a virus containing the SPARC siRNA. These results resembled what was seen *in vivo*, where fibrotic mice instilled with the siRNA containing virus had significantly less collagen accumulation than the fibrotic mice that did not receive the virus. Though the results of this portion of the project are inconclusive until more experiments can be performed, it appears that the silencing of SPARC expression in individuals already suffering from fibrosis may have significant therapeutic potential.

There are several directions with which to take the results presented here in the future. Primarily, more research needs to be performed with the SPARC siRNA containing virus *in vivo*. The three month experiment should be repeated using a non-target negative control instead of the GFP control to determine if the decrease seen in collagen deposition was a result of the siRNA or a response to the presence of the viral vector. Also, the viral incubation period should be shortened in order to detect a reduction in SPARC expression. A similar experiment could be designed for a one month time point as well, because the disease in mice appears to be the most severe at this time and a one month study would complement the three month data.

It is also necessary to study the pathways by which SPARC may be inducing collagen synthesis and deposition. Specifically, the involvement of SPARC in the TGF-β signaling pathways of JNK and SMAD2/3 should be evaluated in an asbestos-induced model of fibrosis. I attempted to evaluate protein expression changes in the SMAD2/3 pathway in mice exposed to asbestos but was unsuccessful in getting a phosphorylated

SMAD antibody to work. Analysis of these pathways as well as the interactions between SPARC and TGF-β would both confirm previous studies and provide more insight into the mechanism by which SPARC contributes to fibrosis development in the lung.

In terms of *in vitro* studies, it would be interesting to use primary lung fibroblasts from SPARC-null mice to study not only the influence of SPARC on collagen expression but also how SPARC influences the expression of other genes involved in the fibrotic response. This would be useful to determine more specifically the mechanism by which SPARC functions in fibroblasts during the development of pulmonary fibrosis. The results from such a study could provide more potential therapeutic targets for the treatment of fibrotic diseases. It would also be beneficial to determine if SPARC was localizing to the nucleus *in vitro* after CRO exposure with nuclear staining. If it is, more insight could be gained as to why SPARC is moving into the nucleus and what the subsequent effects are in both the cell and extracellular space.

More *in vitro* studies could be performed using co-cultures of fibroblasts and epithelial cells. As the role of SPARC in the fibrotic response involves mainly fibroblast and epithelial cells, a co-culture experiment would provide results that may more resemble those seen *in vivo*. A co-culture study would also yield more information regarding the mechanism of action of SPARC as well as the interaction between the two cell types. Furthermore, if the *in vivo* response could be replicated more closely *in vitro*, it would be both cost efficient and time saving.

It has been suggested that the protein Hevin compensates for the lack of SPARC in SPARC-null mice. Though there were significant decreases in collagen accumulation in SP-null mice, there were some significant increases seen in type III collagen mRNA. This may indicate that another protein, like Hevin, could be compensating for SPARC in the

SP-null mice. Therefore, fibrosis studies should be carried out in SPARC/Hevin double-null mice. Results from such a study would confirm if Hevin is in fact compensating for SPARC and may also provide some insight into the similarities between the two genes when compared with results from studies in SP-null mice.

Finally the *in vivo* studies utilizing the SPARC-null mice could be repeated with the addition of an immunosuppressant. The SP-null mice exposed to asbestos showed significantly less collagen deposition in the lungs but no change in the inflammatory response. Silencing of SPARC only addresses half of the fibrotic response. To truly help individuals suffering from fibrosis, it must be dealt with on two fronts. Both the level of collagen production must be reduced and the inflammatory response must be modulated. If it is possible to accomplish both of these tasks, a cure for fibrosis may be developed in the near future.

APPENDIX A: Elutriated Libby Amphibole

The type of amphibole found in the vermiculite mines in Libby is unlike all the other well-studied forms of amphibole asbestos for several reasons. One is the varied composition of the Libby amphibole fibers, which include a variety of fiber types including tremolite, winchite, and richterite (Meeker, 2003). Another is a difference in the chemical composition of the fibers, where the various fibers that compose Libby asbestos all have different proportions of cations like Mg, Ca, Fe, Na, and K (Webber, 2008). Additionally, varied fiber sizes that differ from other well-studied forms of asbestos may cause a different response.

Fiber size plays a significant role in disease development after asbestos exposure. Early studies indicated that fibers greater than 8μm in length are more pathogenic than the shorter fibers (Mossman, 1989) and are more likely to cause mesothelioma (Stanton, 1981). However, more recent studies have suggested that both long and short fibers are equally capable of causing a response (Dodson, 2003; Suzuki, 2005). In fact, it has been hypothesized that after exposure to amphibole similar to those from Libby where there is a mixed fiber size (Meeker, 2003), the longer fibers get trapped in the upper airways where they are removed by mucociliary factors (Shusterman, 2003), and therefore the smaller, respirable fibers are the ones that can travel down to the alveoli at the lung bases. If this is correct, the shorter fibers would be more capable of causing disease *in vivo*.

In order to examine this hypothesis, I was able to utilize Libby amphibole fibers with lengths less than 2.5μm after an elutriation technique was perfomed (Webber, 2008). Dr. Tony Ward at the University of Montana provided the elutriated Libby

amphibole fibers (E.LA) for this study. There were no apparent differences in the chemical composition between the E.LA and the normal LA (Webber, 2008). As was previously described in Chapters 1, 2, and 3, C57Bl/6 WT and SP-null mice were intratracheally instilled with 100μg of the elutriated LA fibers suspended in 30μl PBS or PBS alone as a vehicle control. The mouse lungs were harvested after one month and three month exposures for analysis. The lungs were divided for histological analysis, RNA isolation, protein isolation, and the hydroxyproline assay. Histology along with RNA and protein analysis will not be presented here.

Hydroxyproline content is a surrogate measure for total collagen. Both WT and SP-null lungs were analyzed for total hydroxyproline after one month or three month of exposure to elutriated LA (Figure 33). After both one month (Figure 33A) and three months (Figure 33B) there was a significant increase the level of total hydroxyproline in the lungs of mice exposed to the elutriated Libby amphibole compared to PBS treated controls. As was seen in Chapter 2, lack of SPARC in the mice (SP-null) significantly mitigated this effect.

Figure 33: Elutriated LA Hydroxyproline Assay

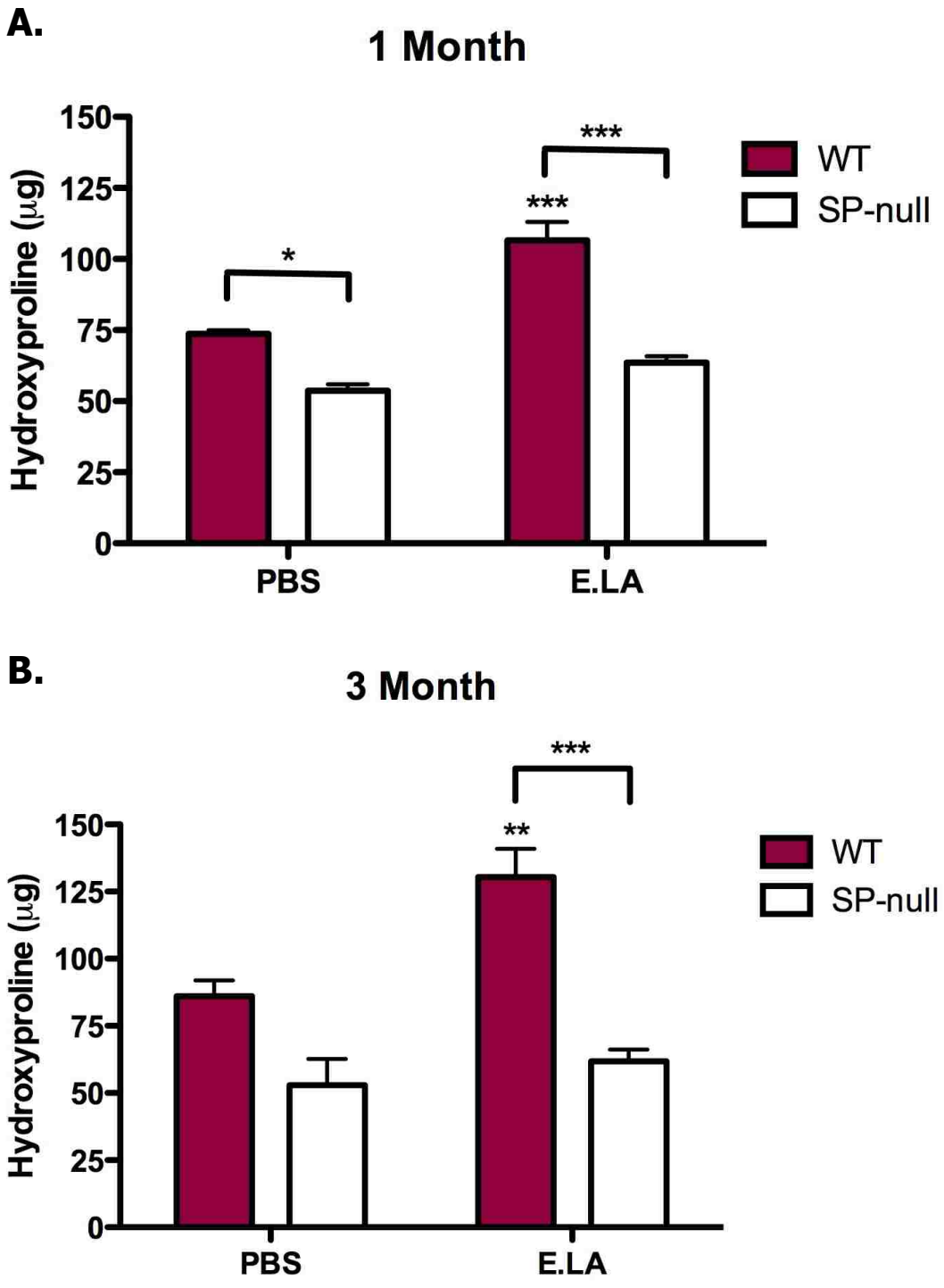

Figure 33 Legend: Total hydroxyproline content from the lungs of WT and SP-null mice exposed to PBS or E.LA. Mice were intratracheally instilled for 1 or 3 months and collagen content of the left lung was determined by measuring hydroxyproline levels in replicate animals. All experiments were done in triplicate. Results are presented as mean values ± SEM for each treatment/time (all groups have n = 6-10). Lungs from both the one month and three month E.LA exposed WT mice have significantly more hydroxyproline than the PBS controls. Hydroxyproline levels of lungs from E.LA exposed SP-null mice are no different than their PBS exposed counterparts. (* = $p < 0.05$, ** = $p < 0.01$, *** = $p < 0.001$).

I also analyzed the new E.LA hydroxyproline data against the previous normal LA data presented in Chapters 1 and 2 (Figure 34). At the one month time point, lungs from mice exposed to both E.LA and normal LA demonstrated a significant increase in hydroxyproline content compared to PBS treated lungs (Figure 34A). There was, however, no difference between the hydroxyproline between E.LA and LA treated lungs. By three months post-exposure, both the LA and E.LA treated lungs contained significantly higher amounts of hydroxyproline compared to PBS treated controls. In addition, at three months after asbestos exposure, the E.LA treated WT lungs also contained significantly more hydroxyproline than the LA treated WT lungs (Figure 34B). This could be an indication that the shorter, elutriated LA fibers cause higher levels of collagen accumulation over time.

Figure 34: Normal vs. Elutriated LA Hydroxyproline Assay

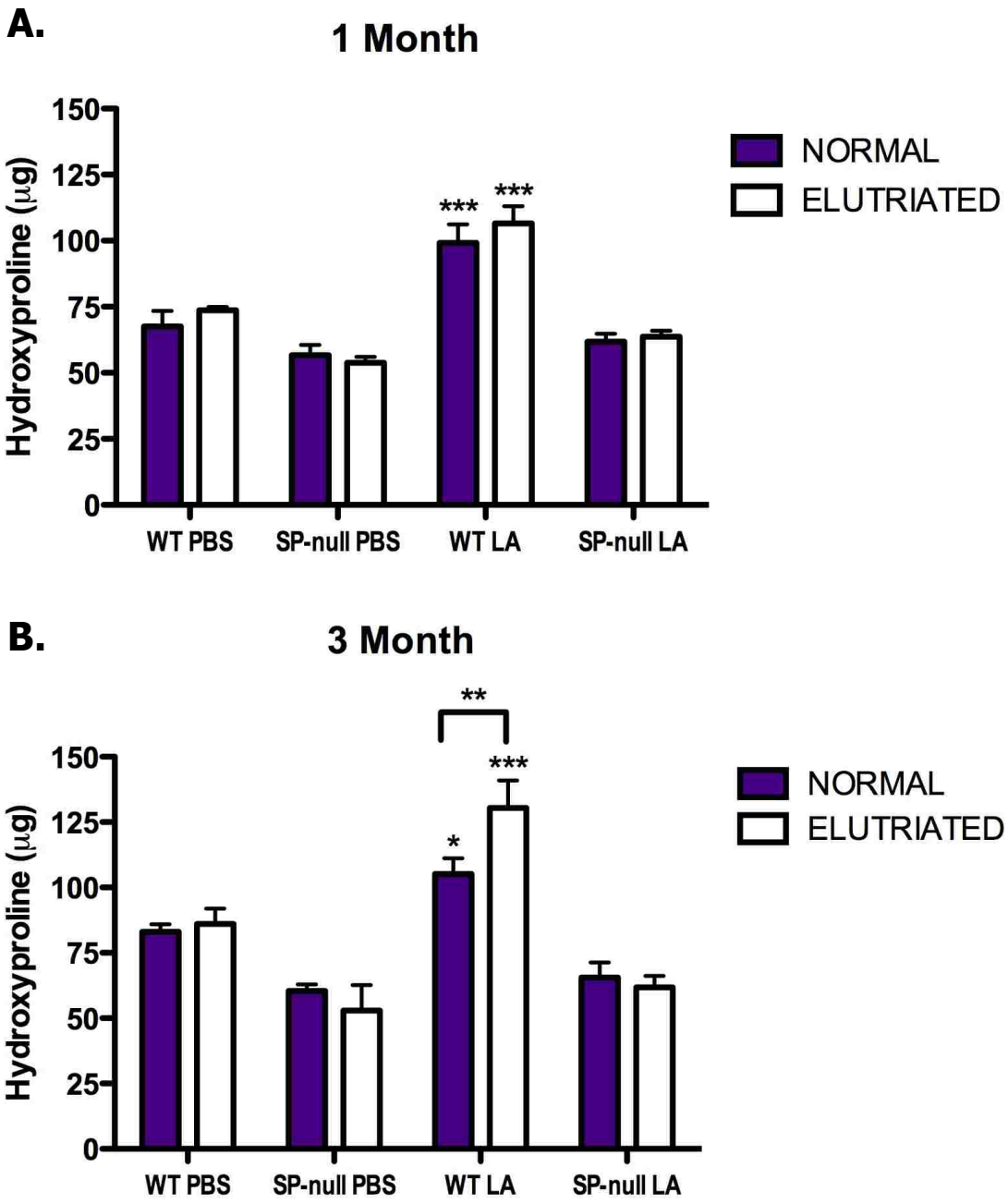

Figure 34 Legend: Total hydroxyproline content from the lungs of WT and SP-null mice exposed to PBS, normal LA, or E.LA. Experiments were perfomed as was previously described in the legend for Figure 31. When compared to the WT normal LA instilled mice, the WT mice instilled with elutriated LA have significantly more hydroxyproline at three months after exposure. (* = $p < 0.05$, ** = $p < 0.01$, *** = $p < 0.001$).

Conclusion:

No significant differences in total hydroxyproline between the normal LA and E.LA treated lungs were seen until three months post-exposure. However, it may be that the shorter fibers are more hazardous in the long run. It is thought that exposure to fibers of different lenghths can cause different asbestos-related diseases (Lippman, 1990). Based on the outcome that shorter fibers caused increased collagen deposition at three months, it is possible that inhalation of these respirable fibers may cause more of a fibrotic disease than a cancerous one. However, this is only one experiment and much more research into this issue must be done in the future to fully understand the differences in pathogenicity between the various fiber lengths.

References:

Dodson RF, Atkinson MA, Levin JL Asbestos fiber length as related to potential pathogenicity: A critical review. *Am. J. Ind. Med.* 44:291–297. 2003.

Lippmann M. Effects of fiber characteristics on lung deposition, retention, and disease. *Environ. Health Perspect.* 88:311–317. 1990.

Meeker GP, Bern AM, Brownfield IK, Lowers HA, Sutley SJ, Hoefen TM, and Vance JS The composition and morphology of amphiboles from the Rainy Creek Complex, Near Libby, Montana. *Am. Mineralogist* 88:1955–1969. 2003.

Mossman BT, Hansen K, Marsh JP, Brew ME, Hill S, Bergeron M, Petruska J. *Mechanisms of fibre-induced superoxide release from alveolar macrophages and induction of superoxide dismutase in the lungs of rats inhaling crocidolite*. IARC Sci. Publ. 81-92. Lyon: IARC Press. 1989.

Shusterman D. Toxicology of nasal irritants. *Curr. Allergy Asthma Rep.* 3:258–265. 2003.

Stanton, MF, Layard M, Tegeris A, Miller E, May M, Morgan E, Smith A. Relation of particle dimension to carcinogenicity in amphibole asbestoses and other fibrous minerals. *J. Natl. Cancer Inst.* 67:965–975. 1981.

Suzuki Y, Yuen SR, Ashley R. Short, thin asbestos fibers contribute to the development of human malignant mesothelioma: Pathological evidence. *Int. J. Hyg Environ. Health* 208:201–210. 2005.

Webber JS, Blake DJ, Ward TJ, Pfau JC. Separation and characterization of respirable amphibole fibers from Libby, Montana. *Inhalation Toxicology.* 20: 733-740. 2008.

APPENDIX B: Hevin

Hevin (also known as SC1, MAST 9, SPARC-like 1, or ECM 2) is a member of the SPARC family that also includes QR1, the testicans and the SMOCs (Vannahme, 2002). Like SPARC, the protein consists of three domains: acidic, follistatin-like, and extracellular calcium-binding (Hambrock, 2003). The last two domains closely resemble those found in SPARC, however the acidic domain has not been found to resemble any other protein. Furthermore, like SPARC, Hevin functions in inhibiting cell adhesion (Bradshaw, 2001), inhibiting cell attachment and spreading (Girard, 1996), and may play a role in cancer as a negative regulator of cell proliferation and growth (Nelson, 1998; Bendik, 1998; Claeskens, 2000). The ability of Hevin to modulate cell-matrix interactions is still under investigation. Regardless, it has been shown that tumors grown in SP-null mice do not present with expected increases in cell proliferation and angiogenesis. (Brekken, 2003).

Based on the similarity in the functioning of both SPARC and Hevin, it has been hypothesized that Hevin may play a compensatory role for SPARC in SP-null mice. To examine this hypothesis, I analyzed both Hevin mRNA and protein levels in SP-null mice exposed to asbestos to see if levels increased in an attempt to compensate for the lack of SPARC. I utilized the same mice instilled for the data presented in chapters 1 and 2. Again, the RNA and protein were isolated in the manner described in previous chapters and analyzed for Hevin expression. Determining the ability of Hevin to compensate for SPARC in a fibrosis model may help to identify the role of Hevin in cell-matrix interactions.

First I examined the levels of Hevin mRNA via quantative Real-Time PCR to determine if there were any expression alterations in either WT or SP-null mice exposed

to asbestos (Figures 35 and 36). There were no significant differences in Hevin expression detected in WT mice at any of the three time points analyzed for any exposure group (Figure 35A). There were, however, significant decreases in Hevin mRNA levels in lungs from SP-null mice exposed to LA at both the one week and three month time points (Figure 35B). When comparing the levels of Hevin mRNA expression between WT and SP-null mice, no differences were found for either the CRO treatment group (Figure 36A) or the LA treatment group (Figure 36B). In terms of mRNA expression, it does not appear that more Hevin mRNA is synthesized to compensate for SPARC in SP-null mice.

Figure 35: Hevin qRT-PCR

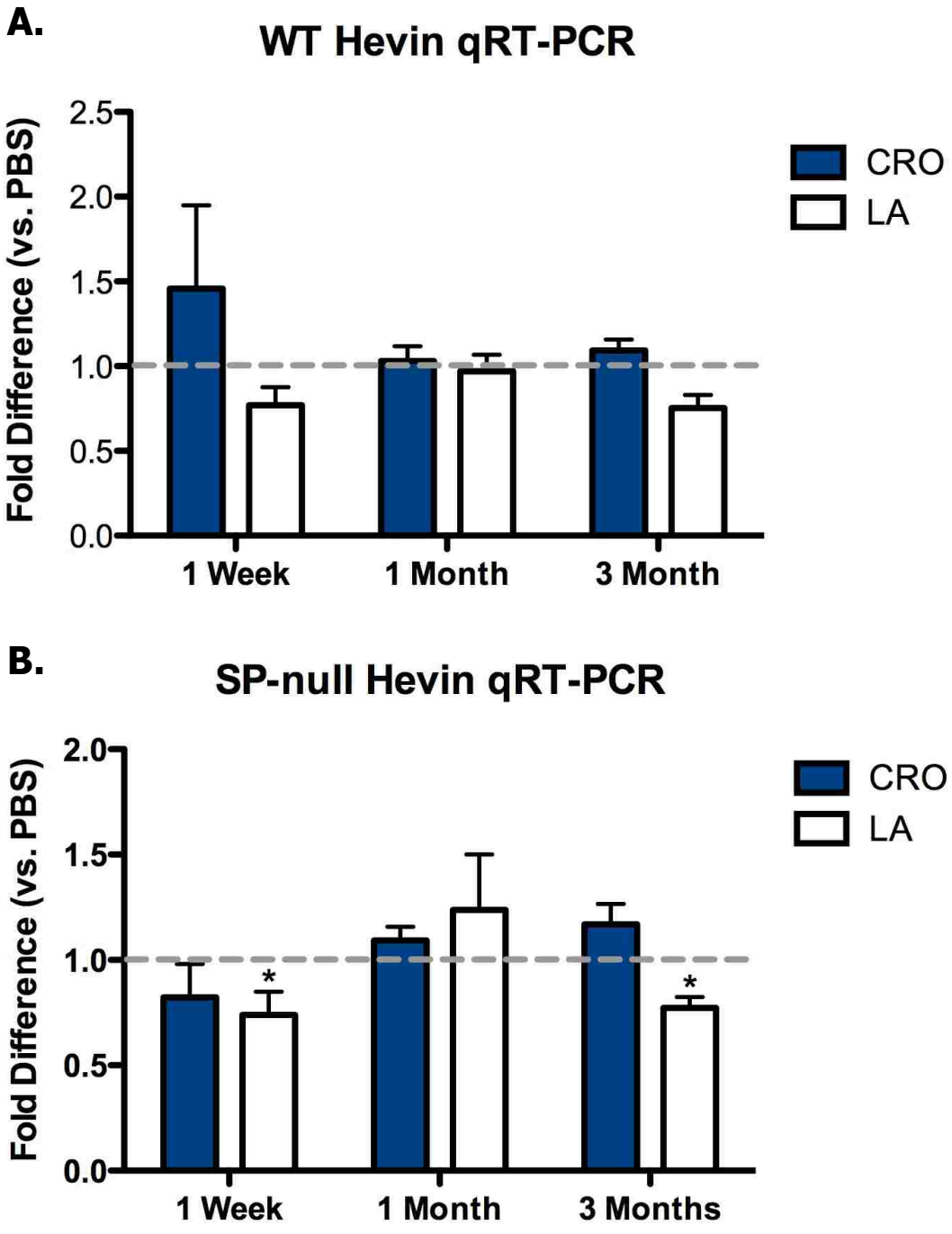

Figure 35 Legend: Real-Time PCR of Hevin mRNA from the lungs of either C57Bl/6 WT or SP-null mice treated with PBS, CRO, or LA. Each experiment was repeated three times. Results from triplicate pools of RNA for each treatment group (n = 10 – 12 per group) were normalized to both Gapdh and β-actin and are presented as mean fold difference ± SEM. The only significant differences in Hevin mRNA expression occur at one week and three month in the LA treatment group when compared to the PBS treatment group. When each treatment group was evaluated for changes over time, no significant differences were discovered. (* = $p < 0.05$)

Figure 36: Wild-Type/SPARC-null Hevin qRT-PCR

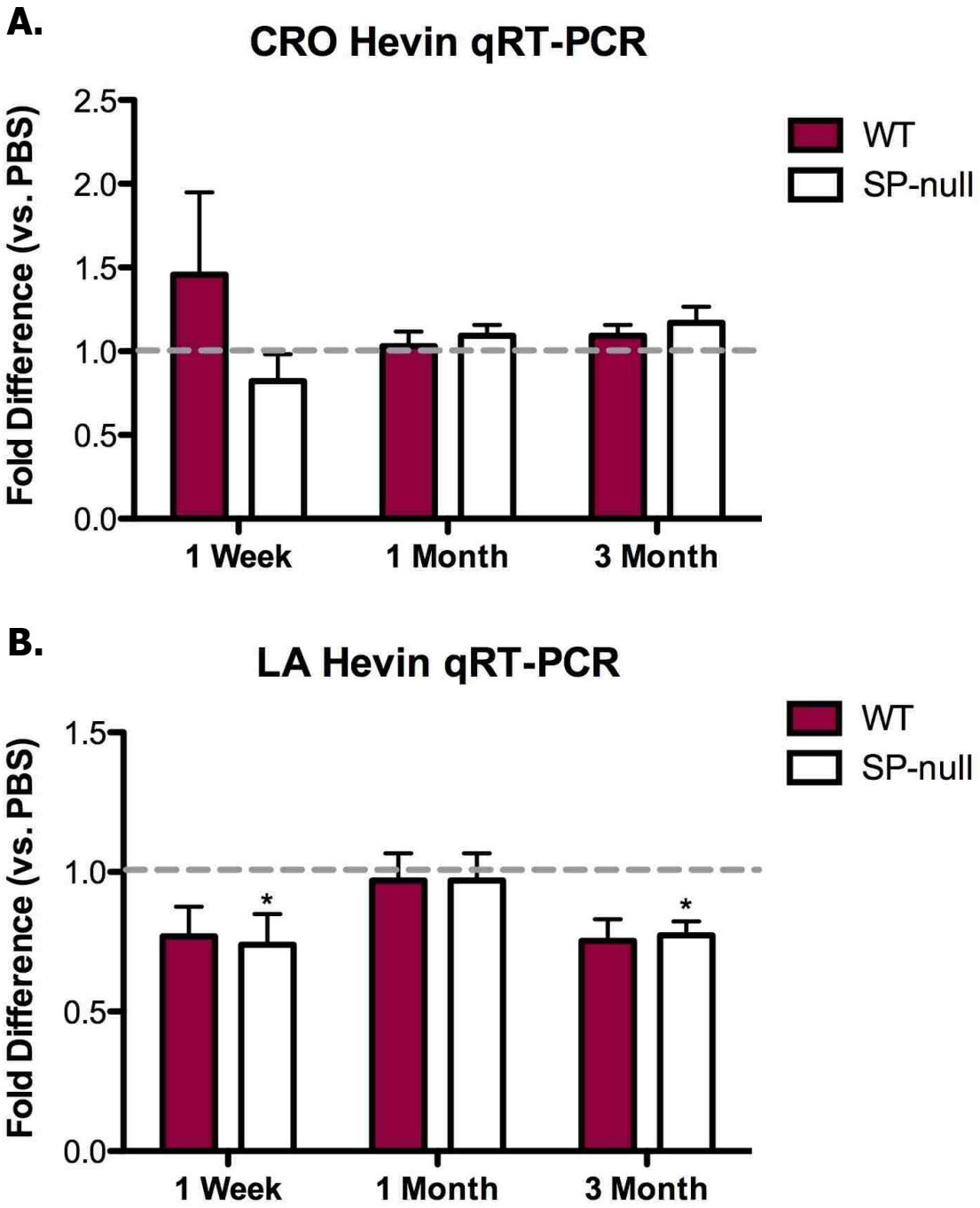

Figure 36 Legend: The same data presented in Figure 33 were also analyzed for differences between WT and SP-null mice. No significant differences were found between the two strains with regards to the expression of Hevin mRNA.

The levels of Hevin protein were also evaluated in both WT and SP-null mice exposed to asbestos (Figures 37 and 38). In WT mice, expression of Hevin protein was significantly increased at one week post LA exposure (Figure 37A). In SP-null mice, expression of Hevin was significantly increased at the one week time point for both amphibole exposure groups and also at the three month time point in CRO exposed animals (Figure 37B). When looking at changes over time, both WT and SP-null mice exposed to LA had a significant decrease in Hevin protein expression from one week to three months post-exposure (Figure 37A and 37B). CRO exposed SP-null mice have a significant decrease in Hevin protein levels from one week to one month, but then a significant increase from the one month to three month time points. Regardless there is still a significant decrease in Hevin from the one week to three month time points overall (Figure 37B). The level of Hevin protein in WT mice compared to SP-null mice was also examined (Figure 38). There were significant increases in Hevin protein in SP-null mice compared to WT mice exposed to CRO asbestos (Figure 38A). There was also a significant increase in Hevin protein levels at the one week time point in SP-null mice exposed to LA compared to their WT counterparts (Figure 38B). Furthermore, Hevin expression was significantly increased in response to LA at the one week time point in both WT and SP-null mouse lungs compared to PBS-treated controls.

Figure 37: Hevin Western Blot

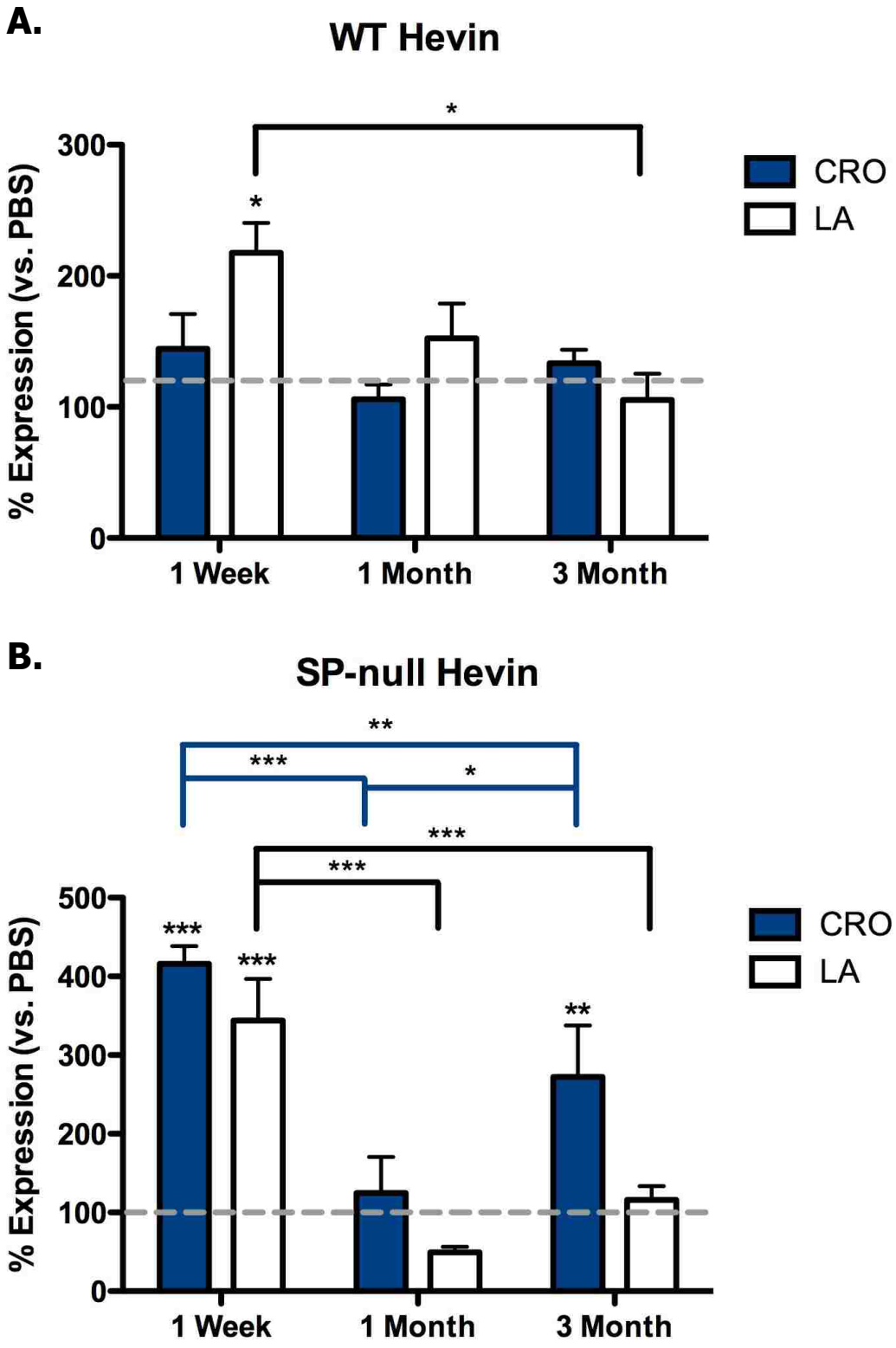

Figure 37 Legend: Immunoblotting of Hevin protein from the lungs of C57Bl/6 WT or SP-null mice exposed to PBS, CRO, or LA. Each blot was repeated three times. Results from triplicate pools of RNA for each treatment group (n = 10 – 12 per group) were normalized to β-actin and are presented as the mean percent expression versus PBS ± SEM. At the one week time point, WT mice exposed to LA had significantly more Hevin protein expression and SP-null mice exposed to either amphibole had significantly higher levels of Hevin. CRO exposed SP-null mice had significantly increased levels of Hevin at three months after exposure. Over time, Hevin expression significantly decreased in LA exposed WT and SP-null mice from the one week to the three month time point. Also in SP-null mice, Hevin protein expression significantly decreased from the one week to one month time point, but then rebounded at the three month time point. (* = $p < 0.05$, ** = $p < 0.01$, *** = $p < 0.001$)

Figure 38: Wild-Type/SPARC-null Hevin Western Blot

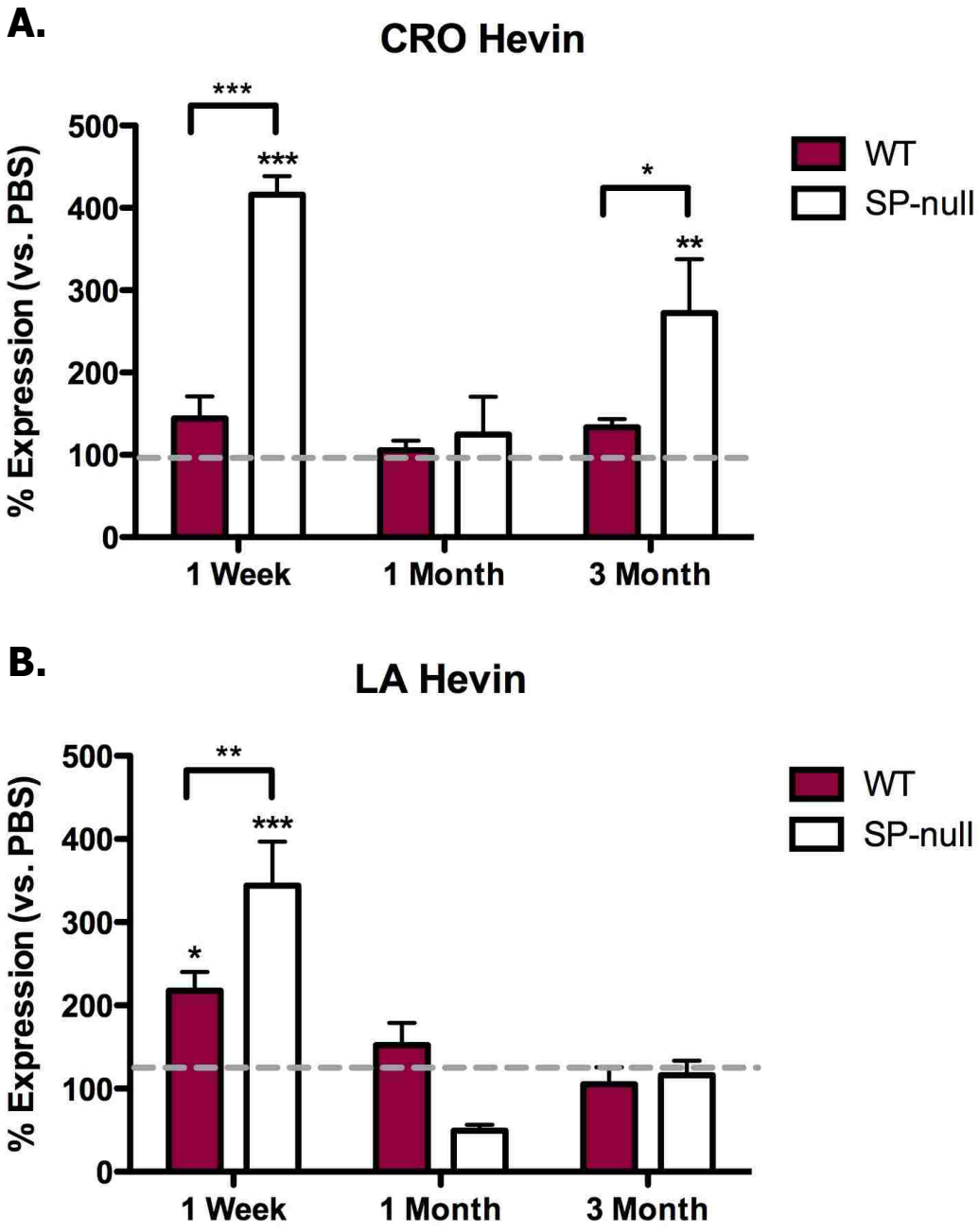

Figure 38 Legend: The same data presented in Figure 35 were also analyzed for differences between WT and SP-null mice. CRO exposed SP-null mice expressed significantly more Hevin protein at both the one week and one month time points than their WT counterparts. LA exposed SP-null mice only had significantly more Hevin expression at the one week time point when compared to LA exposed WT mice. (* = $p < 0.05$, ** = $p < 0.01$, *** = $p < 0.001$)

Conclusion:

Though there were no apparent increases in Hevin mRNA in SP-null mice exposed to asbestos, there were significant increases in Hevin protein. This increase in Hevin protein appeared to occur mainly at one week after asbestos exposure and levels in SP-null mice were significantly higher than WT mice indicating that it may be compensating for SPARC in SP-null mice exposed to asbestos. As there were still significant decreases in hydroxyproline content in SP-null mice exposed to asbestos for one week compared to WT mice (Chapter 2, Figure 20), these results may indicate that if Hevin is compensating for a lack of SPARC, it is not doing so in the area of cell-matrix communication. But again, more research is needed to fully understand Hevin's compensatory abilities.

References:

Bendik I, Schrami P, Ludwig CU. Characterization of MAST9/Hevin, a SPARC-like protein, that is down-regulated in non-small cell lung cancer. Cancer Res. 58: 626-629. 1998.

Bradshaw AD, Sage EH, SPARC, a matricellular protein that functions in cellular differentiation and tissue response to injury. *J Clin Invest.* 107(9):1049-54. 2001

Brekken RA, Puolakkainen P, Graves DC, Workman G, Lubkin SR, Sage EH. Enhanced growth of tumors in SPARC null mice is associated with changes in the ECM. *Journal of Clinical Investigation.* 111: 487-495. 2003.

Claeskens A, Ongenae N, Neefs JM, Cheyns P, Kaijen P, Cools M, Kutoh E. Hevin is down-regulated in many cancers and is a negative regulator of cell growth and proliferation. *Br. J. Cancer.* 82: 1123-1130. 2000.

Girard JP, Springer TA. Modulation of endothelial cell adhesion by hevin, an acidic protein associated with highendothelial venules. *J. Biol. Chem.* 271: 4511-4517. 1996.

Hambrock HO, Nitsche DP, Hansen U, Bruckner P, Paulsson M, Maurer P, Hartmann U. SC1/Hevin: an extracellular calcium-modulated protein that binds collagen I. *J. Biol. Chem.* 278: 11351-11358. 2003.

Nelson PS, Plymate SR, Wang K, True LD, Ware JL, Gan L, Liu AY, Hood L. Hevin, an antiadhesive extracellular matrix protein, is down-regulated in metastatic prostate adenocarcinoma. *Cancer Res.* 58: 232-236. 1998.

Vannahme C, Smyth N, Miosge N, Gosling S, Frie C, Paulsson M, Maurer P, Hartmann U. *J. Biol. Chem.* 277: 37977-37986. 2002.